Combined hydrogen propulsion

for short sea shipping

V. de Vries, 2022

MSc thesis Mechanical Engineering, track Energy & Process Technology

TU Delft

CONOSHIP INTERNATIONAL

Combined hydrogen propulsion

for short sea shipping

by

V. de Vries

To obtain the degree of Master of Science
at the Delft University of Technology

Student number: 1177397
Project duration: September 2020 – January 2022
Thesis committee: Prof. dr. ir. E. L. V. Goetheer, TU Delft, supervisor
Ir. A. A. van der Bles, Conoship B.V., daily supervisor
Dr. ir. L. van Biert, committee member
Prof. Dr. Ir. W. de Jong, committee member

TU Delft

CONOSHIP INTERNATIONAL

Preface

This report presents the master thesis on combined hydrogen propulsion for short sea shipping by Volkmar de Vries. The thesis was executed at Conoship B.V. located in Groningen as part of the track ‘Energy and Process Technology’.

During my professional career as an engineer and (chief) electrician in the offshore industry, I saw that the current ways of working are not sustainable and that a shift in mindset and technology is necessary to reduce the human impact on the world. Although changing everything in the blink of an eye would be great, we have to be realistic in setting our goals. I am glad that I could contribute to the technology of tomorrow with this thesis at Conoship.

I want to thank the people who supported me in completing the EPT track and writing this thesis, especially my supervisor at Conoship Guus van der Bles and my supervisor at the TU Delft Earl Goetheer. They were a great help in reflecting my ideas and identifying areas for improvement. I also want to thank my current employer, Maritime Institute Willem Barentsz (part of NHL Stenden) for allowing me to use their facilities and laboratory for the practical experiments.

V. de Vries
West-Terschelling, January 2022

Summary

Shipping is, and will continue to be, the most important transportation method around the globe. A vital part of the logistic chain, it is also one of the main contributors to the worldwide CO_2 emissions. Current propulsion technologies all rely on the same classic diesel driven technology, as diesel is widely available and has a high energy density.

The goal of this research is to identify greener solutions to propel a vessel sailing for short distances. During a definition study, several fuels and energy converters were studied and benchmarked based on a use case. The results showed that (a combination of) the dual fuel internal combustion, using bio diesel and hydrogen, and the low temperature proton exchange membrane fuel cell, fuelled with hydrogen, is the most feasible setup for the use case. Such a combination in itself is not a new one, but in the literature only an all-electric setup is described. In the proposed solution an internal combustion engine is driving the propellor shaft directly, assisted by an electric motor powered by the fuel cell.

Based on this outcome, the following research question was defined:

How can an internal combustion dual fuel engine and/or LTPEM fuel cell be integrated to form a cost effective solution to propel a short sea ship running on hydrogen?

First, nine designs were created, ranging from a conventional diesel engine setup as a reference case, to a fully electric design powered by fuel cells. All main components in these designs are analyzed regarding part load efficiencies. With these efficiencies, the fuel consumption at different loads are calculated. Based on a use case scenario the total fuel costs are calculated. The CAPEX and the OPEX of the designs are determined to calculate the total costs. As currently no other fuel can compete with diesel, the designs are compared based on the price per tons of CO_2 emissions, as the shipping industry is expected to see a CO_2 emission penalty in the near future. For each design, what the height of this penalty has to be to reach the breakeven point at the end of the use case was calculated. Based on the lowest CO_2 price, an all-electric, fuel cell powered design was identified as the most promising option. Applying additional operational arguments such as redundancy and end user acceptance, it was decided together with Conoship to choose a combination of an internal combustion engine and a fuel cell.

This configuration is worked out in detail to answer the sub questions, covering efficiency improvement and system integration, during which it became apparent that not all information is available to answer all these sub questions. The design needs further research in a multidisciplinary team. A simulation model would be helpful in this further research. A framework and a start to such a model was written together with a list of recommendations.

So far, the chosen design seems to be an economic and practical solution that can be implemented in the near future. It relies on readily available techniques, but the total system integration and control technique is new for the industry.

Contents

Appendices

List of figures

Report

Appendices

List of tables

Report

Appendices

Nomenclature

ABC	Anglo Belgian corporation, engine manufacturer
ASR	Area specific resistance
CO_2	Carbon dioxide
CPP	Controllable pitch propellor
DNV	Det Norske Veritas (Norwegian classification society)
FC	Fuel cell
FPP	Fixed pitch propellor
G_{AC}	Alternating current generator
G_{DC}	Direct current generator
GHG	Greenhouse gas(ses)
GT	Gas turbine
H_2	Hydrogen
HHV	Higher heating value
IBC code	International code for the construction and equipment of ships carrying dangerous chemicals in bulk
ICE	Internal combustion engine
IMO	International maritime organization
KPI	Key performance indicator
kW	Kilowatt
kWe	Kilowatt electric
LHV	Lower heating value
LNG	Liquified natural gas
LOHC	Liquid organic hydrogen carrier
LTPEM	Low temperature proton exchange membrane fuel cell
MARPOL	International convention for the prevention of pollution from ships
$NaBH_4$	Sodium borohydride, option to store hydrogen
NOx	Nitrogen oxides
ORC	Organic Rankine cycle
PM	Particle matter (emission)
PM(M)	Permanent magnet (motor)
PMaSRM	Permanent magnet assisted synchronous reluctance motor
PTI	Power take in
PTO	Power take out
PtX	Power to fuel (green electrical power converted to a liquid or gaseous fuel)
PWM	Pulse width modulation
SOFC	Solid oxide fuel cell
SOLAS	International Convention for the Safety of Life at Sea
SynRM	Synchronous reluctance motor
TCO	Total cost of ownership
THD	Total harmonic disturbance
TRL	Technical readiness level
VFD	Variable frequency drive

A	Fuel cell dependent constant, for LT-PEM mostly 0,06 [V]
E	Theoretical (fuel cell) voltage [V]
I	Current [A]
I	Current density [mA cm^{-2}]
$I_{F(av)}$	Average current through diode [A]
$I_{F(rms)}$	RMS current through diode [A]
i_0	Exchange current density [mA cm^{-2}]
i_n	Internal current density [mA cm^{-2}]
N	Number of windings
R	Resistance [Ω]
R_d	Resistance of diode [Ω]
r	Area specific resistance [kΩ cm^2]
V	Voltage [V]
V_c	Cell voltage [V]
ΔV_{ohm}	Voltage drop caused by ohmic losses [V]
V_{T0}	Forward voltage over diode
Φ	Flux

1 Introduction

The shipping industry still largely relies on the same technologies as in the last few decades, making it a large source of harmful emissions. Legislation is forcing shipowners to look into technologies to reduce their emissions, mainly focusing on sulfur, soot and NOx emissions, as well as their fuel consumption, by, for example, weather routing and slow steaming.

Fuel reduction alone, however, does not lead to a sufficient reduction in carbon dioxide emissions, which are mainly embedded in the fuel used. Therefore, alternatives to diesel are becoming more important. This is economically challenging, as hydrocarbons are cheap and have excellent energy density.

However, preventing emissions is not merely an economic goal, but is also necessary to reduce the human footprint on the earth and climate. Conoship B.V. designs ships and is actively looking into alternatives to reduce this footprint of ships. An example is the 'Econowind' project, a containerized demonstration sail propulsion system usable on ships. This system is already in use in a fixed setup on a short sea shipping vessel.

Another point of interest for Conoship is the use of different fuels and alternative energy converters to use these fuels, making it possible to lower the local emission of CO_2 as low as zero.

As part of the exploration of these new techniques, Conoship offered me a position to perform an MSc thesis to explore the possibilities of these alternative fuels and energy converters.

1.1 Research Scope

During the definition study prior to this thesis, I examined the available literature to set a direction and narrow the research questions. The most promising fuel to fulfill Conoship's vision of no (local) CO_2 emissions is blue or green hydrogen. A comparison based on a use case of 20 years showed that the economic differences between a dual fuel hydrogen internal combustion engine and an LTPEM fuel cell are small. Both are an option in standalone or combined installation. The gas turbine option was omitted because its efficiency is too low. A high temperature SOFC is not feasible in the near future, as its technical readiness level is lower than the LTPEM fuel cell.

These results were used as input for a discussion on how to move forward. Especially the insight that an internal combustion engine can be an economical attractive option compared to a fuel cell, despite the better efficiency of the fuel cell, opens the way to interesting combinations.

Conoship's main focus so far is on standalone options, but is interested in combinations as well. To investigate the different setups, Conoship asked for a study on the implementation and combination of these hydrogen powered technologies. This study includes combinations that are not found in literature.

1.2 Research questions

Using the results of the definition study, the following research question was formulated:

How can an internal combustion dual fuel engine and/or LTPEM fuel cell be integrated to form a cost effective solution to propel a short sea ship running on hydrogen?

The following sub questions were then derived:

1. What are options to propel a ship using an internal combustion engine, an LTPEM fuel cell or a combination of both, and how do these options score regarding CAPEX, OPEX, and efficiency?
2. How can the economic efficiency be maximized by using additional energy recovery equipment and by using a total system integration?
3. Can this setup handle the vessel's power demands or are additional measures, such as batteries or capacitors, needed?
4. In a non-conventional electric system, what is a high-level system integration regarding control techniques?
5. What are the high-level design impacts of the options regarding vessel layout and regulations?

1.3 Boundaries

Not all elements can be worked out in great detail in the relatively short period of this master thesis. To allow a clear framework, the following Limits are used:

- Only dual fuel internal combustion engines are covered as these are close to commercial implementation.
- The LTPEM fuel cell is used.
- The fuels used are green or blue hydrogen and PtX or biodiesel as a pilot fuel.
- Bunkering and storage of hydrogen is not examined.
- This report is focussed on the use case (see Section 1.4).
- The setup of the necessary electrical installation is limited to single line diagrams.

1.4 Use case

The installation and techniques should be suitable to install in a short sea shipping type vessel (3600 tdw). The total installed power will be around 1 MW, but the power on the propellor shaft is limited to 750 kW. This 750 kW limit is important to avoid additional costs, as an additional crew member is needed for larger propellor shaft powers. The time in between refuelling is between five days and two weeks. The economic lifetime for the vessel and its installation is set on 20 years. In this life time, the following use case scenario is used:

- Vessel in port: 50% of the time
- Vessel sailing at 25% power: 5% of the time
- Vessel sailing at 50% power: 5% of the time
- Vessel sailing at 75% power: 35% of the time
- Vessel sailing at 100% power: 5% of the time.

This sailing profile is based on numbers used within Conoship.

1.5 Approach

To answer the main research question, an objective framework was realized. The definition study showed that one of Conoship's main goals is to reduce CO_2 emissions. In an ideal world, the budget to do so would be unlimited. In reality, this effort must be paid for by the shipowner. Currently, no configuration is as economical as a single diesel engine driving a propellor with a gear reduction, both in terms of fuel economy and in terms of volume of the installation and fuel tanks. The definition study also showed that the dual fuel combustion engine and the LTPEM fuel cell can reduce the CO_2 emissions against an economic viable price difference. Both have a TRL level that allows a (combined) installation with the current technology. Finally, the definition study showed hydrogen as a fuel, and biodiesel as a pilot fuel for the dual fuel internal combustion engine.

Current government policy encourages green developments and discourages investments in polluting technologies. One way to do so is to introduce financial instruments to make investing in new technologies to reduce emissions more attractive. One such an example is European Union Emissions Trading System (EU ETS). Companies with high CO_2 emissions must participate. Each ton of CO_2 emitted costs a company one emission right. By limiting and slowly reducing the emission rights, companies are forced to invest in more environmentally friendly alternatives. Another option is to buy additional emission rights from other companies. If the number of available rights drops, the price increases.

Such a system is not yet in place for the shipping industry but several important institutes, such as DNV, forecast that this is only a matter of time. Therefore, the possible configurations should at least contain the sum of (additional) investments, operational costs and the fuel costs, compared to the reduction in CO_2 emissions. This used method is illustrated in Figure 1.

To calculate this ratio, the following information and approach were used:

1. Design possible setups, including dual fuel internal combustion engine and fuel cell technology.
2. Determine the (part load) efficiencies of the components involved.
3. Based on the use case scenario and the efficiencies, calculate the fuel costs.
4. Based on the use case, calculate the operational (OPEX) costs.
5. Estimate the costs of installation (CAPEX) with applicable interest.
6. Calculate the total CO_2 emissions in the use case for all configurations and compare them with the reference configuration.
7. Divide the additional costs by the reduction in CO_2 emissions compared to the reference case to obtain the CO_2 price per ton to reach the breakeven point for 20 years of lifetime.

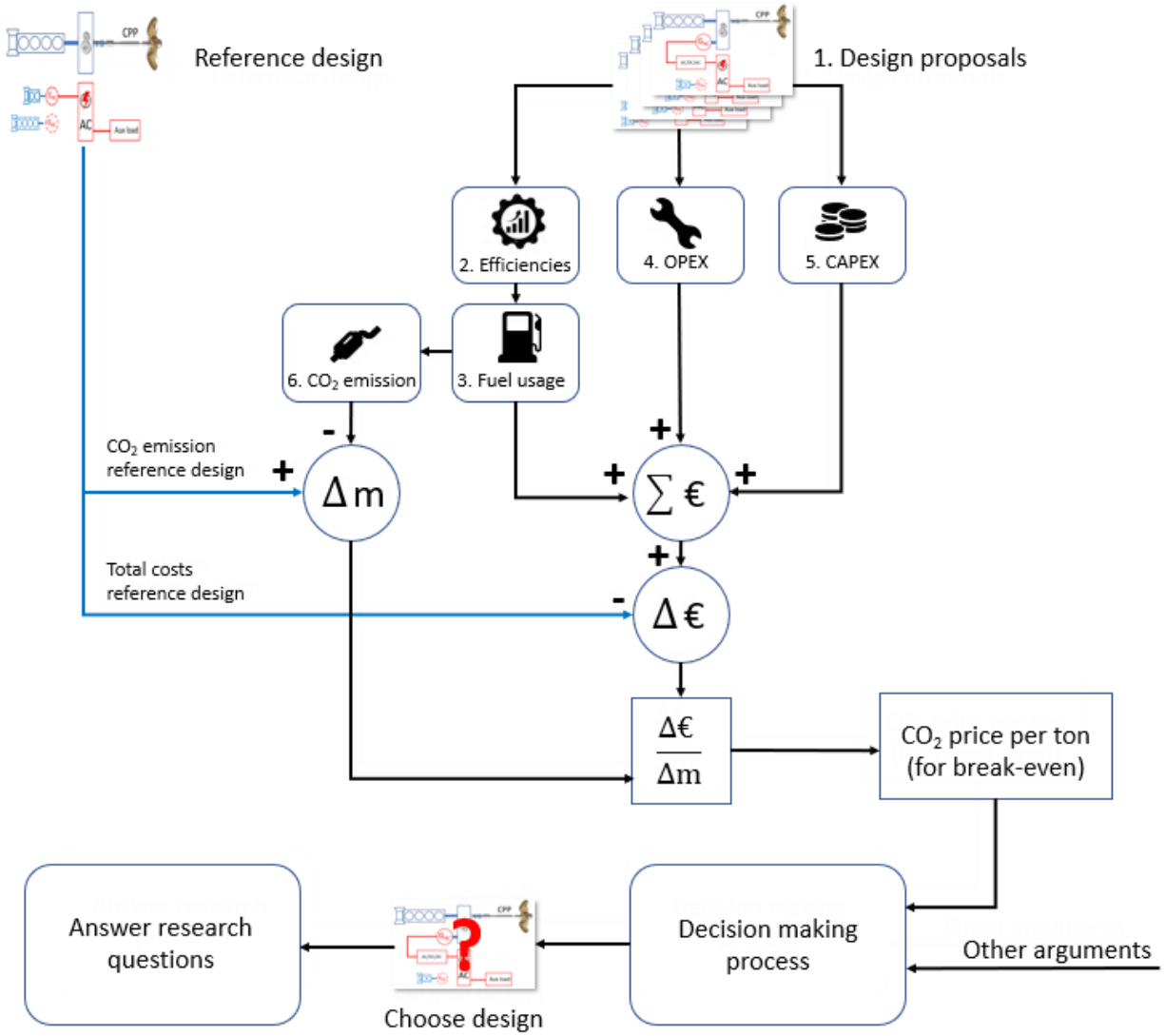

Figure 1: Research approach

The calculated CO_2 price reflects the minimum CO_2 'penalty' the industry will have to pay in the near future to make the investment in a different configuration economical, based on the use case. It does not reflect any ethical decisions by shipowners or their clients, or that customers might be willing to pay more to ship their products on a CO_2-neutral vessel.

The reference case is the currently common single internal combustion engine running on marine diesel oil. This engine drives a propellor shaft via a gearbox. The propellor is a controllable pitch propellor.

The CO_2 price per ton is used as an input for the decision-making process within Conoship. Based on the CO_2 price per ton and other technical and operational arguments to be discussed, a design setup was chosen.

1.6 Structure of the report

Chapter 2 explores the different design options. Each design is briefly described. The goal of this chapter is to identify the main components. The efficiencies of these components are explored in Chapter 3. The background of the efficiencies used in this chapter are explained in more detail in Appendices A and B. Appendix C is included on the technical background and main processes of the LTPEM fuel cell.

Chapter 4 uses the efficiencies to calculate the fuel and urea consumption based on the use case. The fuel consumption is the base for calculating the CO_2 emissions. Appendix D provides background on the need for urea and the operating envelope of an internal combustion engine. In Chapter 5, the financial background is introduced and the CO_2 price per ton for breakeven is calculated. Based on that number and other arguments, a design is selected in Chapter 6. This design is further explored to answer the sub questions in Chapter 7. Finally, the conclusions and recommendations are presented in Chapter 8. Based on the conclusions and recommendations, Appendix E presents an example and recommendations for a simulation model and small scale test setup that can be used for further research.

2 Design proposals

General

The first step is to have the different possible setups defined. These setups are based on technology readily available. It is, however, not said that the combinations of these technologies are already widespread. Shipping industry tends to be conservative and new technologies take time to be accepted, not only by the ship owners and operators, but also by class societies, responsible for the legislation. The proposed designs start at the reference case, a conventional controllable pitch propellor driven by a standard diesel engine. This design is then changed in steps until a completely electrical driven, fuel cell powered design is the final result. Below the designs are briefly described. Blue colors indicate mechanical power transmission, red lines electrical power transmission. The drawings are based on the situation when sailing. Components not in use during sailing are drawn with dashed lines.

Auxiliary load

For the auxiliary load during sailing, the figures of a Damen Combifreighter 3850 were used. The load balance [9] states a sea-going load of 65 kW. This value increases to 87 kW during manoeuvring. As this type of ship might often be sailing in relatively small fairways using additional steering gear pumps, the mean sea going load is increased slightly to 70 kW.

However, the ship from the load balance uses heavy fuel oil. For the designs in this study only MDO is used, so all heating, heat tracing and part of the fuel oil treatment system is removed from the load balance. This lowers the sea going auxiliary load to 60 kW.

Point of attention is that the load balance is not very recent (2006). Switching to power saving alternatives such as LED lighting will lower the electricity consumption. After discussing with a designer of electrical installations for ships (Alewijnse), for this effect an estimated 5 kW is deducted for a conventional internal combustion design running on MDO, bringing the load for that setup to 55 kW. This deduction is cancelled out for the designs with a dual fuel hydrogen engine as this setup will need additional ventilation to comply with the rules and regulations. Those designs have a load of 60 kW.

When a fuel cell (FC) is included in the configuration, an additional auxiliary load was added for the fuel cell pumps and fans. For a 250 kW FC, 10% or 25 kW was added, and for a 500 kW, 7,5% or 37,5 kW was added. [34] As certain overlaps occur, for example for ventilation and cooling water, based on elaborated discussion within Conoship in both cases 10 kW was deducted. When only an FC was used, another 5 kW was deducted as no lubricating oil pumps and separators are needed.

The installed bow thruster requires 288 kW. As the bow thruster is only used during a short period, this bow thruster was not used for the efficiency calculations but only for the configuration layout.

In the harbor, the electrical load is around 25 kW for an MDO setup and around 45 kW during loading/unloading operations. For the efficiency calculations, we used a constant load of 35 kW. When an FC is installed, based on the lack of information in this stage, a worst case assumption has been made and the same 25 kW is added to this load.

Dual fuel technology

Many proposed designs use dual fuel hydrogen internal combustion engine. Conventional diesel engines all rely on the diesel principle, igniting the fuel by the heat generated during compression. Engines using the Otto principle do not rely on compression heat, but use a spark plug to ignite the fuel. This requires a fuel with a low flashpoint, so diesel is not suitable for the Otto process.

Gas engines can work with the Otto principle. Mostly the gas is injected in the intake manifold, just before the intake valves, the so-called port fuel injection (PFI). This can be continuous or timed, although the continuous system produces undesirable combustion problems and is less flexible and controllable. [47] This principle of spark-ignition gas or spark gas (SG) is mostly used with a pre chamber. This pre chamber is filled with a sperate gas supply, leading to a rich blend with an air/fuel ratio (lambda) between 1.1 and 1.3 that can be easily ignited with a spark plug. The mixture in the cylinder has a higher lambda of about 1.5 to 2.2. [30]

To allow a spark plug free design, manufacturers use a dual fuel (DF) technology. Air is first compressed in the cylinder and the gas with a pressure of 200–300 bar is directly injected in the cylinder, immediately followed by a small amount of liquid fuel. In this case, the liquid fuel ignites first, providing the energy for the ignition of the air-gas mixture.

Another widely adopted DF technology is injecting the gas in the intake manifold, just before the intake valve, with a relatively low pressure of 5–10 bar. After being compressed during the compression stroke, a small amount of liquid fuel is injected at a high pressure (1000–2000 bar) just before the top position. The temperature ignites this liquid fuel that in turn ignites the air-gas mixture. [30]. The advantage of this system, compared with the direct injection described above, is the higher mixture homogeneity. This results in higher engine efficiencies, extended lean operation, lower cyclic variation and lower NO_x production. [47].

Several manufacturers are working on dual fuel hydrogen engines. Conoship has contacts with the company ABC engines, which developed a fully operational prototype of a 1 MW DF hydrogen engine for maritime applications. This dual fuel engine can operate on up to 80% hydrogen (mass based) or 100% diesel oil, resulting in a fully redundant setup. A spark ignition 100% hydrogen engine is planned for the (near) future. ABC’s engine has a diesel oil injector and gas admission valve per cylinder that admits the hydrogen in the intake air.

Designs 1a (reference case) , 1b: Conventional propulsion setup

In design 1a, an internal combustion engine running on MDO drives a controllable pitch propellor via a gearbox, as drawn in Figure 1. The gearbox is needed to lower the speed of the diesel engine to an optimal propellor speed. Although the gearbox reduces the efficiency, it would be less efficient to have the propellor rotating at a higher speed. The weak point of a diesel engine is its ability to deliver sufficient torque at low speeds. At low speeds, the turbo charger is not in its optimal working range. As the diesel engine has only limited combustion air supply, it is not possible to admit unlimited fuel. To overcome problems when manoeuvring the vessel, a controllable pitch propellor (CPP) is used. This allows the engine to run at a higher speed while the thrust of the propellor is changed by adjusting the propellor blade angle. This enables stepless changes between forward thrust and backward thrust. The disadvantage of a controllable pitch propellor is that the hydrodynamic design cannot be optimized due to the large propellor hub and that the blades do not have a fixed angle.

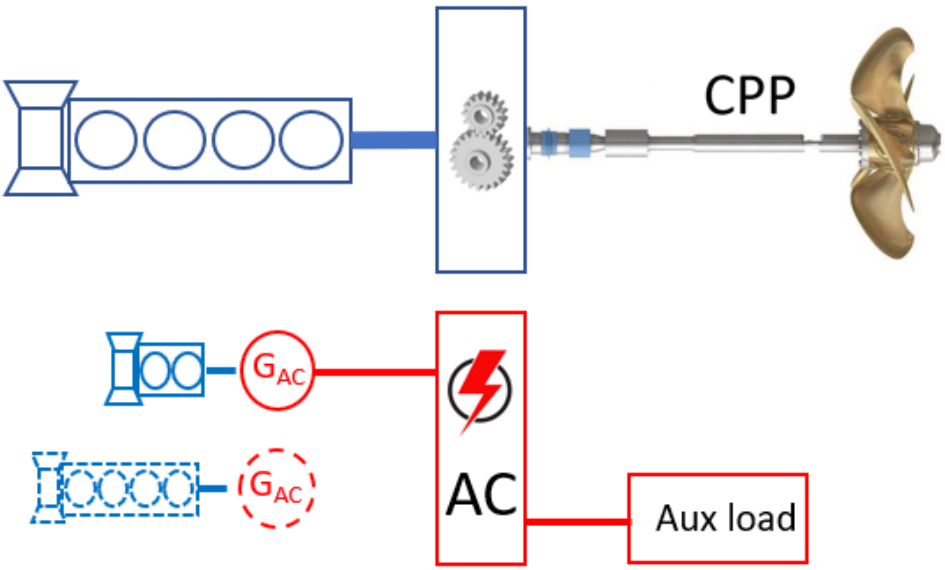

Figure 2: Designs 1a, 1b: Conventional propulsion setup

Two diesel generators provide electrical power to an alternating current (AC) switchboard. During sailing, a small generator of 100 kWe is running in part load. This is sufficient to power the vessel systems of around 60 kW. During manoeuvring, the bow thruster of around 220 kW is used. A second generator of 300 kWe, drawn with a dashed line in Figure 2, is installed to power the bow thruster, and if necessary, the vessel auxiliaries. This design is used in two versions. Design 1a is the reference case with an internal combustion engine running on MDO.

Version 1b has the same design, but powered by a duel fuel hydrogen engine. This engine uses diesel oil as a pilot fuel to ignite hydrogen. It can run on 100% diesel oil or a mixture of diesel oil and hydrogen. Running on 100% hydrogen is not possible. Chapter 7.2 provides more detailed information about the dual fuel hydrogen technology.

The auxiliary load is for design 1a is 55 kW when sailing and 30 kW in port. For design 1b the auxiliary load is 60 kW when sailing and 35 kW in port.

Design 2: Conventional propulsion with constant rpm shaft generator

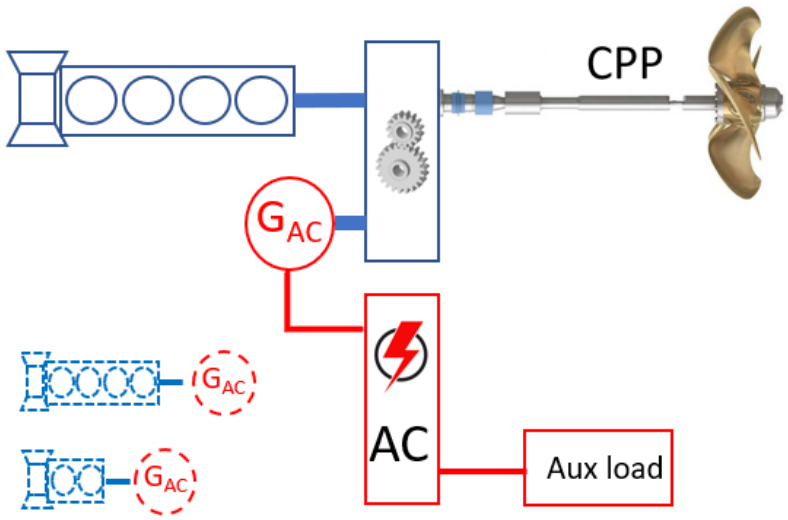

Figure 3: Design 2: Conventional propulsion setup with constant rpm shaft generator

This setup differs from the previous regarding the power supply of the hotel load and auxiliaries, as drawn in Figure 3. When sailing at higher loads, the engine has sufficient and constant revolutions to drive the shaft generator connected to the gear box of the main engine. In this situation the shaft generator is feeding the auxiliaries. The propulsion power at fixed rpm is controlled with the CPP. The shaft-generator has to be big enough to power the auxiliary load with some reserve. Therefore, a 100 kWe shaft generator is used.

When the vessel sails at a low speed the shaft generator is switched off and the auxiliary engine has to power the hotel load, auxiliaries and the bow thruster. Therefore, this generator set is sized at 300 kWe. During port operations, a smaller 100 kWe diesel generator feeds the vessels power supply. This design is only considered with a dual fuel engine.

Design 3: Conventional propulsion with variable rpm shaft generator

This configuration is almost the same as the previous design, except for the technology of the shaft generator. By using power electronics, the AC/DC/AC block in Figure 4, the shaft generator can be used over almost the full rpm range of the main engine. During manoeuvring, the bow thruster is driven by this shaft generator as well, explaining the sizing of this generator (300–400 kWe). The auxiliary generator is the same as in the previous examples (100 kWe). The drawback is that the main engine must have a certain minimum speed during manoeuvring to have enough torque available to drive both the propellor and the bow thruster via the generator. This will lead to a decrease in efficiency. The time that the vessel is running in this condition is limited, so for now this is not taken into account.

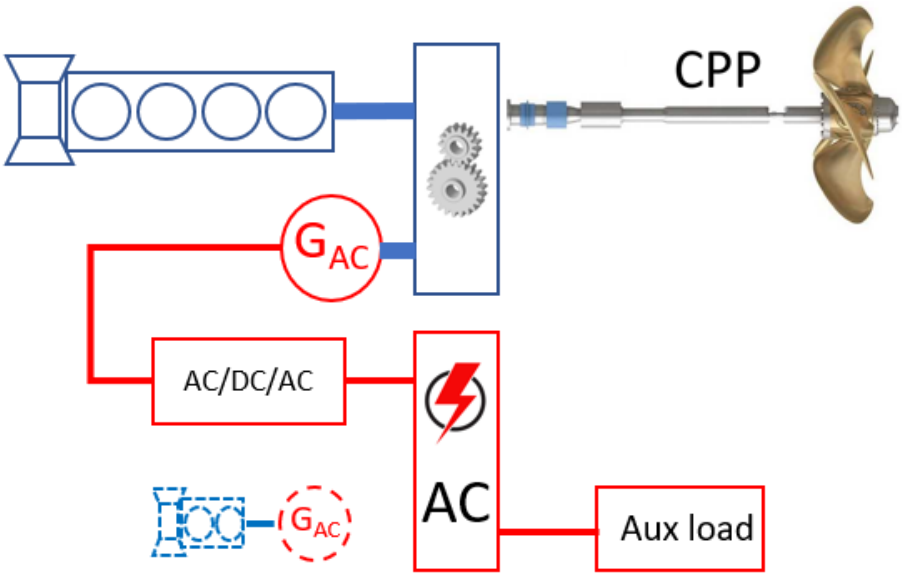

Figure 4: Design 3: Dual fuel, CPP with variable rpm generator and conventional diesel generator

Design 4: Dual fuel electric with an AC network

In this configuration, a constant rpm dual fuel combustion engine drives an AC generator at a fixed speed. The propellor shaft is driven by two electric motors, as class requires redundancy. Each motor can drive half the propellor load (around 375 kW). Typically, this size of electric motor delivers maximum power at around 1500 or 1800 rpm, far too high to directly drive the propellor. Therefore, a gearbox is installed to lower the speed to around 170 rpm for the propellor. Another option would be to install a synchronous motor, which are capable of lower speeds. The downside is that these motors are larger and more expensive. Also, the combination of a low speed and a low power is not common for these types of motors. To avoid harmonic distortion in the electrical system, a transformer is used to supply the converter with a 12 pulse supply source. More information on this topic can be found in Appendix A-1. Some vessels use a dedicated propulsion system separated from the auxiliary, but that requires a second generator constantly running. As an electric motor has a large torque available at low, nearly zero speed, a fixed pitch propellor (FPP) can be used. The advantage of such a propellor is that the hub is smaller and the blade shape can be optimized to maximize efficiency. In port, a 100 kWe AC generator is used.

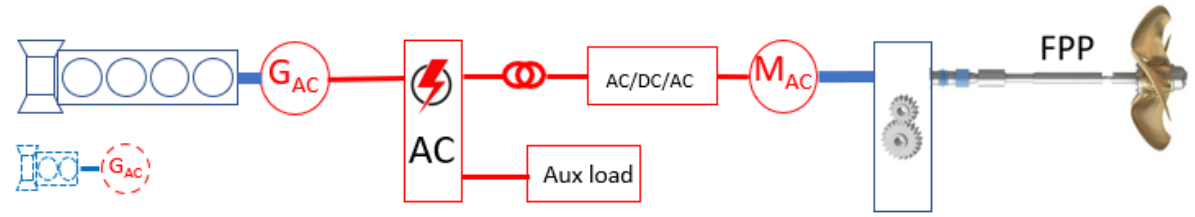

Figure 5: Design 4: Dual fuel electric with an AC network. For clarity only one electric motor and frequency converter is drawn but for class requirements two motors and drives have to be installed.

Design 5: Dual fuel electric with a DC network

This setup is the same as in the previous design, except that a DC network is used. This implies that the dual fuel engine can run at a variable rpm, making it possible to optimize its efficiency. Additionally, the transformers are not necessary anymore. In this configuration, two electric motors are used to drive the propellor shaft and a fixed pitch propellor is used. The diesel generator set for port use is for now a standard 100 kWe AC generator. This implies that in port, the auxiliary load is directly supplied with an AC power source. A DC generator could also be used for this purpose.

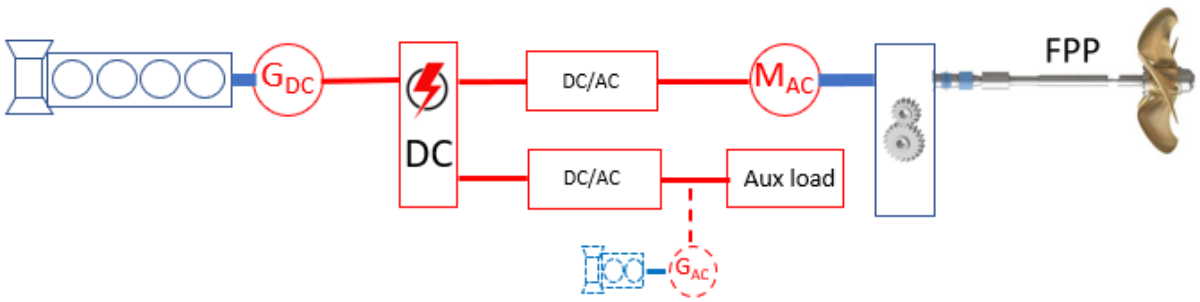

Figure 6: Design 5: Dual fuel engine with a DC network

Designs 6a and 6b: Dual fuel ICE, fuel cell assisted

This configuration uses a fuel cell to power the auxiliary load. The setup is drawn in Figure 7. Two options were considered. In the first option, the FC is 500 kWe, large enough to power the auxiliary load and the bow thruster during manoeuvring. This design does not need the 100 kW and 300 kW generator set, compared to the reference design. The ICE is around 500 kW. The FC consist of several strings, as described in Chapter 7.4. Each string is sufficient to power the aux load, so 5 out of 6 strings can be shut down in port to save on running hours. To simplify the possible combinations for this first calculation, a fuel cell was used of only two strings of 250 kW each, each connected to a 250 kW DC/DC converter.

In the second setup, the FC is sized 250 kWe and the ICE is 750 kWe. This is not sufficient to power the bow thruster and the auxiliary load. This can be solved using an electric motor, which can also function as a generator. In this way, the ICE can feed the electrical system. Another option is to use a separate generator set or diesel engine only for driving the bow thruster. For now, we used this last option. Contrary to the 500 kW FC option, the 250 kW FC has a diesel engine directly driving the bow thruster, so the 100 kW generator set was deducted from the reference design.

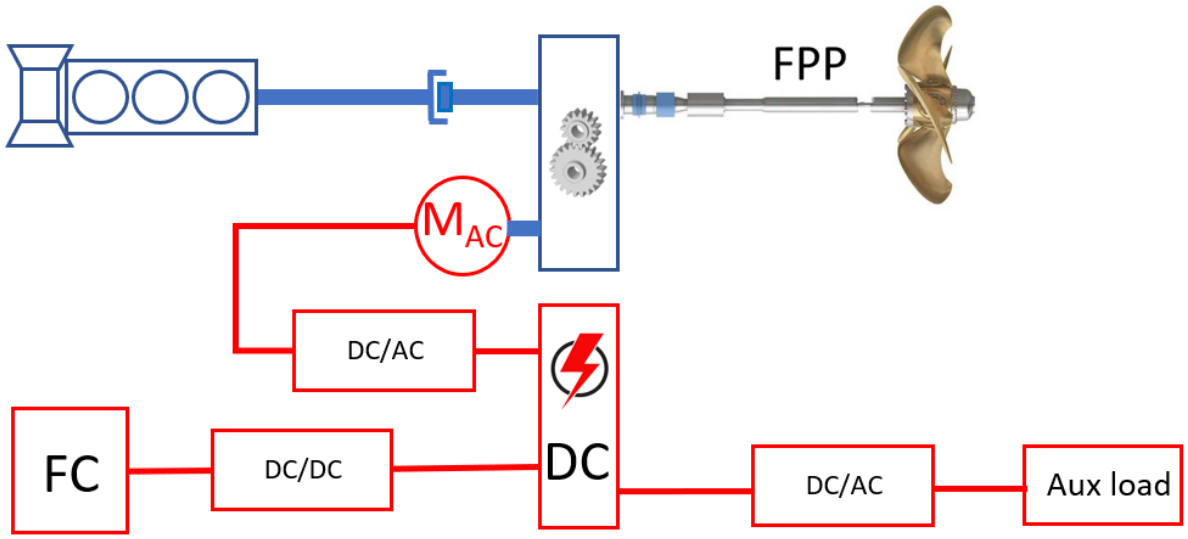

Figure 7: Designs 6a, 6b: dual fuel internal combustion engine, fuel cell assisted

At low speeds, the fuel cell drives the propellor shaft. In that case, the internal combustion engine is disengaged from the gearbox with a clutch.

Designs 7a and 7b: Dual fuel ICE with an AC network, fuel cell assisted

This configuration is basically the same as in the previous paragraph, except the propellor shaft is now electrically driven by two electric motors. Two electric motors were used due to class requirements, as described before. The dual fuel engine is now driving a constant speed AC generator. The design setup is drawn in Figure 8.

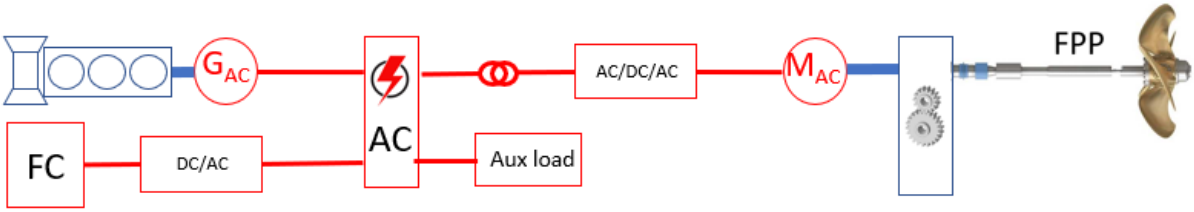

Figure 8: Designs 7a, 7b: Dual fuel internal combustion engine with an AC network, fuel cell assisted. For clarity only one of the two electric motors is drawn.

This setup was also calculated for a 500 kWe dual fuel motor combined with a 500 kWe fuel cell, as well as for a combination of a 750 kWe motor and a 250 kWe fuel cell. In port, the fuel cell is powering the vessel and at low speeds the fuel cell is electrically driving the propellor shaft. At higher loads, the dual fuel engine is started and the propellor is driven by both engine and the fuel cell.

The bow thruster can be operated with the 500 kW fuel cell. In the 250 kW fuel cell design, the bow thruster has a dedicated standalone diesel generator directly driving the bow thruster.

Designs 8a and 8b: Dual fuel ICE with a DC network, fuel cell assisted

This configuration is identical to designs 7a and 7b, except that it uses a DC network, allowing the internal combustion engine to run at a variable speed. Additionally, the transformer was removed, as it was not necessary in this setup as drawn in Figure 9.

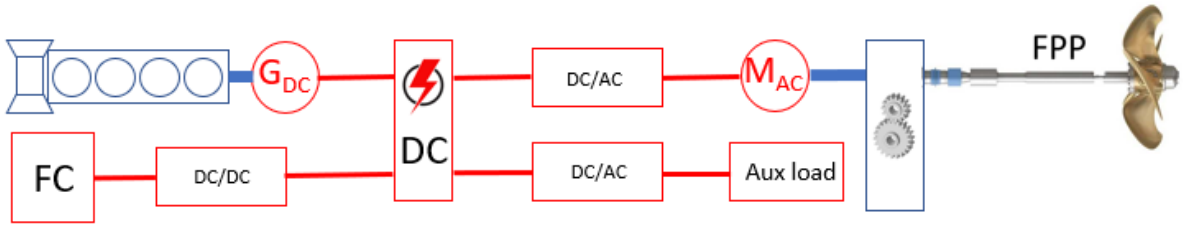

Figure 9: Designs 8a, 8b: DF ICE diesel electric with DC network, FC assisted

This configuration was calculated in a setup with an equal sized internal combustion motor and fuel cell of 500 kWe and with a 750 kWe combustion engine and a 250 kWe fuel cell. The design with a 250 kW fuel cell has a dedicated diesel generator for driving the bow thruster.

Design 9: Fuel cell only configuration

The last setup for this report is an FC only configuration, drawn in Figure 10. In this thesis, the fuel cell was treated as one big 1 MW fuel cell. In reality, this setup would consist of 24 fuel cell strings. This 1 MW is sufficient to have 750 kW available for the propellor and to provide the auxiliaries, even in case of a problem with one fuel cell string.

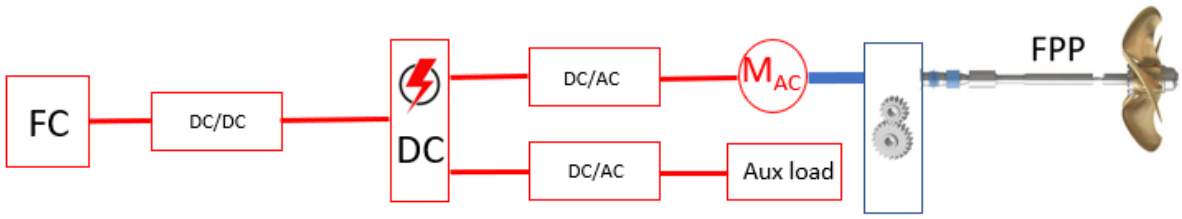

Figure 10: Design 9: Fuel cell only configuration

Depending on the design choices based on costs, redundancy and efficiency, these strings are divided across several DC/DC converters. In this thesis, we treated the system as 4 fuel cells strings each of 250 kWe. Depending on the load, one or more fuel cells strings are online. The reason for this is that the auxiliary power needed depends on the amount of online fuel cells. For a single 250 kWe fuel cell, this is around 25 kW. As more fuel cells are brought online, the relatively required power decreases, as some auxiliaries, such as ventilation, are shared. In this example, we used propellor load 1 FC at 25%, 2 FC at 50%, 3 FC at 75% and 4 FC at 100% propellor load. The amount of fuel cell strings online also affects the running hours of these strings.

Conclusions

In this chapter, nine setups were described and illustrated with a high level diagram. These setups will the basis for the determination the overall system efficiencies.

3 Efficiencies

3.1 Introduction

To gain insight into the total efficiency, the complete propulsion packages described in the previous chapter are analyzed. All main components that induce a loss were examined. Minor losses that can only be calculated when all details are known, such as losses in electrical cables or in propellor shaft bearings, were not included. These losses are used to calculate the fuel consumption of the designs.

An example of such a calculation is illustrated in Figure 11. This figure shows a controllable pitch propellor driven by a dual fuel internal combustion engine. When the lever on the bridge is set on to a certain speed, the engine will follow this speed setpoint command. As the vessel increases speed, the propellor shaft power will follow the propellor curve that has a third order relationship with the propellor speed. When the load on the propellor shaft increases, the losses in the gearbox also rise. These losses are the topic of this chapter. The engine has to deliver more power to compensate. The fuel consumption and the ratio between hydrogen and pilot diesel is a function of the power and engine speed and is obtained from contour plots from the manufacturer. The urea consumption, used to neutralize the NOx emitted by the engine, is related to the diesel oil consumption, as explained in Attachment B-5.

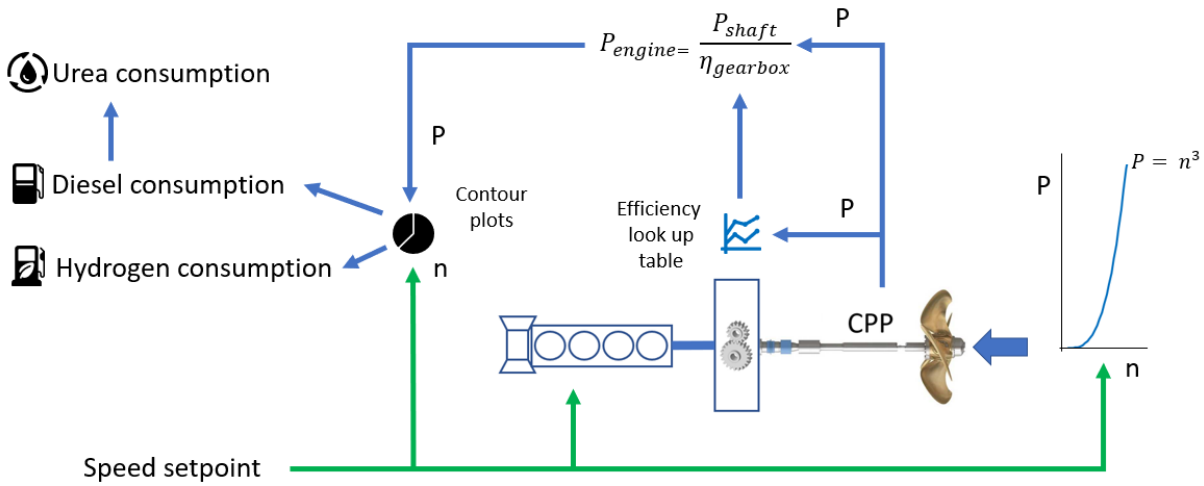

Figure 11: Example of fuel use calculation for a dual fuel engine

The same principle is applied to the electrical installation and combinations of electrical and mechanical designs. Figure 12 shows a dual fuel engine driving a fixed pitch propellor by means of an electrical AC power distribution. As explained later, the shaft power for a fixed pitch propellor is reduced by 5%. Then the efficiencies of the gearbox, electric motor, frequency converter, transformer and generator are needed to calculate the power the engine

must deliver to drive the propellor. For a mechanical contribution or efficiency, the items are blue, for an electrical contribution or efficiency, the items are red.

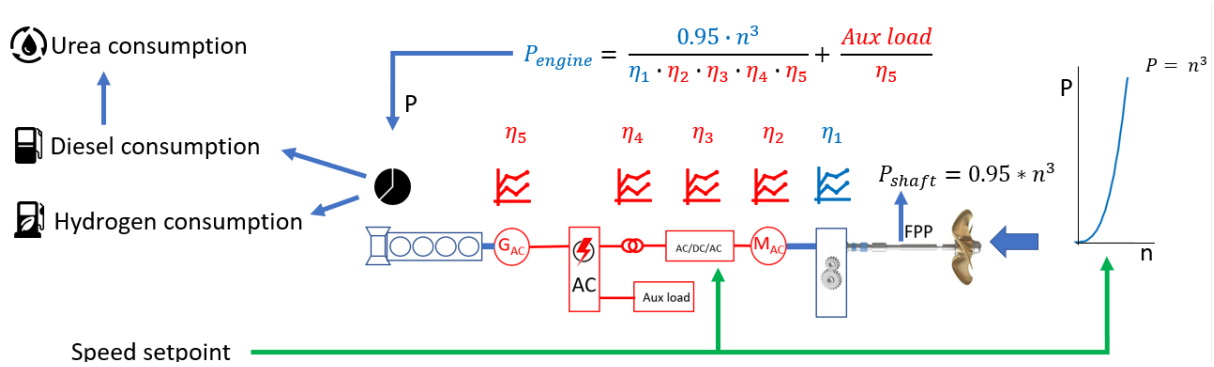

Figure 12: Example of fuel use calculation for a duel fuel engine in an electrical setup

As the engine is running in a constant speed mode, the speed is not an input and the contour plots are a line.

In section 3.2 and 3.3, the efficiencies of the components are described. This section summarizes the relevant information from the attachments. The biggest challenge is to obtain information about part load efficiencies. Manufacturers tend to give the highest achievable efficiency. When running in various operating points, this efficiency is not realistic. This is mostly due to constant losses, such as ventilation and the power supply to electronics. This is more or less the same for all operating points. Therefore, these losses are relatively high in low load conditions. For all components, the efficiencies are found for at least 4 points: 25%, 50%, 75% and 100% load. With these results, in between values can be interpolated with sufficient accuracy. Some components have graphs available for part load conditions.

3.2 Electrical components

For the electrical items, literature research was performed manufacturers were contacted. Appendix A-1 and A-2 describe AC and DC equipment respectively. The values mentioned in this section are explained in these attachments.

For an AC generator, the values of Figure 39 to Figure 42 in Appendix A-1 were used. DC generators were treated the same as AC generators, except that the efficiency is corrected with the 99,5% efficiency of the rectifier.

For the electric motor, the Nidec FLSHRM 355LTC Permanent magnet motor was chosen. It has the highest efficiency, especially in combination with a variable frequency drive (VFD). Due to the absence of current in the rotor, only stator losses are present. It is important to mention the maintainability of this motor. Due to the large magnetic forces, it could be challenging to exchange the bearings in a small space, such as on board a vessel. Additionally, this motor is only available with a relatively high rpm of 3600. This is not suitable for a standard marine gearbox. As the developments for these types of motors is still ongoing, it is assumed that a lower rpm motor will become available. In the meantime, this type of motor can still be used with a custom gearbox.

For the drive, a Nidec 400 kW drive is used. The drive efficiency is not linear with the load. According to Nidec, the efficiency is 98% [36]. Normally, they use this as a fixed value, but

as explained in Attachment A-1, this is not representative for our application. Based on the manufacturer documentation, the table below was created.

	Power (propellor)			
	25%	50%	75%	100%
Drive 400 kW efficiency [%]	96,58	97,82	98,25	98,55
Nidec 408 kW/3600rpm PM AC motor efficiency [%]	94,1	96,1	96,6	96,9
Total efficiency [%]	90,88	94,01	94,91	95,49

Table 1: Drive/motor efficiencies

In this thesis, transformers were only used in an AC diesel electric power train as a measure to limit harmonic distortion. In this setup, the 3 phase AC voltage waves are converted into 2 times three phase AC voltage with a phase shift. Doing so opens the way to use a 12 pulse AC drive, lowering the total harmonic distortion (THD). This setup requires two 400 kVA transformers. As no data for such a transformer was found, the values of a 500 kVA transformer were used, as plotted in Figure 43 in Appendix A-1. As described in Attachment A-1, the efficiencies were corrected for the additional harmonic losses.

	Transformer load			
	25%	50%	75%	100%
Transformer (500 kVA) efficiency [%]	98,7	99	98,8	98,6
Additional harmonic losses [%]	0,02	0,08	0,19	0,33
Total transformer efficiency [%]	98,68	98,92	98,61	98,27

Table 2: Transformer efficiencies (500 kVA)

In some setups, an Aradex VP5000 DC-DC converter were used with the following efficiencies [13]:

	Power			
	25%	50%	75%	100%
DC-DC converter efficiency [%]	99,1	99,1	98,9	98,8

Table 3: Efficiency of a 200 kW DC-DC converter (Aradex VP5000)

For the fuel cell, information from a fuel cell supplier is used [35] to determine the hydrogen consumption. The losses in switchboards and cables were neglected, as their contribution on small vessels will be minimal if the installation is well engineered.

3.3 Mechanical components

The efficiencies of mechanical components, including generator sets and the dual fuel engine, are described in Attachment B. As explained in Attachment B-1, the following efficiencies were used for the gearbox:

	Power			
	25%	50%	75%	100%
Gearbox 1PTI efficiency [%]	94	97	98	98,5
Gearbox 2PTI efficiency [%]	92	96	97,3	98

Table 4: Gearbox efficiencies at different loading points

The fuel and urea consumption was determined with the graphs shown in Attachments B-4 and B-5. The formulas of the fourth order polynomials of these graphs were used in the Excel tables to calculate the fuel and urea consumption based on the delivered power of the engine.

For the auxiliary generator sets, the values of Figure 53 (efficiencies of Caterpillar generator sets) were used to determine the (part load) efficiencies.

3.4 Conclusion

In this chapter, the method of efficiency and fuel consumption calculation was explained. More information on component efficiencies is given in Attachments A and B. Using this information, the fuel consumption is calculated in Chapter 4 based on the use case.

4 Fuel consumption

4.1 Introduction

By integrating the previously described use case, installation designs and efficiencies of the components, the fuel consumption, an important contributor to the total costs, can be calculated. For the calculation the use case scenario is applied.

The power needed to propel the vessel follows the propellor law:

$$P \sim n^3 \qquad 1$$

In theory, the speed of the vessel is linearly related to the propellor's revolutions. In reality, many factors influence the relationship between speed, propellor revolutions and power. Over the years, the vessel will be affected by marine growth on the hull and propellor and the propellor might lose efficiency due to wear and tear. Additionally, the vessel will experience resistance from waves and weather. As there are no restrictions regarding the vessel speed in our use case, however, these influences are not part of this report. In our case, the maximum power on the propellor shaft is limited to 750 kW due to legislation on the minimum safe manning.

Based on the flow shown in Figure 12, the engine or fuel cell load is calculated based on the propellor load. The engine or fuel cell load was then used to calculate the fuel consumption. To explain the way of calculation, one of the more complicated designs (8a) was used as an example.

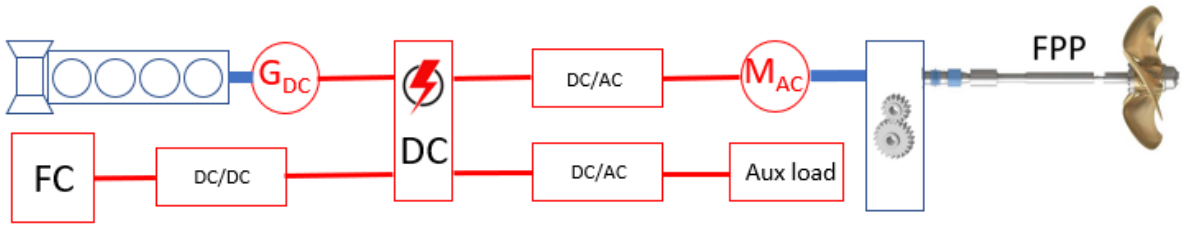

Figure 13: Design 8a: Dual fuel internal combustion engine with a DC network, fuel cell assisted (example)

This design uses both a dual fuel generator set and a fuel cell to provide electrical energy to the installation. The division of the power between these two energy sources is regulated by the power management system. At low power, the propellor can be run only on the fuel cell to minimize the diesel consumption and thus the CO_2 emissions. How long the fuel cell can operate alone depends on its size. This setup involves one mechanical efficiency (gearbox) and 4 electrical efficiencies (AC/DC/AC converter, transformer, generator and DC/AC converter). These efficiencies, together with the power division by the power management system, dictates the load of the generator set and the fuel cell.

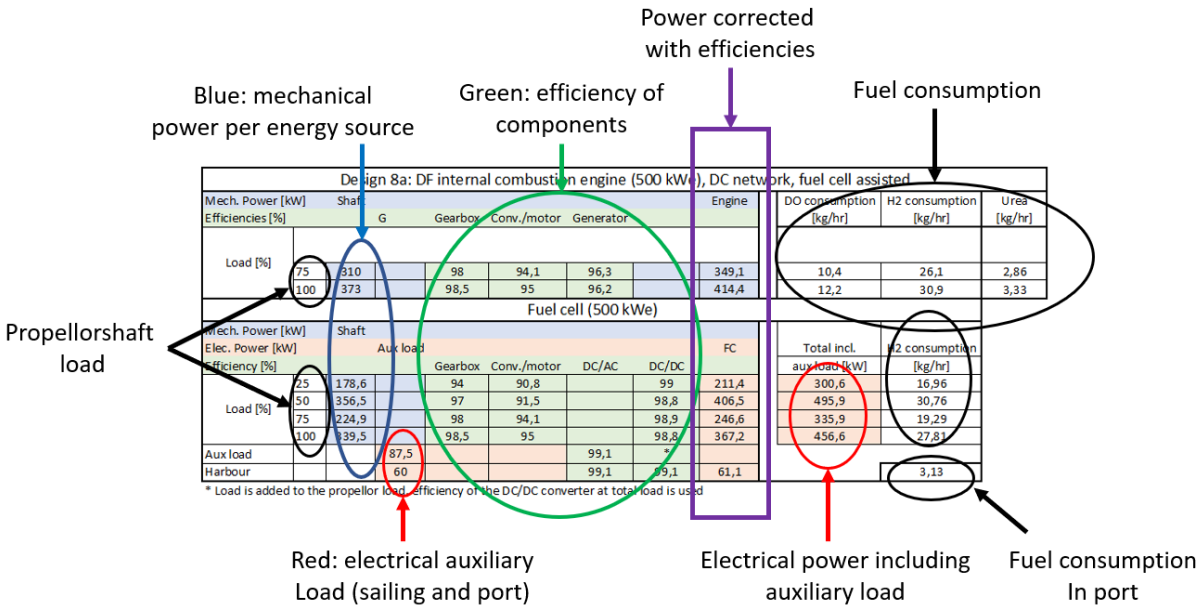

Figure 14: Fuel consumption table for design 8a (example)

Figure 14 represents the fuel consumption table of design 8a. In this example, a 500 kW dual fuel engine is combined with a 500 kW fuel cell. The engine is the upper part of the table, the fuel cell the lower. On the left the propellor shaft, loads are given. At 25% load, 188 kW is expected. The fuel cell is large enough so the combustion engine is not running at this load. This explains the white lines at the combustion engine. The 25% propellor shaft load row in the fuel cell shows a load of 178,6 kW. This is because this configuration uses a fixed pitch propellor. This improves efficiency by at least 5%, so the same propellor function is obtained with 5% less shaft power. This is the difference between 188 and 178,6 kW. Staying on the same line, going to the right, the efficiencies for the gearbox (94%), converter and motor (90,8%) and DC/DC converter (99,1%) are listed. This results in a load of 211,2 kW for the fuel cell. The auxiliary load is corrected with the DC/AC converter (99,1%) and DC/DC converter (99,1%) efficiencies. The resulting 89,1 kW is added to the 211,2 kW, giving a total of 300,2 kW for the fuel cell. The fuel cell is built of two 250 kW strings so 2 strings are needed. This results in a loading of 60% for each fuel cell string. With the fitted polynomials from Attachment I, the efficiency and the hydrogen consumption were calculated for this operating point.

The same was done for the other operating points. At a propellor load of 75%, the fuel cell does not have enough power to feed the propulsion and the auxiliary load on its own. The dual fuel internal combustion must therefore contribute to the propulsion of the vessel. The power delivered by the combustion engine is chosen such that both the efficiency and the hydrogen/diesel oil ratio are as high as possible.

The aforementioned setup has limitations but is intended to be a reasonable representation of the fuel consumption. For a more accurate representation for each model, an extensive simulation must be set up, including the following factors:

- A complete sailing profile, including all in between load points with their time.
- A power management system that continuously determines the number of active fuel cell strings and the load division between fuel cell and dual fuel motor.
- Polynomials for all efficiencies.

The biggest challenge is the settings for the power management system. Switching off a fuel cell string will save running hours, but decrease the efficiency of the operating fuel cells. Decreasing the load of the fuel cells will increase their efficiency, but will increase the CO_2 emissions of the diesel engine. These conflicts are all subject to many variables that can only be determined through many iterations. For now, the methods presented in Section 4.2 are sufficient to find reasonable figures to support decision making.

4.2 Fuel consumption calculations

Designs 1a (reference case) and 1b: Conventional propulsion setup

Design 1a and 1b have a conventional setup with a controllable pitch propellor driven by an internal combustion engine, with a gearbox in between. Tables 5 and 6 therefore only include the efficiency of the gearbox. Design 1a is the reference case and is a diesel oil only vessel. The fuel consumption was obtained by applying the specific fuel consumption. This is slightly different from the following examples, as this engine only runs on diesel oil.

Design 1b is the same except it uses a duel fuel engine. The auxiliary engine still runs only on diesel oil as small marine dual fuel engines are not yet available. The other difference is the auxiliary load, which is slightly higher compared to design 1a due to the additional ventilation.

Design 1a: Internal combustion engine running on DO								
Mech. Power [kW]		Shaft		Engine		sfc engine	DO consumption	Urea
Efficiencies [%]			Gearbox			[g/kWh]	[l/hr] [kg/hr]	[kg/hr]
Load [%]	25	188	94	200,0		210	49,0 42,0	5,31
	50	375	97	386,6		205,7	92,8 79,5	7,75
	75	563	98	574,5		201	134,7 115,5	9,69
	100	750	98,5	761,4		206,1	183,1 156,9	11,09
Auxiliary engine running on DO (100 kWe nominal)								
Elec. Power [kW]		Aux load					DO consumption	Urea
Efficiency [%]			Generatorset				[kg/hr]	[kg/hr]
Normal		55	33,1				14,0	0,84
Harbour		30	31,6				8,0	0,48

Table 5: Fuel calculation for design 1a (reference case): Conventional propulsion setup with an internal combustion engine running on diesel oil

Design 1b: DF internal combustion engine running on DO and hydrogen								
Mech. Power [kW]		Shaft		Engine		DO consumption [kg/hr]	H2 consumption [kg/hr]	Urea [kg/hr]
Efficiencies [%]			Gearbox					
Load [%]	25	188	94	200,0		16,7	10,6	6,57
	50	375	97	386,6		27,0	18,8	7,31
	75	563	98	574,5		25,4	34,8	7,84
	100	750	98,5	761,4		20,7	53,2	8,15
Auxiliary engine running on DO (100 kWe nominal)								
Elec. Power [kW]		Aux load					DO consumption [kg/hr]	Urea [kg/hr]
Efficiency [%]			Generatorset					
Normal		60	33,4				15,1	0,91
Harbour		35	32				9,2	0,55

Table 6: Fuel calculation for design 1b: Conventional propulsion setup with a dual fuel internal combustion engine running on hydrogen and diesel oil

Design 2: Conventional propulsion with constant rpm shaft generator

Table 7 contains the results of this configuration. In contrast to the previous tables, the upper part with the data of the ICE now also contains red fields. At higher loads (and therefore higher shaft speeds), the shaft generator is used to feed the auxiliary load. During lower loads, the auxiliary engine feeds these auxiliaries. The efficiency of the shaft generator is given in Figure 42 in Appendix A-1, using a power factor of 0,8. As the installed shaft generator is slightly smaller than the generator used to draw the figure, the efficiency is slightly better than seen in the figure.

When the shaft generator is used, two efficiencies are involved: of the generator and the gearbox. Table 7 shows that at 75% load, the main engine has to deliver 563 [kW] to drive the propellor and 60 [kW] for the auxiliary load.

Design 2: DF internal combustion engine running on DO and hydrogen, 100 kWe shaft generator									
Mech. Power [kW]		Shaft				Engine		DO consumption [kg/hr]	H2 consumption [kg/hr]	Urea [kg/hr]
Elec. Power [kW]			Aux load							
Efficiencies [%]				Generator	Gearbox					
Load [%]	25	188			92	204,3		16,8	10,7	6,59
	50	375			96	390,6		27,7	18,8	7,33
	75	563			97,3	578,6		27,5	38,8	7,99
			60	91	97,3	67,8				
	100	750			98	765,3		26,7	54,8	8,21
			60	91	98	67,3				
Auxiliary engine (100 kWe nominal)										
Elec. Power [kW]			Aux load					DO consumption [kg/hr]	Urea [kg/hr]	
Efficiency [%]					Generatorset					
Normal			60		33,4			15,1	0,91	
Harbour			35		32			9,2	0,55	

Table 7: Fuel calculation for design 2: Dual fuel internal combustion engine with a constant rpm shaft generator

Design 3: Conventional propulsion with variable rpm shaft generator

The advantage of this setup is that it saves an additional generator set, as the shaft generator can be used to power the bow thruster. The downside is lower generator efficiency at low loads when the bow thruster is not in use. It is below the standard efficiency graph of the manufacturer (Figure 40 in Appendix A-1) and has to be extrapolated as 91%. A solution

could be to use a 300 kWe shaft generator and run it and the auxiliary generator in parallel when the bow thruster is used. However, stable parallel operation with big power swings is difficult due to the size difference of the dual fuel engine and the smaller diesel generator.

This setup introduces an additional loss: the power electronics in the AC/DC/AC converter. The efficiencies of the converter of the shaft generator are based on Table 27 and Figure 48 in Appendix A-1.

Design 3: DF internal combustion engine running on DO and hydrogen, 400 kWe shaft generator										
Mech. Power [kW]		Shaft					Engine			
Elec. Power [kW]			Aux load							
Efficiencies [%]				Converter	Generator	Gearbox				
Load [%]	25	188				92	204,3		31,7	13,1	6,91
			60	96	91	92	74,7				
	50	375				96	390,6		59,2	13,5	7,55
			60	96	91	96	71,5				
	75	563				97,3	578,6		27,6	39,0	7,99
			60	96	91	97,3	70,6				
	100	750				98	765,3		27,0	54,9	8,21
			60	96	91	98	70,1				
Auxiliary engine (100 kWe nominal)										
Elec. Power [kW]			Aux load						DO consumption [kg/hr]	Urea [kg/hr]	
Efficiency [%]						Generatorset					
Harbour			35			32			9,2	0,55	

Table 8: Fuel calculation for design 3: Dual fuel internal combustion engine with a variable rpm shaft generator

Design 4: Dual fuel electric with an AC network

This setup is the first to use a fixed pitch propellor, causing a different shaft power as explained before. The efficiencies of the total harmonic disturbance (THD) limiting transformers are taken from Table 2. The motors, converters and transformers must be redundant by class requirements. Therefore, the power must be divided by two to find the efficiencies.

For the generator, the graph of Figure 39 is used. A power factor of 0,8 was used at 25% load and a power factor of 0,9 for larger loads, as the DC link of the large AC/DC/AC converter causes a higher power factor. For port operations, a 100kWe generator was installed.

Design 4: DF electric with an AC network, 900 kWe generator											
Mech. Power [kW]		Shaft						Engine			
Elec. Power [kW]			Aux load								
Efficiencies [%]				Gearbox	Conv./motor	Transformer	Generator				
Load [%]	25	178,6		94	90,8	98,5	95,7	222,0		16,5	21,8	2,01
			60				95,7	62,7				
	50	356,3		97	91,5	98,7	96,7	420,6		15,1	37,1	1,84
			60				96,7	62,0				
	75	534,9		98	94,1	98,8	96,8	606,5		16,3	49,6	3,04
			60				96,8	62,0				
	100	712,5		98,5	95	98,2	96,7	801,8		30,2	55,3	5,72
			60				96,7	62,0				
Auxiliary engine (100 kWe nominal)											
Elec. Power [kW]			Aux load							DO consumption [kg/hr]	Urea [kg/hr]	
Efficiency [%]							Gen. set					
Harbour			35				32			9,2	0,55	

Table 9: Fuel calculation for design 4: Dual fuel electric with an AC network

Design 5: Dual fuel electric with a DC network

In this setup, the generator efficiency is slightly less than an AC generator due to the rectifier, but as this rectifier is not necessary in the DC/AC converters, this cancels out. The power factor of the DC (consisting of a three phase AC generator with a rectifier) is nearly 1.

As the combustion engine can operate with a variable speed, the speed can be chosen that provides optimal efficiency. However, an optimal efficiency does not mean that the local CO_2 emissions is the lowest possible. As described in Appendix B-4, a strategy combining both a reasonable efficiency and a hydrogen/diesel ratio as high as possible was chosen. As explained in Appendix B-5, the urea consumption was estimated using the mean value of the generator curve and the propellor curve.

Desgin 5: DF electric with a DC network, 900 kWe generator											
Mech. Power [kW]		Shaft						Engine			
Elec. Power [kW]			Aux load						DO consumption [kg/hr]	H2 consumption [kg/hr]	Urea [kg/hr]
Efficiencies [%]				Converter	Gearbox	Conv./motor	Generator				
Load [%]	25	178,6			94	90,8	96,1	217,7	16,3	16,0	4,47
			60	96,5			96,1	64,7			
	50	356,3			97	91,5	97	413,9	19,8	30,0	4,71
			60	97			97	63,8			
	75	534,9			98	94,1	97,2	596,7	19,7	46,1	5,49
			60	97,5			97,2	63,3			
	100	712,5			98,5	95	97,1	784,2	24,3	59,3	6,83
			60	98			97,1	63,1			
Auxiliary engine (100 kWe nominal)											
Elec. Power [kW]			Aux load						DO consumption [kg/hr]	Urea [kg/hr]	
Efficiency [%]							Gen. set				
Harbour			35				32		9,2	0,55	

Table 10: Fuel calculation for design 5: Dual fuel electric with a DC network

Designs 6a and 6b: Dual fuel ICE, fuel cell assisted

In this design, two dual fuel internal combustion engines were tested: one of 500 kW and one of 750 kW. No information is available yet about smaller size DF hydrogen engines. Table 31 in Appendix B-3 shows the efficiencies for several diesel generator sets, which allowed us to estimate the difference in efficiency between a 1 MW and a 500 kW engine. The efficiency and the hydrogen/diesel ratio were taken from the 1 MW DF engine chart. Then the efficiency was lowered by 2% for the 500 kWe and 1% for the 750 kWe version to compensate for the smaller engine size.

In design 6a the FC is used for propellor loads up to 50%, above that the combustion engine is used while the FC compensated for fluctuations. In design 6b, the FC only mode is used up to 25% propellor load. At low loads, when running on the fuel cell only, the 250 kWe cell fuel is loaded over its nominal power. The fuel cell is slightly oversized by its manufacturer, but the load is too high for the fuel cell. In reality, the engine would be switched on just before this overloading starts.

For the 500 kW fuel cell, both 250 kW strings are in operation all the time, except in port, where one is sufficient. The efficiency of both the fuel cell and the DC/DC converter are related to their load.

For the DC/AC converter and electric motor, the values of Table 1 were used. As a rectifier is unnecessary, the efficiencies increase by 0,5%. For the auxiliary load, a 150 kW DC/AC converter is installed. For this converter, the values of Table 1 were also used, but in this case, the efficiency was not increased by 0,5% to compensate for the values of the table being for a larger converter.

For the urea we use the same relationship as with the 1 MW engine. The load of the 500 kWe engine in the table is doubled, then the urea use is calculated with the polynomials for the 1 MW engine as before. This urea use is divided by two to scale back to the 500 kWe engine. The same procedure was performed for the 750kWe engine but with a different scale factor.

Design 6a: DF internal combustion engine (500 kWe), fuel cell assisted											
Mech. Power [kW]		Shaft						Engine		DO consumption [kg/hr]	H2 consumption [kg/hr]	Urea [kg/hr]
Efficiencies [%]							Gearbox					
Load [%]												
	75	310					98,5	314,7		14,2	20,0	3,98
	100	373					98,5	378,7		10,9	28,0	4,07
Fuel cell (500 kWe)												
Mech. Power [kW]		Shaft										
Elec. Power [kW]			Aux load					FC		Total incl.	H2 consumption	
Efficiency [%]				DC/AC	Gearbox	Conv./motor	DC/DC			aux load [kW]	[kg/hr]	
Load [%]	25	188			92	91,4	99	225,8		316,0	17,97	
	50	375			96	95,6	98,8	413,6		503,9	31,37	
	75	253			97,3	94,5	98,9	260,6		350,9	20,30	
	100	377			98	91,4	98,8	406,7		497,1	30,85	
Aux load			87,5	98			*					
Harbour			60	97,9			99,1	61,8			3,17	

* Load is added to the propellor load, efficiency of the DC/DC converter at total load is used

Table 11: Fuel calculation for design 6a: Dual fuel internal combustion engine (500 kW), fuel cell assisted

Design 6b: DF internal combustion engine (750 kWe), fuel cell assisted											
Mech. Power [kW]		Shaft						Engine		DO consumption [kg/hr]	H2 consumption [kg/hr]	Urea [kg/hr]
Efficiencies [%]							Gearbox					
Load [%]												
	50	275					98,5	279,2		19,1	19,8	5,46
	75	463					98,5	470,1		20,7	29,1	5,97
	100	650					98,5	659,9		17,6	45,3	6,19
Fuel cell (250 kWe)												
Mech. Power [kW]		Shaft										
Elec. Power [kW]			Aux load					FC		Total incl.	H2 consumption	
Efficiency [%]				DC/AC	Gearbox	Conv./motor	DC/DC			aux load [kW]	[kg/hr]	
Load [%]	25	188			92	91,4	98,8	226,3		303,8	19,81	
	50	100			96	95,6	98,9	94,5		171,9	9,91	
	75	100			97,3	94,5	99	84,0		161,3	9,20	
	100	100			98	91,4	99	79,8		157,1	8,92	
Aux load			75	98			*					
Harbour			60	97,9			99,1	61,8			3,17	

* Load is added to the propellor load, efficiency of the DC/DC converter at total load is used

Table 12: Fuel calculation for design 6b: Dual fuel internal combustion engine (750 kW), fuel cell assisted

Designs 7a and 7b: Dual fuel ICE with an AC network, fuel cell assisted

This design is an all electrical setup with an AC installation. This dictates that the dual fuel engine must run at a constant speed. The division of power, efficiency of combustion engines and the amount of fuel cells strings active from design 6a and 6b also apply to this design. Instead of a DC/DC converter, a DC/AC converter is used. There are no reliable efficiency figures available, but they will be in line with a DC/DC converter as similar components are used and the maximum efficiency is comparable.

As the propellor shaft is driven by electric motors, a fixed pitch propellor is used, giving an additional efficiency improvement of 5%. No clutch is needed behind the combustion engine, as there is no direct connection with the propellor shaft anymore. In design 7b, the fuel cell is overloaded at 25% propellor load. In reality, the combustion would be started just before this situation occurs.

Design 7a: DF internal combustion engine (500kWe), AC network, fuel cell assisted											
Mech. Power [kW]		Shaft						Engine		DO consumption	H2 consumption	Urea
Efficiencies [%]			G	Gearbox	Conv./motor	Transformer	Generator			[kg/hr]	[kg/hr]	[kg/hr]
Load [%]												
	75	310		98	94,1	98,8	96,3	353,3		9,4	27,1	1,73
	100	373		98,5	95	98,2	96,2	422,0		14,7	29,0	2,69
Fuel cell (500 kWe)												
Mech. Power [kW]		Shaft										
Elec. Power [kW]			Aux load					FC		Total incl.	H2 consumption	
Efficiency [%]				Gearbox	Conv./motor	Transformer	DC/AC			aux load [kW]	[kg/hr]	
Load [%]	25	178,6		94	90,8	98,5	99	214,6		303,0	17,11	
	50	356,5		97	91,5	98,7	98,8	411,9		500,5	31,11	
	75	224,9		98	94,1	98,8	98,9	249,6		338,1	19,44	
	100	339,5		98,5	95	98,2	98,8	373,9		462,5	28,25	
Aux load			87,5				*					
Harbour			60				99,1	60,5			3,09	

* Load is added to the propellor load, efficiency of the DC/DC converter at total load is used

Table 13: Fuel calculation for design 7a: Dual fuel internal combustion engine (500 kW) with an AC network, fuel cell assisted

Design 7b: DF internal combustion engine (750 kWe), AC network, fuel cell assisted											
Mech. Power [kW]		Shaft						Engine		DO consumption	H2 consumption	Urea
Efficiencies [%]			G	Gearbox	Conv./motor	Transformer	Generator			[kg/hr]	[kg/hr]	[kg/hr]
Load [%]												
	50	256,3		97	94,1	98,8	96,3	295,1		12,35	23,18	1,30
	75	434,9		98	94,1	98,8	96,3	495,7		12,40	38,00	2,22
	100	612,5		98,5	95	98,2	96,2	692,9		29,54	43,14	5,10
Fuel cell (250 kWe)												
Mech. Power [kW]		Shaft										
Elec. Power [kW]			Aux load					FC		Total incl.	H2 consumption	
Efficiency [%]				Gearbox	Conv./motor	Transformer	DC/AC			aux load [kW]	[kg/hr]	
Load [%]	25	178,6		94	90,8	98,5	98,8	215,0		290,9	18,76	
	50	100		98,5	91,5	98,7	98,9	113,7		189,5	11,12	
	75	100		98,5	94,1	98,8	98,9	110,4		186,2	10,89	
	100	100		98,5	95	98,2	98,9	110,0		185,9	10,87	
Aux load			75				*					
Harbour			60				99,1	60,5			3,09	

* Load is added to the propellor load, efficiency of the DC/DC converter at total load is used

Table 14: Fuel calculation for design 7b: Dual fuel internal combustion engine (750 kW) with an AC network, fuel cell assisted

Designs 8a and 8b: Dual fuel ICE with a DC network, fuel cell assisted

This design only differs from the previous one in the electrical system. Here, DC system is used, allowing the speed of the combustion engine to be varied. This optimizes the efficiency and hydrogen/diesel ratio. These designs do not use transformers.

Design 8a: DF internal combustion engine (500 kWe), DC network, fuel cell assisted											
Mech. Power [kW]		Shaft						Engine		DO consumption [kg/hr]	H2 consumption [kg/hr]	Urea [kg/hr]
Efficiencies [%]			G	Gearbox	Conv./motor	Generator						
Load [%]	75	310		98	94,1	96,3		349,1		10,4	26,1	2,86
	100	373		98,5	95	96,2		414,4		12,2	30,9	3,33
Fuel cell (500 kWe)												
Mech. Power [kW]		Shaft									
Elec. Power [kW]			Aux load					FC		Total incl.	H2 consumption
Efficiency [%]				Gearbox	Conv./motor	DC/AC	DC/DC			aux load [kW]	[kg/hr]
Load [%]	25	178,6		94	90,8		99	211,4		300,6	16,96
	50	356,5		97	91,5		98,8	406,5		495,9	30,76
	75	224,9		98	94,1		98,9	246,6		335,9	19,29
	100	339,5		98,5	95		98,8	367,2		456,6	27,81
Aux load			87,5			99,1	*				
Harbour			60			99,1	99,1	61,1			3,13

* Load is added to the propellor load, efficiency of the DC/DC converter at total load is used

Table 15: Fuel calculation for design 8a: Dual fuel internal combustion engine (500 kW) with a DC network, fuel cell assisted

Design 8b: DF internal combustion engine (750 kWe), DC network, fuel cell assisted											
Mech. Power [kW]		Shaft						Engine		DO consumption [kg/hr]	H2 consumption [kg/hr]	Urea [kg/hr]
Efficiencies [%]			G	Gearbox	Conv./motor	Generator						
Load [%]	50	256,3		97	94,1	96,3		291,6		14,4	17,8	3,40
	75	434,9		98	94,1	96,3		489,7		15,2	35,0	4,09
	100	612,5		98,5	95	96,2		680,4		23,3	46,9	5,53
Fuel cell (250 kWe)												
Mech. Power [kW]		Shaft									
Elec. Power [kW]			Aux load					FC		Total incl.	H2 consumption
Efficiency [%]				Gearbox	Conv./motor	DC/AC	DC/DC			aux load [kW]	[kg/hr]
Load [%]	25	178,6		94	90,8		98,8	211,8		288,4	18,55
	50	100		97	91,5		98,9	113,9		190,4	11,18
	75	100		98	94,1		98,9	109,6		186,2	10,89
	100	100		98,5	95		98,9	108,1		184,6	10,78
Aux load			75			99,1	*				
Harbour			60			99,1	99,1	61,1			3,13

* Load is added to the propellor load, efficiency of the DC/DC converter at total load is used

Table 16: Fuel calculation for design 8b: Dual fuel internal combustion engine (750 kW) with a DC network, fuel cell assisted

Design 9: Fuel cell only configuration

The last design uses fuel cells as the sole energy source. All strings are 250 kWe, allowing 1 string to be online in port and during sailing at 25%, load 2 strings at 50%, 3 strings at 75% and 4 strings at 100%. As in this case ventilation and cooling cannot be combined with the combustion engine, each additional string will cause the auxiliary load to increase. This is not fully linear, as at a certain point there will be a synergy between the auxiliaries.

Design 9: Fuel cell only (1MWe)										
Mech. Power [kW]		Shaft								
Elec. Power [kW]			Aux load					FC	Total incl.	H2 consumption
Efficiency [%]				Gearbox	Conv./motor	DC/AC	DC/DC		aux load [kW]	[kg/hr]
Load [%]	25	178,6		94	90,8	98,8	98,8	201,5	278,1	17,73
	50	356,5		97	91,5	98,8	98,8	399,1	488,6	30,20
	75	534,9		98	94,1	98,8	98,8	582,3	684,6	41,69
	100	712,5		98,5	95	98,9	98,9	766,8	879,2	53,12
Aux load 1 FC			75			99,1	*			
Aux load 2 FC			87,5			99	*			
Aux load 3 FC			100			99	*			
Aux load 4 FC			110			98,9	*			
Harbour			60			99,1	99,1	61,1		3,00

* Load is added to the propellor load, efficiency of the DC/DC converter at total load is used

Table 17: Fuel calculation for design 9: Fuel cell only

4.3 Conclusions

In this chapter, the fuel and urea consumptions for all designs were calculated. These are listed in Table 18. This allows calculation of the fuel costs and CO_2 emissions in the use case. This chapter showed that a gearbox and the combination of converter and electric motor have a relatively large impact on the efficiency. Currently, the gearbox is necessary in all setups, as no electric motors are available in the required power range that have a sufficiently low speed (around 170 rpm). Such a motor can be custom built, but this would make the vessel vulnerable to damage as no standard replacement would be available. This motor would also be larger, which could conflict with the space requirements.

Design		Fuel usage [Ton/year]		
		Hydrogen	DO	Urea
1a	Conventional Propulsion DO (reference design)	0	572	46,1
1b	Conventional Propulsion DF	147	213	40,1
2	Conv. Prop. Constant rpm shaft gen.	156	169	40,6
3	Conv. Prop. Variable rpm shaft gen.	155	177	39,3
4	Dual fuel electric with an AC network	202	117	15,9
5	Dual fuel electric with a DC network	160	168	26,3
6a	Dual fuel ICE (500 kW) fuel cell assisted	185	48	14,0
6b	Dual fuel ICE (750 kW) fuel cell assisted	177	80	23,4
7a	DF ICE (500 kW), AC network, FC assisted	203	35	6,5
7b	DF ICE (750 kW), AC network, FC assisted	210	56	9,6
8a	DF ICE (500 kW), DC network, FC assisted	200	37	10,2
8b	DF ICE (750 kW), DC network, FC assisted	201	63	16,4
9	Fuel cell only	185	0	0,0
DO: Diesel oil, DF: Dual fuel, ICE: Internal combustion engine, AC: Alternating current, DC: Direct current, FC: Fuel cell				

Table 18: Fuel usage per year

5 Financial framework

5.1 Introduction

In this chapter, the cost estimation is explained and illustrated in Figure 15. The main cost contributions are:

- Fuel costs
- OPEX (operational expenses)
- CAPEX (capital expenses)

Although the calculation for the fuel costs is straightforward, the big unknown factor is the changing fuel prices. In section 5.2 an approach towards a more uniform view point on these prices is given. Additionally, the definition of OPEX and CAPEX as used in this research are explained in section 5.3.

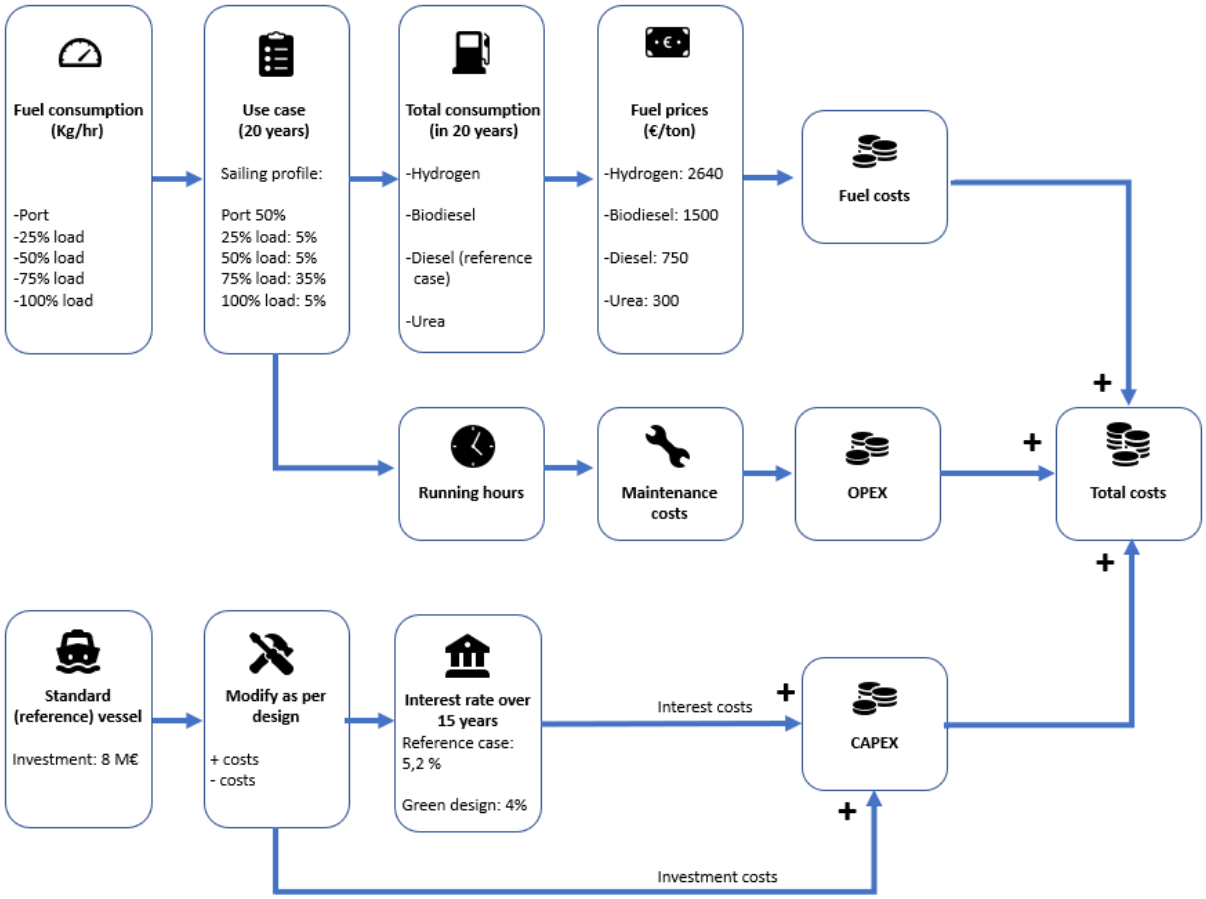

Figure 15: Flow sheet for cost calculation

5.2 Fuel costs

The most important parameters in the cost estimation are the fuel costs. As these costs change over time, it is difficult to estimate them over 20 years. Forecasts vary largely depending on the source. In general, most agree that green hydrogen will became cheaper as more green energy becomes available. It is not clear at what rate this will occur, however, as this also depends on the electricity infrastructure. Currently the price is around €5000/ton [61]. This is only economically feasible with a very high CO_2 penalty. This is further discussed in the sensitivity analysis of the hydrogen price in Section **Error! Reference source not found.**. Here the relationship between the hydrogen price and the CO_2 price per ton is given.

Blue hydrogen relies on the natural gas price. The price has recently varied between €1275/ton and €3000/ton. Forecasts suggest the cost levelling out at €1060–1700/ton [20]. For now, after a discussion within Conoship, a price of €2200/ton was used. To cover the costs of transportation and bunkering, a surcharge will be applicable. Currently it is not possible to obtain an exact number and also the surcharge will depend on the storage form chosen and location in the world. For now and estimate of 20% is used.

In September 2021, standard diesel oil was around €510/ton in Rotterdam, excluding bunker charges [49]. This will likely increase, based on the current oil price trend and because fossil fuel use is expected to decrease. After discussion with Conoship, a value of €750/ton was used for the calculation. A sensitivity plot is included for a MDO price between €250/ton and €1500/ton in Appendix H-1.

For biodiesel, HVO100 has the best potential, being nearly identical to fossil-fuel diesel but completely fossil-fuel free. Including delivery, this fuel is currently around €1500/ton [21][60]. An increase in the use of this fuel might lower the price. On the other hand, the raw materials for this fuel are not endless, so this might be a reason that the price rises. For now the price is treated as steady and a sensitivity plot is included in Appendix H-1.

Urea prices are currently (September 2021) around €300/ton [58]. As the urea use is only 4%-6% of the diesel oil use, as explained in Appendix D, no sensitivity analysis is made for this price.

5.3 Equipment costs

To calculate the economic feasibility of the options, the additional price of the installation compared to a standard diesel oil setup (design 1a) was determined.

All prices mentioned below are for the equipment itself. Installing and engineering is put in the tables as an additional field. Although the prices for the equipment are known, the additional engineering and installation are difficult to estimate, especially as there is a research and development component in the first projects.

The equipment prices were obtained through personal communication with Pon Power, Alewijnse, Nedstack, AMW-Marine, Berger Maritiem and Aradex.

Internal combustion engines

For the internal combustion engines, the prices for several Caterpillar generator skids have been separated in their main components. Table 19 is an overview of the prices for several Caterpillar generator sets. It is used for the price estimation of the different designs.

Internal combustion engines under 130 kW do not need to comply with IMO tier III regarding NOx reduction. However, as Conoship intends to build environmentally friendly vessels, these small engines are fitted with a selective catalytic reduction (SCR), as described in Attachment 0. The same SCR as fitted on the 150 kWe and 100 kWe engines can be used used on to the 250 kWe set. For the C18 generator set, two SCR modules are used. Above this size, a different setup is used, explaining the relatively low step between the C18 and C32 generator set.

	Power	Maintenance	Prices [k€]				
Type	[kWe]	[€/hr]	Total	Generator	Skid	Engine	SCR
C4.4	100	2	70	6	2	27	35
C7.1	150	2,75	95	10	3	47	35
C9.3	250	3,25	135	15	4	81	35
C18	500	4,5	220	20	6	124	70
C32	945	5,5	300	30	8	182	80

Table 19: Prices for different generator sets and components

Based on the current information, it is not clear what the additional costs for a dual fuel hydrogen engine are. However, Pon Power estimates that alternative fuels, such as hydrogen, will only require a small conversion. The conversion making an internal combustion engine suitable to run on hydrogen is not very costly. An additional 25% should be sufficient [45].

Fuel cells (including DC/DC converter)

For the fuel cells, the manufacturer provided the following information. The current price for a complete system, including the auxiliaries, is around 2500 €/kW for a several hundred kW system. This price will drop in the future when more systems are sold, but highly depends on the price of platina that is used as a catalyst in these fuel cells. The manufacturer is optimistic and speculate that a price drop towards 1250 €/kW in 20 years is likely. Future will tell if such a price drop occurs, but for the use case a conservative price drop of 1% a year for the first 5 years was presumed. After this, the price drop was set to 2% a year. This price drop only influences the stack refurbishment/replacement. The stack replacement costs are estimated at 20% of the investment costs. If a stack is refurbished after 8 years this will be less costly than a refurbishment after 4 years.

The interval between the stack replacements is 24000 hours, but the goal of the manufacturer is to stretch this to 40000 hours. Also the quality of the hydrogen also influences this lifetime. For this report, an interval of 30000 hours was used to calculate the costs. Compared to a diesel engine, the maintenance costs are relatively low due to the absence of moving parts. Therefore, these are considered to be covered in the stack replacement costs.

The installations from the manufacturer consists of several stacks of 13.5 kW. In larger systems, such as the systems proposed in this report, these stacks are combined into modules of around 100 kW. Each module needs a DC-DC converter regulate the voltage. The price of a 100 kW converter is around €9k. There is little difference between AC and DC converters [8].

Electric motor with drive and transformer

For our setup, we need 400 kW electric motors. A package (Motor and converter) for a 500 kW conventional squirrel cage motor is around €30k. A permanent magnet assisted synchronous reluctance (PMaSRM) motor (as described in Attachment A-1) with drive is around €55k [37]. Currently, these PMaSRM motors are only available in higher speeds (around 3600 RPM). To run these motors at a lower speed requires either a gearbox or more poles. The second option has a better efficiency. As these motors are larger, however, they might not be feasible for a vessel with limited space. Also, due to the lower production quantity, spare parts may have a longer lead time, potentially leading to longer downtime in case of a malfunction. For now a PMaSRM motor is used. This implicates a more expensive gearbox, as described in the section describing the gearbox and propellor in this chapter.

When using an AC installation, a transformer with double secondary windings might be necessary to lower harmonic distortion. A 500 kW transformer is around €30k.

Shaft generator

Depending on the configuration, the shaft generator might need a converter. The first option is a 100 kWe shaft generator without a converter, costing roughly €6k (Table 19). The other option is a 400 kWe generator with a converter. This costs around €20k for the generator (Table 19) and €15k for the converter [8].

General electric installation

When using a larger electrical installation, the electrical items, such as switchboards, are more complicated. To compensate for this, an additional €100k was added for both a fully electrical vessel and for the combination of an ICE with a fuel cell [8]. There is also a slight difference between a DC and an AC installation. DC switchboards are a little cheaper, but as this technology is relatively new, the required additional engineering would make up for any savings. When a DC generator is used, a rectifier is necessary. The price of a rectifier was set to €15k for a 1 MW rectifier and €10k for a 500 kW rectifier [8]. In certain setups, the auxiliary AC load is fed from a DC/AC converter. This converter costs around €10k [8].

Gearbox and propellor

The simplest gearbox has one power take in (PTI) and one power take out (PTO). When using a combination of an internal combustion engine with an electric motor, a second power take in is needed. Also, the Power take in of the combustion engine must have a clutch to disengage the combustion engine from the power train. The additional costs for the extra PTI and the clutch are €50k–75k [10]. For this report, we used the higher number, as there might be additional costs involved since the electric motor has a relatively high speed. Mounting a shaft generator requires an additional power take out. This costs around €20k.

As explained in Attachment B-2, a fixed pitch propellor can be used when driving the propellor shaft with an electric motor. The engineering department of Conoship estimates that a fixed fitch propellor saves approximately €50k compared to a controllable pitch propellor.

Hydrogen installation

Hydrogen can be stored as a compressed gas, a cryogenic liquid, or embedded in porous carbon or metal-organic frameworks. Other options are organic carriers, such as LOHC, or chemical hydrides, such as $NaBH_4$. Much research has been conducted on hydrogen storage and all options have advantages and challenges. This report does not explore the storage options, but they all have a much higher fuel volume compared to diesel oil. This might affect the cargo volume of the vessel, possibly decreasing the profits. As all configurations are based on hydrogen use, this effect will be nearly the same for all cases except the reference case. Currently, Conoship has design setups that do not affect the cargo volume, so a possible profit decrease is not included. The investment in the storage system will depend on the system that is installed. To provide a basis for comparison, the storage costs were set at €1m after elaborate discussion with Conoship. This number is based on the fact that both the pressurised option and the cryogenic option have a large impact on the vessel design. Further research is needed to have a more accurate estimate.

Besides the storage, the hydrogen system must be integrated in the vessel. Transportation and treatment along with all safety and ventilation systems systems were set at €500k, also after discussion with Conoship. Also for this number the advice is to have a more detailed research done to make a more accurate estimate.

CAPEX

The CAPEX in this reports includes the hardware investment costs and the interest costs. The hardware investment costs includes the base design of the reference case and the additional costs (or savings) for converting it to a different design.

Large investments in the shipping industry are mostly financed by a mix of bank equity and external investors. There are numerous financial constructions with various pros and cons. Without going into detail, the method of a thesis of Bob Hillen was used. This MSc thesis was performed at Conoship and examined the use of Redox flow batteries. For the use case in that thesis, Conoship internally decided to an investment that will be fully repaid in 15 years on a straight-line basis. To be able to calculate the total resource needed for the interest the hardware cost is divided by two and multiplied by the interest rate to get the cumulative interest rate over 15 years. This interest period of 15 years differs from the use case period of 20 years but as all designs are calculated in the same way this is consistent.

The investment for a conventional diesel configuration, the reference case, is around €8m. For this investment case, an interest rate of 5,2% was used. For the other, hydrogen based, designs, a 100% bank equity is possible, resulting in a lower interest rate of 4%.

As it is difficult to give a sound estimation for the hardware investment costs Appendix H-2 contains a sensitivity plot for the CAPEX.

OPEX

All maintenance costs are included in the OPEX. Apart from the initial investment, the internal combustion engine needs regular maintenance. Estimated maintenance costs are given in Table 19a. These figures are a rule of thumb used by Pon Power, a dealer of these engines, for regular maintenance costs performed in the Netherlands. For the dual fuel internal combustion engine, the figures were increased by 20%, as the engine has more components. Lubrication oil is not included in the OPEX, as its contribution will be small.

Fuel cells need less maintenance, as there are fewer moving components. The daily maintenance is limited to exchanging filters and occasionally replacing a component. These costs are not further specified in this report, as the combustion engine also requires breakdown maintenance.

Other operational costs, such as regular vessel maintenance and crewing, were not included in this report, as these costs are nearly the same for all vessels. The main difference might come in crewing costs, especially in the first years. The crew must be trained to work with the new technologies. It might be difficult to find suitable engineers, leading to higher wages. This effect was not included in the figures.

5.4 Conclusion

This chapter provided the bases for the total cost estimation in Chapter 6. The largest uncertainty is how fuel prices will change. These prices are affected by technical developments, political choices and availability, and have a large impact on the total costs. Equipment costs can be estimated accurately. The system integration is more difficult, but that aspect is common to all new designs.

6 Design selection

6.1 Introduction

In this chapter, the fuel, CAPEX and OPEX costs are combined based on the use case of 20 years.

The fuel costs were calculated based on the efficiency. The running hours of the equipment led to maintenance costs. For fuel cells, it is assumed that the strings are 250 kW. So if a configuration has a stack of 500 kW, one string can be deactivated in port to save on running hours. In reality, the strings are smaller, around 100 kW, which allows for further reduction of the running hours. This depends on the time spent in port, as it is not advisable to switch stacks on and off more than once a day [34]. An automated schedule can be created to spread the running hours evenly over the strings.

6.2 Costs per design

The costs for all designs are summarized in tables in Attachment G. For clarity, two tables are described to illustrate the method used.

Design 1a: reference case

Table 20 is the overview of the reference case. The orange top part specifies the OPEX costs, in our case the maintenance costs. Based on the use case scenario, the running hours of the engines were calculated. The main engine only runs when sailing. The 100 kWe auxiliary engine runs most of the time. The 300 kWe generator runs when manoeuvring, when more power is needed for loading operations and during maintenance to the 100 kWe generator set. The division chosen is 90% of the time for the 100 kW set and 10% of the time for the 300 kW set. These hours were multiplied by the maintenance costs per running hour, as stated in Table 19, giving the total maintenance costs. Table 23 contains an overview of the running hours for all the designs.

The investment costs for the reference vessel were set at €8m. As this is not a 'green' investment, the interest rate is 5,2% per year. As described before, the investment is paid for linearly over 15 years. The total interest is therefore 15 times 5,2% of €4m, or €3.15m. The total CAPEX cost are the interest costs plus the investment costs.

Design 1a: Internal combustion engine running on MDO			
OPEX			
	€/hr	€/yr	Total [M€]
Maintenance Main engine	5,5	24090	0,482
Maintenance 100 kWe auxiliary engine	2	15768	0,315
Maintenance 300 kWe auxiliary engine	3,5	3066	0,061
		Total maintenance:	0,9
CAPEX			
Capex vessel			8,000
		Total Capex:	8,000
Interest (5,25%)			3,150
Total Capex costs			11,2
Fuel and Urea costs			
DO costs			8,586
Urea costs			0,276
		Total Fuel and Urea costs	8,9
		Total over 20 years:	20,9

Table 20: Total costs design 1a: Internal combustion engine running on MDO (reference case)

The grey rows represent the fuel and urea costs. Based on the fuel consumption per hour calculated before, and with the use case scenario determining the total hours, the total fuel and urea costs were calculated. Adding these three cost components results in the total costs for the use case.

Design 6a: Dual fuel internal combustion engine (500kW), fuel cell assisted

The method for the next example is the same, so only the differences are highlighted. The stacks from the fuel cell plant must be replaced after about 30000 hours. The running hours were calculated based on the use case. In port and at low loads one string is switched off to save running hours. Based on these two figures, the number of stack replacements was calculated. The cost of the stack replacements was based on the method described in Section 5.3. As the stack replacement price slowly decreases, the replacement cost varies. The total cost of all stack replacements is part of the OPEX. For the CAPEX, the same €8m for the base vessel was used. To convert this design into the intended setup, the internal combustion engine has to be converted to dual fuel and fuel cells added. The conversion of the internal combustion engine means additional costs for converting it to dual fuel and a cost deduction as a smaller engine is used. The hydrogen storage and installation are priced the same for all hydrogen designs. Electrical components are added, meaning an additional charge for designing and installing a larger, more complicated electrical installation. Also, the auxiliary generator sets are not needed as the fuel cell can deliver all necessary electrical power.

Common systems, such as cooling, ventilation and systems for the crew and accommodation will be largely the same. Differences such as the increase in ventilation capacity are included in the ‘hydrogen installation’ scope.

Design 6a: DF internal combustion engine (500 kWe), fuel cell assisted			
OPEX			
	€/hr	€/yr	Total [M€]
Maintenance Main engine	5,4	18921,6	0,378
Stack replacement			0,841
		Total maintenance:	1,2
CAPEX			
Capex vessel			8,000
Main engine additional dual fuel components			0,023
Fuel cell			1,250
6 pcs 100 kWe DC/DC converter			0,054
Hydrogen storage			1,000
Hydrogen installation			0,500
400 kW electric motor with converter			0,070
Gearbox with 2 PTI and clutch, additonal costs			0,075
Larger electrical installation			0,100
150 kWe DC/AC converter for auxiliary load			0,010
Smaller ICE (500 kWe instead of 1000 Mwe)			-0,058
FPP instead of a CPP			-0,050
One generatorset (100 kWe) less			-0,070
One generatorset (300 kWe) less			-0,150
		Total Capex:	10,8
Interest (4%)			3,226
Total Capex costs			14,0
Fuel and Urea costs			
DO costs			1,452
Urea costs			0,084
Hydrogen costs			9,753
		Total Fuel and Urea costs	11,3
		Total over 20 years:	26,5

Table 21: Total costs design 6a: Internal combustion engine (500 kW), fuel cell assisted

As this configuration is green, the interest rate is 4%. The total costs over 20 years were again calculated by adding the CAPEX, OPEX and fuel costs.

6.3 Summary of information

Costs of different designs

The aforementioned method was followed for all designs. The tables for each design are given in Appendix G. Table 22 is the summary of all the designs.

Scenario		Costs in Million Euro [M€]			
		OPEX	Capex	Fuel	Total
1a	Conventional Propulsion DO (reference)	0,9	11,2	8,9	20,9
1b	Conventional Propulsion DF	1,0	12,4	14,4	27,8
2	Conv. Prop. Constant rpm shaft gen.	0,8	12,4	13,6	26,8
3	Conv. Prop. Variable rpm shaft gen.	0,8	12,3	13,7	26,8
4	Dual fuel electric with an AC network	0,8	12,7	14,3	27,8
5	Dual fuel electric with a DC network	0,8	12,6	13,6	27,1
6a	Dual fuel ICE (500 kW) fuel cell assisted	1,2	14,0	11,3	26,5
6b	Dual fuel ICE (750 kW) fuel cell assisted	1,0	13,3	11,9	26,2
7a	DF ICE (500 kW), AC network, FC assisted	1,2	14,2	11,8	27,2
7b	DF ICE (750 kW), AC network, FC assisted	1,0	13,6	12,9	27,4
8a	DF ICE (500 kW), DC network, FC assisted	1,2	14,1	11,7	27,0
8b	DF ICE (750 kW), DC network, FC assisted	1,0	13,5	12,6	27,2
9	Fuel cell only	1,1	15,5	9,8	26,4

DO: Diesel oil, DF: Dual fuel, ICE: Internal combustion engine, AC: Alternating current, DC: Direct current, FC: Fuel cell

Table 22: Summary of costs for all designs

Investing in new technologies is more expensive than the classic diesel engine setup. Together with (much) higher fuel prices, this leads to a large gap between the reference design and green options.

Local CO_2 emission

However, the design will not be chosen merely based on the above costs. Therefore, the local CO_2 emissions of all options are determined next.

Scenario		Fuel usage [Ton/year]			Local CO_2	Running hours [hr/year]			
		Hydrogen	DO	Urea	[Ton/year]	FC	ME	AE small	AE large
1a	Conventional Propulsion DO (reference)	0	572	46,1	1815	na	4380	7884	876
1b	Conventional Propulsion DF	147	213	40,1	675	na	4380	7884	876
2	Conv. Prop. Constant rpm shaft gen.	156	169	40,6	537	na	4380	4818	438
3	Conv. Prop. Variable rpm shaft gen.	155	177	39,3	560	na	4380	4380	na
4	Dual fuel electric with an AC network	202	117	15,9	372	na	4380	4380	na
5	Dual fuel electric with a DC network	160	168	26,3	532	na	4380	4380	na
6a	Dual fuel ICE (500 kW) fuel cell assisted	185	48	14,0	153	13140	3504	na	na
6b	Dual fuel ICE (750 kW) fuel cell assisted	177	80	23,4	253	8760	3942	na	na
7a	DF ICE (500 kW), AC network, FC assisted	203	35	6,5	111	13140	3504	na	na
7b	DF ICE (750 kW), AC network, FC assisted	210	56	9,6	179	8760	3942	na	na
8a	DF ICE (500 kW), DC network, FC assisted	200	37	10,2	118	13140	3504	na	na
8b	DF ICE (750 kW), DC network, FC assisted	201	63	16,4	200	8760	3942	na	na
9	Fuel cell only	185	0	0,0	0	16644	na	na	na

DO: Diesel oil, DF: Dual fuel, ICE: Internal combustion engine, AC: Alternating current, DC: Direct current, FC: Fuel cell, na: not applicable

Table 23: Local CO_2 emissions and running hours for all designs

Burning one kg of MDO leads to local emissions of 3,17 kg CO_2 [57]. By multiplying the amount of MDO used with this number, the local CO_2 emissions during the use case were calculated. Hydrogen has no local CO_2 emissions. Table 23 summarizes the fuel use and the calculated local CO_2 emissions. It also shows the running hours for the fuel cell and internal combustion engines.

CO_2 penalty

By combining Table 22 and Table 23, the CO_2 reduction of the different scenarios compared to the diesel oil reference case were calculated. Dividing the additional costs compared to the diesel oil reference case by the CO_2 reduction, the minimal CO_2 penalty per ton to reach the breakeven point during 20 years was calculated. For example, design 1b, the dual fuel internal combustion engine, costs €6,9m more than the reference case. The CO_2 reduction compared to the reference case is 22789 tons. Dividing these numbers gives a penalty of 304 €/ton to reach the breakeven point after 20 years.

Design		Costs [M€]	CO_2 [Ton/usecase]	CO_2 reduction [%]	CO_2 b.e. price €/ton
1a	Conventional Propulsion DO (reference)	20,9	36291	-	-
1b	Conventional Propulsion DF	27,8	13502	63	304
2	Conv. Prop. Constant rpm shaft gen.	26,8	10737	70	232
3	Conv. Prop. Variable rpm shaft gen.	26,8	11209	69	237
4	Dual fuel electric with an AC network	27,8	7446	79	239
5	Dual fuel electric with a DC network	27,1	10636	71	242
6a	Dual fuel ICE (500 kW) fuel cell assisted	26,5	3069	92	169
6b	Dual fuel ICE (750 kW) fuel cell assisted	26,2	5054	86	170
7a	DF ICE (500 kW), AC network, FC assisted	27,2	2229	94	185
7b	DF ICE (750 kW), AC network, FC assisted	27,4	3574	90	200
8a	DF ICE (500 kW), DC network, FC assisted	27,0	2361	93	182
8b	DF ICE (750 kW), DC network, FC assisted	27,2	4009	89	195
9	Fuel cell only	26,4	0	100	153
DO: Diesel oil, DF: Dual fuel, ICE: Internal combustion engine, AC: Alternating current, DC: Direct current, FC: Fuel cell, b.e.: break even					

Table 24: Cost overview of the different scenarios and the CO_2 price necessary to reach the breakeven point

Figure 16 summarizes the cost division and the CO_2 price to reach the breakeven point during the use case of 20 years.

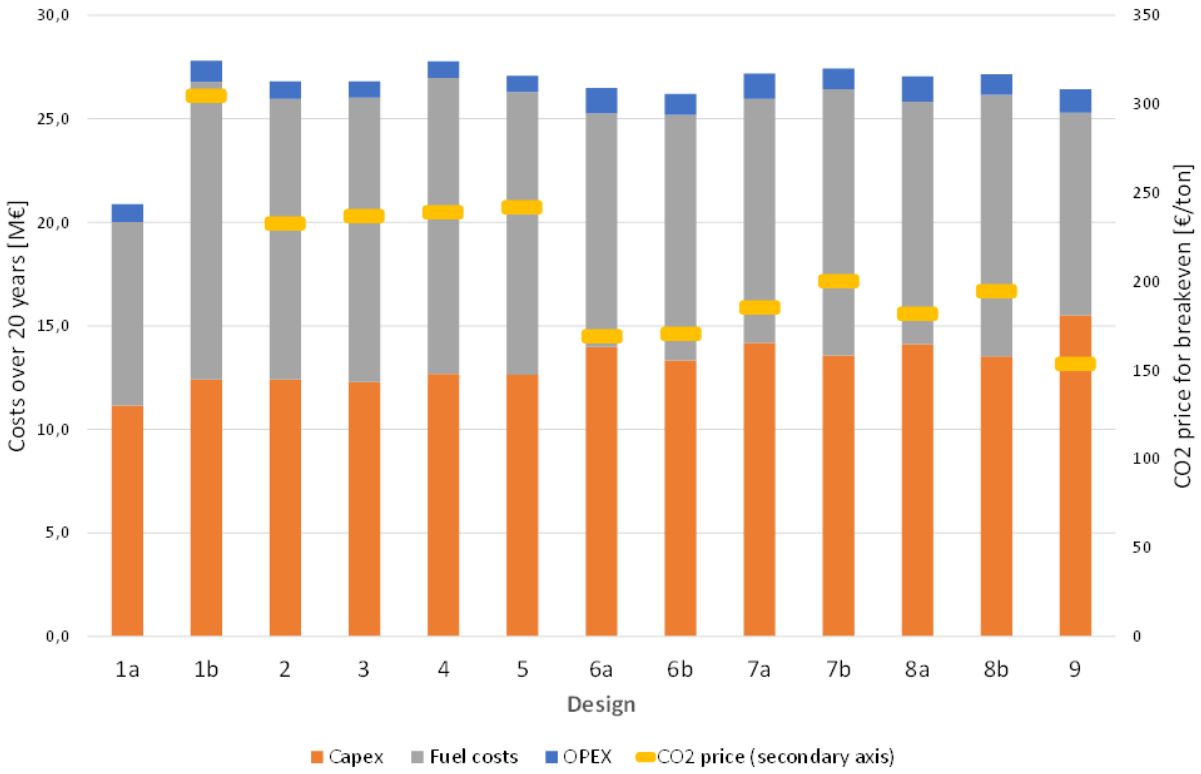

Figure 16: Cost overview of the different scenarios and the CO_2 price necessary to reach the breakeven point

Discussion

When only taking the CAPEX into account, the reference case is best. This case has also the best figures regarding the fuel costs. For the calculations, 750 €/ton was used, but currently the price is even lower, around 550 €/ton, making the difference between the reference case and green options even larger.

CAPEX costs rise when using a dual fuel hydrogen engine. Making some investments in shaft generators or an all-electric setup saves on using an auxiliary generator set, as in designs 2, 3, 4 and 5. This reduces the CO_2 emissions and so lowers the necessary CO_2 penalty. The all electric designs 4 and 5 have a slightly lower efficiency. The OPEX costs also decrease slightly as auxiliary engines are used less.

Starting with design 6a the fuel cells, are introduced. The CAPEX increases but the fuel use decreases due to the better efficiency. This causes the total costs to be lower than design 1b with a dual fuel only configuration. Designs 6a and 6b, with an internal combustion engine directly driving the propellor shaft and assisted with an electric motor, has a slightly better efficiency than designs 7a, 7b, 8a and 8b, which have additional losses due to the all-electric setup. The CO_2 emissions reduction of 6a and 6b, however, is slightly less than 7a, 7b, 8a and 8b. Based on the CO_2 penalty, designs 6a and 6b are preferred above 7a, 7b, 8a and 8b.

The all fuel cell setup (design 9) has the highest CAPEX but this pays back with a lower fuel consumption and zero local CO_2 emissions. Therefore, this setup has the lowest CO_2 penalty for breakeven.

Choice of design

Solely based on economic considerations, the design with only fuel cells is most promising. Due to its high efficiency, the pay-back time is the lowest and the local CO_2 emissions are zero. Conoship is already looking into this all-electric FC setup as a concept. However, their customers (shipowners) must also be convinced to invest in new technologies.

From that perspective, a combination of a fuel cell with an internal combustion engine is also an interesting option. Shipowners and the crew already know a lot about internal combustion engine technology, taking them less out of their comfort zone. An important other benefit is that having an internal combustion engine gives the vessel the ability to sail on conventional MDO or biodiesel in case no hydrogen bunkering facilities are available. It also solves the legal requirement that vessels sailing with a low flashpoint fuel must include a redundant system.

Based on these arguments, Conoship did not choose the all-electric fuel cell concept for this report. Instead, they are interested in the concept of an internal combustion engine driving the propellor shaft via a gearbox, assisted by an electric motor mounted on the same gearbox (designs 6a and 6b). This motor is powered by a fuel cell. The size of the ICE and fuel cell is for further research to examine, but so far one setup has an ICE of 750 kW combined with an FC of 250 kWe, the second one an ICE of 500 kW and an FC of 500 kWe. It must be noted that these size engines are not available yet.

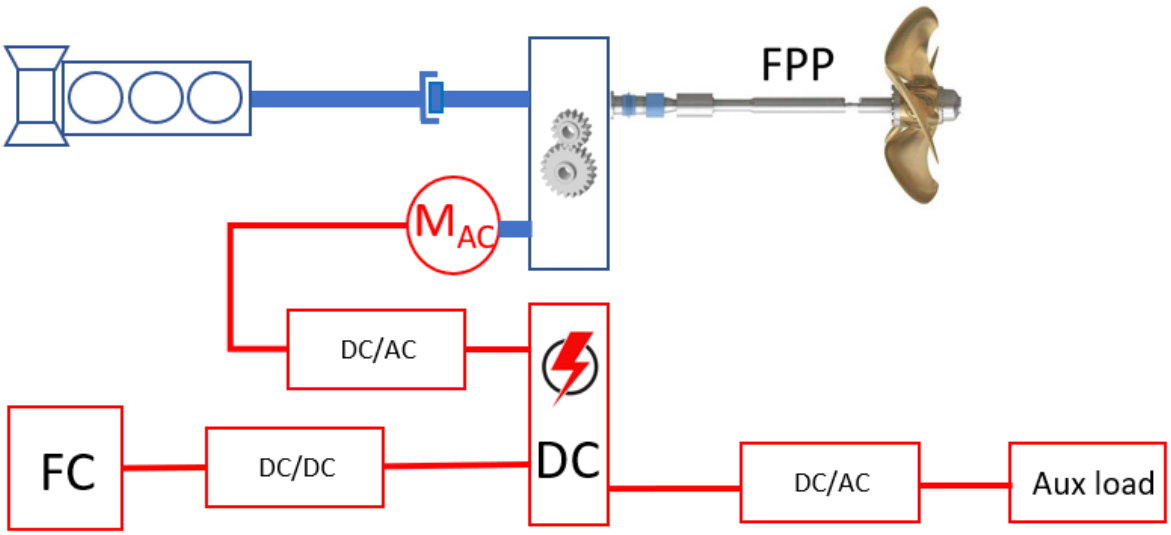

Figure 17: Selected setup 6a and 6b

One of the reasons to choose this design is to be able to run the vessel on diesel only. In this scenario, the fuel cell cannot supply electrical power. The auxiliary load and the bow thruster must therefore be powered in a different way. Also, the power available on the propellor shaft will be lower as the installed dual fuel internal combustion engine is smaller compared to the reference case. This can be solved by installing a diesel generator set. If it is sufficiently large, around 300 kW, it can be a complete replacement for the fuel cell. This generator set can also be used to power the electric motor during sailing and manoeuvring. This last point is important, as the optimized fixed pitch propellor is used in this design, and the torque required during manoeuvring might be too large for the internal combustion engine alone.

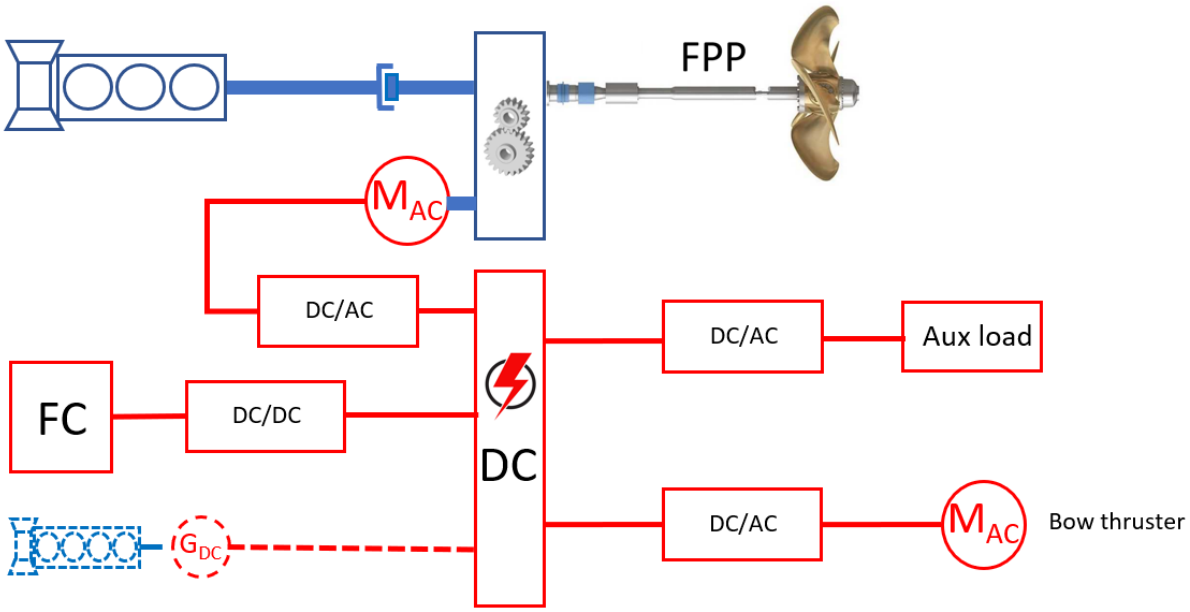

Figure 18: Selected setup with additional DC generator to run on (bio)diesel only

By adding a 300 kW generator, the CAPEX increases by about €150k [45] . As the OPEX depends on the running hours, and those should be close to zero in the optimal situation, these costs are not increased. The CO_2 penalty for breakeven rises in that case from 169 €/ton to 175 €/ton for the design with a 500 kW internal combustion engine. For design 6b, with a 750 kW internal combustion engine, a 300 kW engine was already installed for directly driving the bow thruster. Connecting it to the switchboard and installing a DC/AC converter for the bow thruster will be slightly more expensive than directly driving it, so €50k was added to the CAPEX, which raises the CO_2 penalty from 170 €/ton to 173 €/ton.

Sensitivity

To determine the sensitivity of the parameters used for the results, sensitivity plots were created for the CAPEX and fuel costs, as these have a far larger impact on the outcome than the OPEX. For these sensitivity plots 3 designs are used, being design 1b (dual fuel internal combustion motor), 6b (duel fuel internal combustion engine (750 kW), fuel cell assisted) and design 9 (fuel cell only).

For the fuel costs, sensitivity plots were created for the hydrogen, MDO and biodiesel prices. Figure 19 shows this plot for the hydrogen price. The other plots are given in Appendix H-1and H-2. As expected, the outcome depends on the fuel prices. The hydrogen price will be subject to changes in the future and has a large impact on the CO_2 penalty. The MDO price is not likely to become much lower than current prices (around 550 €/ton). As long as the MDO price lowers not far below the current price, a successful business case is possible for the chosen design. A changing MDO price only influences the reference case as the other designs involving a dual fuel hydrogen internal combustion engine use biodiesel as pilot fuel. The slope of the biodiesel sensitivity plot for design 6b is not steep, so fluctuation in the biodiesel price have little influence.

For the CAPEX, two options were plotted. In the first option, the CAPEX of the reference case is not changed. The CAPEXs of design 1b (dual fuel internal combustion motor), 6b (duel fuel internal combustion engine (750 kW), fuel cell assisted) and design 9 (fuel cell

only) range between 80% and 130% of the reference design. In this option, the CAPEX changes due to unforeseen positive or negative influences during design and building of the alterative designs. This could be due to additional engineering (more investment) or lower costs for the storage (less investment). The second option, involves more fluctuations in the price of materials and labor, affecting both the reference case and the alternative designs. As expected, the sensitivity in this option is lower, as both the reference case and the alternative designs change in the same direction.

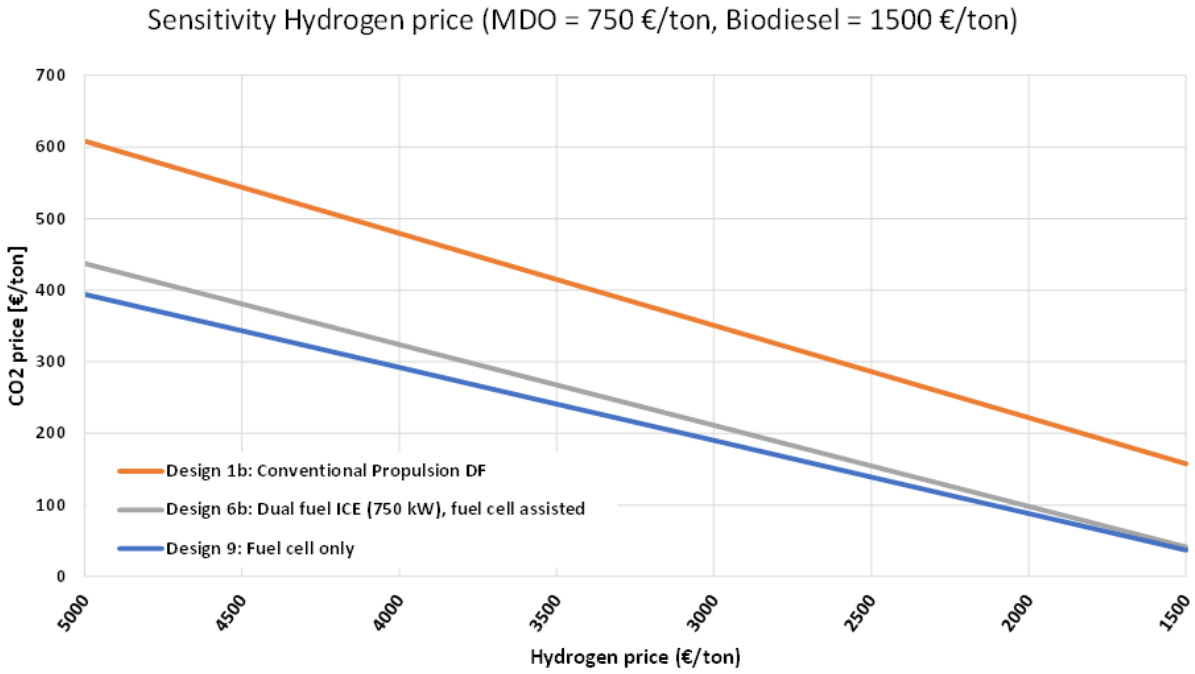

Figure 19: Sensitivity plot hydrogen price

Discussion

The chosen design is not the most economic, but it has practical benefits, primarily the ability to run on (bio) diesel alone. During the transition to green energy sources, hydrogen might not be available in every port, so this is essential to avoid losing contracts. During the building process, the costs must be kept within budgets, as an additional 10% of initial investment raises the CO_2 penalty for breakeven by 50 €/ton. Conoship can influence these costs. In contrast, the fuel costs are harder to influence or predict.

7 Design exploration

7.1 General

The design has been determined, and in this chapter the options and technical challenges are explored to answer the sub questions. The concept of a mechanical (ICE) driven shaft line in combination with electric support is not new. In previous designs, however, the electric motor is mostly driven by a constant rpm diesel powered generator. The dynamic load response of diesel engines is readily available from datasheets and all components used have a proven track record. In our setup, a dual fuel (hydrogen) ICE is used in combination with a fuel cell. Both components are (relatively) new in the shipping industry, so little or no data is available.

In this chapter many topics are discussed. To have an overview Figure 20 shows an overview of these topics.

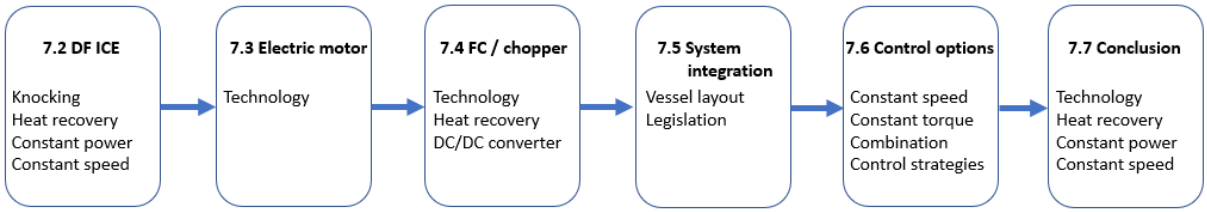

Figure 20: Chapter 7 structure

7.2 Dual fuel internal combustion engine

Introduction

Chapter 2 contains a brief introduction to the working principle of a dual fuel hydrogen engine. This sections presents some more detailed topics.

Knocking

Running on (partly) hydrogen makes an engine vulnerable to auto ignition, as hydrogen requires little energy to ignite. This requires a good engine design to prevent any possible local hotspots. Too early auto ignition is called knocking and is potentially harmful to the engine.

Due to the high flame velocity and rate expansion, the heat release in the cylinder occurs earlier compared to a diesel engine, potentially leading to higher NOx emissions than a diesel. One solution is to dilute the mixture, decreasing the flame velocity and so delaying the heat release. Nevertheless, a DF hydrogen engine still requires an exhaust gas treatment plant to comply with the IMO tier III requirements. Particle matter (PM) emissions and soot formation

are reduced with an increased hydrogen ratio and are less than the emissions of a diesel engine.

Currently the efficiency is comparable with a common diesel engine and it is expected to be slightly higher when the engine is fully developed [5]. This could be possible due to the high flame velocity, more closely approaching the thermodynamically ideal engine cycle. More background on the emissions is given in Appendix D.

Potential knocking is a common problem for (DF) gas engines. During an informal talk with a Llodys surveyor, he mentioned that he encountered many (DF) gas engines that ran into reliability issues and breakdowns stemming from using gas as a fuel. Although these were not hydrogen engines, the problems were related to knocking issues. Unfortunately, he was not allowed to share information about this subject. However this information is in line with other information within my personal network indicating that DF engines have more (reliability) issues than standard diesel engines. ABC states that they do not see any issues, however they prefer the engine to be running as constantly as possible. This minimizes the risk of knocking issues, as the mixture can be held constant.

Apart from this, the dynamics of the DF hydrogen are comparable with a conventional diesel engine. In the lower load ranges, the response to a load jump are slightly slower (10% more time needed to recover), from two third of the maximum load, the hydrogen engine is slightly faster [5].

Heat recovery

The heat recovery possibilities for the ABC DF engine are comparable with a standard diesel engine regarding the exhaust gas flows and temperatures. The same applies to the potential heat recovery from the jacket cooling water. This is because they operate with the same efficiency and nearly the same principle.

Large diesel engine installations could use a conventional steam installation according the Rankine cycle, but this is a bulky and costly installation. Furthermore, such an installation does not use the full exergy of the heat media as the (compressed) water boils at high temperatures. An alternative is an organic Rankine cycle (ORC) installation. This operates according to the same principle but uses a different medium. For the ORCAN efficiency pack, the thermal media R245fa is used. This boils at 15 degrees Celsius, making it possible to extract heat from the cooling water. The energy generated by the turbine or rotating screw expander can be converted directly into mechanical or electrical energy.

The specific heat c_p for the exhaust gasses is 1,05 [kJ/kgK] [39]. Ideally, the exhaust gasses are cooled as much as possible, but in reality condensation in the exhaust line must be avoided and heat potential must be kept in the exhaust gasses to let them rise away from the funnel. Comparing the 1 MW DF engine with a diesel engine of around the same size reveals that the DF engine has a slightly lower exhaust gas temperature with a higher mass flow. The amount of energy is almost the same, although the exergy of the higher temperature gasses is higher. At 50% load, the energy is almost half compared to full load, but because the temperature is higher, it will be easier to use the energy.

As with all these technologies, the efficiency of the total system depends on many factors. Manufacturers mostly give the highest efficiencies possible for sales purposes. Luckily, the

new ferries of Rederij Doeksen, sailing between Harlingen and Terschelling, have this system installed, so practical values are available. During normal running conditions, the MTU 16V4000 M55 engines of these vessels, running on LNG only, are loaded up to 50% of their maximum rating of 1492 kW. This is around 750 kW. In this case, the ORCAN system recovers 45 kW electrical power. 2 kW is consumed by its auxiliaries, so the net power is 43 kW, or 5,7% of the delivered power. The system is designed to deliver a net maximum of 75 kW at 1492 kW, which is 5%. The small difference is most likely caused by the higher temperature of the exhaust gasses at lower loads.

Based on these figures, Table 25 was created for a 1 MW ABC DF hydrogen engine. The exhaust gas data was taken from an ABC document and the heat was calculated with a funnel temperature of 40 °C. The same percentages were used for both the 750 kW and 500 kW engines (design 6a and 6b), as no data is available for these engine sizes. A comparable 1 MW 6DZC engine further produces 289 kW energy in its high temperature cooling water and 51 kW in heat radiation [11]. The heat from the high temperature cooling water is also fed into the ORCAN ORC unit.

Engine			Exhaust gasses			Heat recovery	
Speed [rpm]	Load [%]	Load [kW]	Temperature [°C]	Mass flow [kg/s]	Heat [kW]	[% of engine load]	[kW]
1000	100	1000	289	2,986	780,6	5	50,0
910	75	750	296	2,463	662,0	5,1	38,3
800	50	500	358	1,358	453,5	5,7	28,5
630	25	250	341	0,670	211,7	5,5	13,8

Table 25: Estimated heat recovery with an ORCAN system based on exhaust gas heat recovery and cooling water heat recovery for a 1 MW ABC DF internal combustion engine. Heat in exhaust gasses based on a cp of 1,005 [kJ/kgK] and a funnel temperature of 40 °C.

Based on this information, the hydrogen savings over 20 years are €230k for the 500 kW ICE/500 kW FC option and €360k for the 750 kW ICE/250 kW FC option. The firm Berger Maritiem delivered the ORCAN systems for the ferries of Rederij Doeksen. The rough investment figures they gave were around €200k for the components, including the heat exchangers for the exhaust gasses and jacket cooling water system. For the system integration and installation, they estimate another 25%, adding up to around €250k. They stated that it must be carefully calculated if such a system is worthwhile for our case. The smallest 100 kWe system they deliver is basically designed for a 1 MW engine. Although our total system also has a total power of 1 MW, the cooling water from the fuel cell has too low a temperature to extract heat from. Based on the calculations above it is not likely that this system is useful for our setup.

Another option could be to use the heat to produce pure water. This water can then be used in an installation to convert $NaBH_4$ to hydrogen. James Miller reported in 2003 that it requires 11–60 kJ/kg water to produce water with a reverse osmosis reactor [38]. As this principle relies on high pressure pumps, the waste heat must first be converted to electricity, such as with the OrCad system above. As described above, this is not an economical option. Another option is a vacuum water maker to make the desalinated water in combination with additional filters. The question remains whether the water will be pure enough to be used for this purpose. This is further discussed in the follow up list.

If one would use a liquid organic hydrogen carrier (LOHC) to store hydrogen heat is needed for dehydrogenation of the hydrogen. Using the heat from the exhaust gasses for dehydrogenation of LOHC is not an option, as this requires a temperature of 300 °C. This temperature is not reached throughout the whole operating range. To dehydrogenate 1 mol H2 from, for example, H18-DBT, 65 kJ are needed [19]. To dehydrogenate 1 kg of hydrogen requires 32,2 mJ. The figures in Table 25 show that at 800 RPM, the exhaust gas flow is 1,358 kg/s with a temperature of 358 °C. In the ideal world without any losses, it would be possible to cool these gasses to 300 °C to obtain 82,7 kJ of energy. With this energy, 9,3 kg hydrogen can be dehydrogenated per hour. In reality, this will be lower due to losses. Even the ideal amount is far too low to cover the hydrogen use of the installation.

Finally, the heat from the engine could be used to heat the accommodations and domestic water. This is only a small potential saving, but the implementation is straightforward and depending on the type of heating, even the lower temperature cooling water is usable for this purpose.

Summarized the ORCAD ORC system is not suitable for our design and the heat is not sufficient for pure water production. The only usable way for heat recovery is heating purposes for the accommodation and domestic water.

Constant power vs constant speed

As the chosen setup involves a directly driven propellor, the engine speed has to remain relatively fixed to maintain a constant transit speed. Traditionally, the lever on the bridge sends a speed setpoint to the governor of the engine. The governor controls the fuel rack and therefore the amount of fuel injected into the engine. If the speed is too low, more fuel is injected, leading to more torque produced by the engine. As long as this torque is higher than the torque required by the propellor, the speed increases. Vice versa, if the speed is too high, the amount of fuel is reduced. This process results in a constantly varying amount of injected fuel in the engine.

In a common diesel engine, this process is easy to control, as diesel is not compressible and the injection mechanism, whether electronic or mechanical, has a direct relationship with the amount of fuel injected. In a dual fuel or gas engine, this is more difficult. When admitting the gas in the combustion, the amount of gas, and so energy, depends on the gas pressure, combustion air pressure and the opening time of the valve. The gas pressure is regulated by a control valve, but this cannot be completely steady, as there is a delay time in the system caused by the gas piping. The same applies to the combustion air pressure. The pressure depends on the operating point of the turbocharger, which in turn depends on the load (fluctuations). All together, this can cause the governor to constantly adjust the amount of gas injected. Together with the possible knocking effects in a DF motor, this leads to a more challenging controller setup.

As mentioned before, ABC, a Lloyds surveyor and end users all stated that DF gas engines have issues with their reliability and maintenance intervals caused by knocking effects. ABC states that a DF hydrogen engine should to run as constantly as possible. Apart from these issues, not constantly increasing and decreasing the amount of injected fuel to keep the engine at a constant speed might improve efficiency.

A different option to control the engine is to keep the power (or more accurately the torque) constant instead of the speed. This is analogous to setting the fuel rack of a classic diesel engine in a fixed position. The amount of fuel injected in each cylinder remains constant and thus so does the torque. This is only true if the engine speed is within a certain frame to maintain nearly constant operating conditions for all components, including the turbocharger. If the torque on the propellor shaft increases, this will lead to a decrease in propellor speed and vice versa. In this situation, the thermal and mechanical loading of the engine remains as constant as possible. Also, the gas regulating valve and the gas pressure will remain nearly constant. Safeties have to be in place to protect the engine for an overspeed situation in case the propellor shaft suddenly decreases, such as when the propellor comes (partly) out of the water during heavy seas.

Summarized the constant power or constant torque mode seems to be a good control mode for a dual fuel hydrogen engine to keep it running as constant as possible, and to prevent knocking.

7.3 Electric motor

Technology

The electric motor converts the energy from a fuel cell or battery into mechanical energy. Appendix A describes the different types of AC motors. The same appendix explains that a DC motor is not preferred due to the carbon brushes and the high rotor currents. So-called brushless DC motors are available but these are actually AC motors driven by power electronics from a DC source.

The most common AC motor, the squirrel cage motor, is simple and reliable. By using a permanent magnet motor, the efficiency is improved, as no losses originate from the rotor current. A combination of these techniques is also possible. A practical challenge with PM motors is that it could be difficult to change the bearings due to the strong magnetic fields. When designing the vessel, this must be planned for, for example by building a hatch to remove the motor so it can be serviced in a workshop.

Both the squirrel cage and PM motors are controllable with a variable frequency drive. The different types are described in Appendix A. These drives can control the motor’s speed and torque. A system integrator from the company D&A Electric remarked that although the efficiency of a PM motor is higher than a squirrel cage motor, in some cases the total efficiency of the latter system is better. If the overall efficiency will be improved by filtering out fast load fluctuations, the control of a squirrel cage motor is more direct and flexible, as the designer can control both the stator and rotor currents. This is not a standard technique, however, so the system integrator needs to learn by trial and error. Whether such a design is feasible and useful remains to be investigated.

A standard drive fed with an AC source consists of a rectifier producing a DC voltage and an inverter converting this DC voltage to a variable three phase voltage. Figure 21 shows an overview of such a converter. In our case, the rectifier is not necessary, as the fuel cell already outputs a DC voltage.

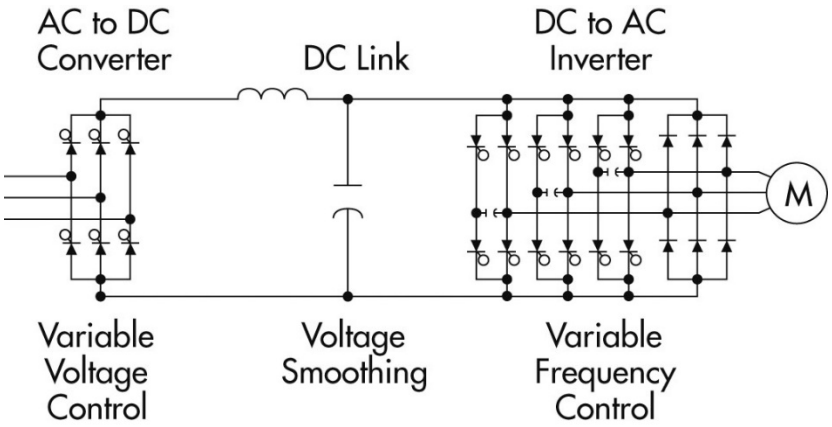

Figure 21: Pulse width modulated variable frequency drive overview (source www.nrcan.gc.ca)

A squirrel cage motor has a higher speed than an internal combustion engine. This increases the size and cost of the gearbox. By using a synchronous motor, the speed can be lowered, but currently there are not many permanent magnet, SynRM or PMaSynRM motors available that have the required power (around 350 kW) and a low speed (below 1200 rpm).

The exact type of motor to be used is a topic for further research. The outcome of the conclusions in this report will not change based on this choice as the efficiencies do not differ very much.

7.4 Fuel cell and DC chopper

For this report, the PEM fuel cell is used, as this is currently the most mature option for maritime use. Its relatively low operating temperature of 60 °C makes it safe and easy to integrate in a vessel. Nedstack delivers fuel cells in a containerized version, but they can also be built in the vessel in a dedicated fuel cell room. Within Conoship, a study was already performed on how to integrate a fuel cell only installation in a vessel.

Technology

The term fuel cell is a container term describing the complete fuel cell package. This includes the actual fuel cell and the auxiliaries, such as the hydrogen regulating and feeding circuit, the air supply, both for supplying oxygen and cooling, the cooling system and the water management system to feed off the produced water. These systems are responsible for the good operation of the fuel cell and must be matched to the fuel cell setup to have an optimal response. Conoship's preferred vendor is Nedstack. Nedstack operates a test plant in Delfzijl, which has been running for many years in a salty environment. This gives a good reference for the lifetime expectance in a marine environment. The information below was obtained from Nedstack.

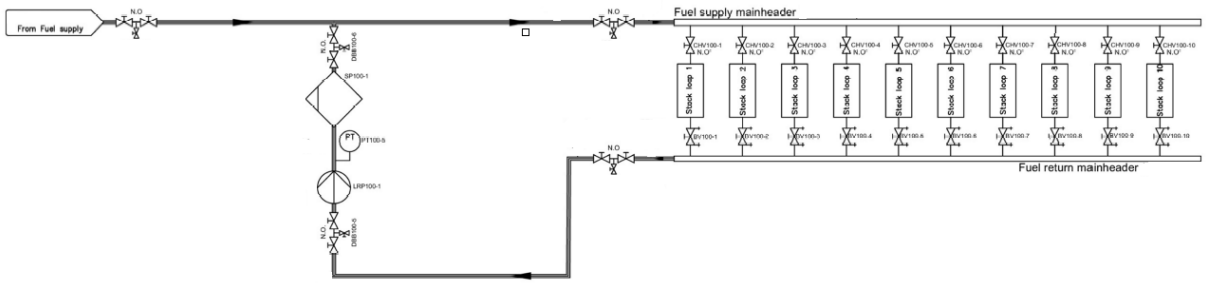

Figure 22: Simplified hydrogen diagram for a fuel cell installation (based on BSc thesis of D. Jansen, Conoship)

For the dynamic response of the system, the most important circuits are the hydrogen and air feed systems. These circuits have to ensure that the reactants (hydrogen and oxygen) are sufficiently present. Hydrogen is fed as a pure substance, while the oxygen is brought into the fuel cell with air.

Figure 22 is a simplified diagram of the hydrogen circuit. The hydrogen is fed into the system with a pressure regulating valve. Depending on how the hydrogen is stored, the pressure can be up to a few hundred bars in the storage system, although the fuel cell needs a pressure of under one bar. Expanding the hydrogen causes a temperature drop that must be compensated by a heat exchanger to prevent cold hydrogen entering the fuel cell. This heat exchanger is not drawn Figure 22. Via the fuel supply main header the hydrogen is fed to the separate strings. The system is set such that the excess ratio of the hydrogen is around 20% above the stochiometric ratio after the strings. This ensures that there is always enough hydrogen in the system to make load steps possible. The excess hydrogen is than compressed with a compressor and fed through a filter and a condenser and combined with the flow of hydrogen from the pressure regulating valve.

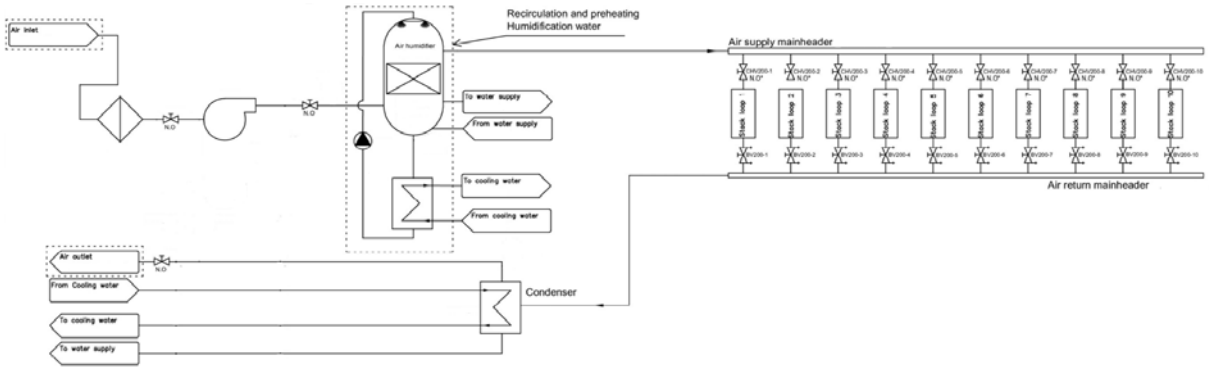

Figure 23: Simplified air diagram for a fuel cell installation (based on BSc thesis of D. Jansen, Conoship)

Figure 23 shows the simplified air diagram. The oxygen is brought in with normal, outside air. This air is heated and humidified before it enters the stacks. As the content of oxygen in air is only 21%, more air is needed than hydrogen to ensure enough oxygen is available. As the air supply is more likely to be the limiting factor during load steps, the control loop for this system uses both the pressure after the stacks and a feed forward loop based on the electrical load to keep the oxygen percentage around 100% above the stochiometric ratio. As soon as a load step occurs, the air supply is increased, even before the pressure drops after the stacks.

When operating at different load conditions, the optimum number of stacks changes. The fact that a load cell is performing at a better efficiency is contradicting with the fact that this leads to more running hours. At a certain point, it could be beneficial to switch off one or more

stacks. This can be achieved by closing the supply valves of the hydrogen and air valves. Currently, the strategy is then to make the stack inert with nitrogen. Nedstack states that switching off a stack is not a problem, as long as it is not done more than once a day [34]. Nedstack did not explain this limit, if it would be harmful to do so more often, or if a stack could be switched off for a short period (say a day or less) without making it inert.

Nedstack performed step load changes on a 100 kW string and found that steps up to 40% of the nominal load are possible. However, these tests were performed with a water load bank rather than resistors and coils. This water load bank is a large tank filled with sea water that is continuously refreshed. Copper conductors are lowered into this tank. The amount of copper surface relates to the power drawn. Although this is a simple method, the load steps are not actually steps, as the conductors are lowered with a mechanism and this takes time. This is clearly visible in Figure 24, where load steps of around 20% are performed. Based on this information, it will be difficult to really determine the response of the system, as this graph contains all time constants from the fuel stack and from the auxiliary systems. To model this system, these circuits must be benchmarked one by one.

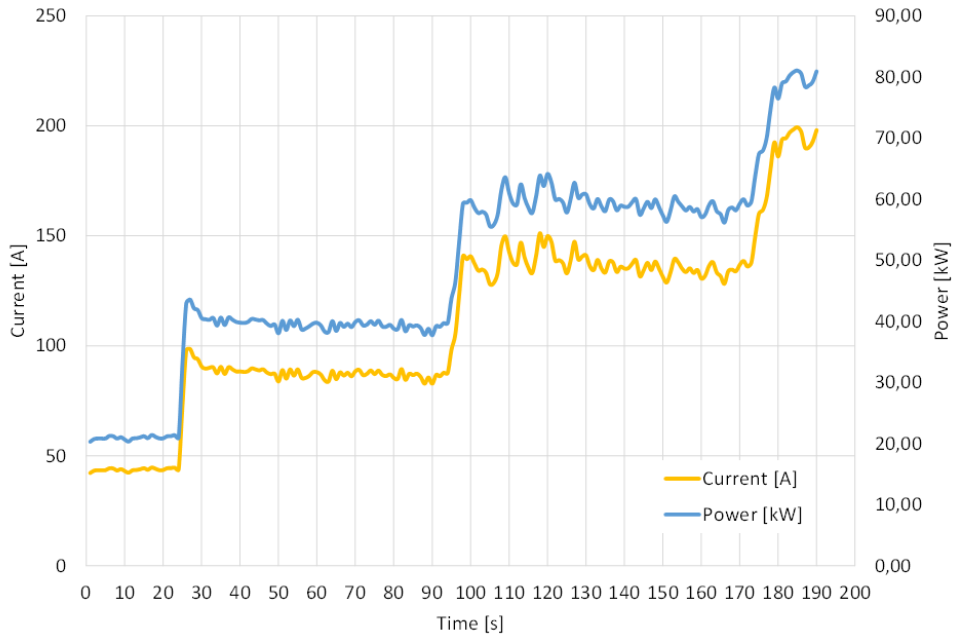

Figure 24: 100 kW Nedstack PEM load response (data source: Nedstack)

Nedstack is not using simulation tools and does not provide the time constants of the equipment. They are interested in developing such tools, so it might a good topic for another thesis. A time constant of 6 seconds is mentioned in a datasheet from an old fuel cell stack. However, the measurement method is not specified, so it is unclear what the system boundaries are.

Recent practical experiences of Nedstack show that there might be problems with current ripples of a higher frequency. Such current ripples could influence the aging process of the fuel cell. The processes behind this phenomenon and the frequency and amplitude of the ripple are not known. Research in this topic has recently started in Nedstack. This issue could impact our propulsion system. Besides the kHz region current ripples induced by the power electronics, disturbances of a few hundred Hertz caused by propellor-hull interaction could occur. Their impact is unclear, so this should be monitored in the future.

Heat recovery from fuel cell

The advantage of being easy to integrate in a ship is a disadvantage for heat recovery. Due to the low operating temperature of 60 °C, the exergy in the waste heat of the fuel cell is low compared to that of the internal combustion engine. It is therefore only usable to heat the air used in the fuel cell and to heat auxiliaries for the crew.

DC/DC converter

As explained in detail in Apendix C, a fuel cell has a non-constant voltage. At lower load, the terminal voltage is higher than when the fuel cell is loaded. Especially in the first part of the curve, the output voltage is non-linear with the current. This DC voltage feeds the inverter shown in the previous section. This voltage must be within a certain range, which depends on the inverter powering the electric motor. Additionally, when combining techniques such as fuel cells, batteries and/or super capacitors, the output voltage of these separate devices determines the division of the load. Therefore, the output voltage of the fuel cell must be controllable. Increasing the voltage lowers the current and the losses associated with this current. Practically, the voltage is mostly limited by the electronic components. For installations in our size (below 1 Mwe), a DC operating voltage between 690V and 1000 V is common. To achieve this, the fuel cells are put in series to form a stack.

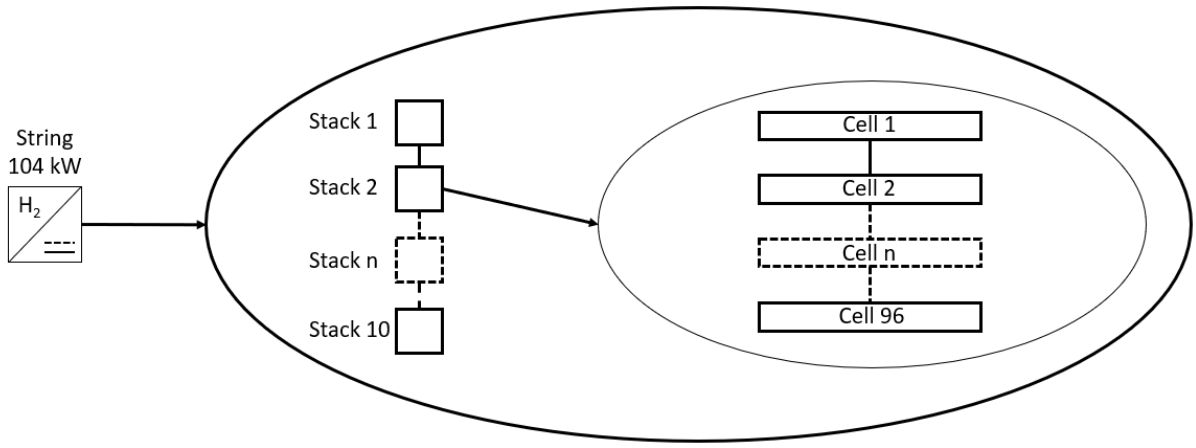

Figure 25: Composition of a fuel cell string

Several of these stacks are also put in series to form a fuel cell string or module. The Nedstack PemGen 500 consists of 6 strings, each containing 10 stacks. Each stack is built of 96 cells. The theoretical maximum power of this PemGen is 624 kWe. The rated power is 500 kWe. The difference between the two is to make sure that the fuel cells can deliver 500 kWe after they age.

As shown in Figure 61, the cell voltage depends on the load. This might not be a problem in a DC installation, but to control the division of load between several power sources, a converter should be added after the string. This converter keeps the output voltage constant and controls the division of load. For an AC installation, a converter is required, as AC installations must have a fixed voltage and frequency. Depending on the size of the installation, several strings are put parallel. This layout also adds redundancy, as a failure in one cell can render an entire string unusable. In this report the string size is around 100 kW.

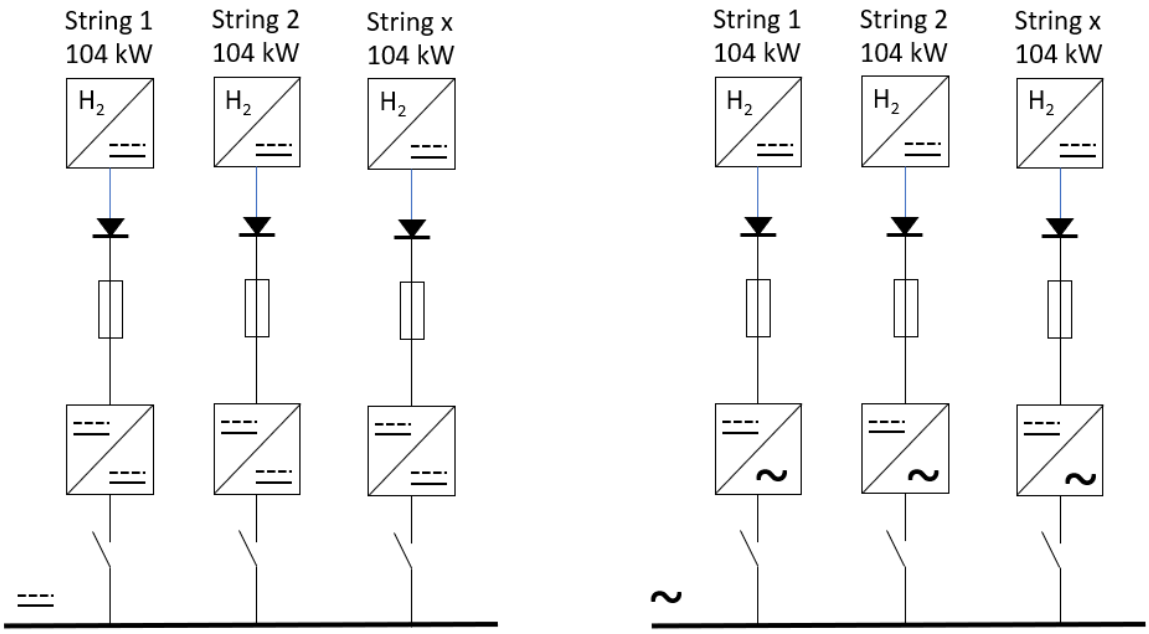

Figure 26: DC installation (left) and AC installation (right)

Another advantage is the ability to switch fuel cells on and off depending on the load. Currently stacks have to be replaced after about 24000 hours. This is independent of the load during the running hours. Switching off a string means fewer running hours for that string and therefore fewer stack replacements. The downside is that running with fewer strings means a higher load, and so a lower efficiency, of the remaining strings. As mentioned before, switching strings on and off is also limited to one or two times a day and involves making that string inert with nitrogen. Determining a final strategy is an optimalisation problem that depends on many variables.

Figure 26 shows two examples of a fuel cell installation. The diodes after the strings indicate that the power flow is only into the system. Fuses are needed as a protection. Depending on the installation, the converter is DC/DC or DC/AC. In our installation. the DC/DC converter, a so-called chopper. is used. Using DC makes it easier to combine other techniques, such as batteries or supercapacitors, to support the fuel cell system. Both batteries and supercapacitors temporarily charge and discharge electrical energy. They can be used to filter out energy fluctuations and provide a more constant load on the internal combustion engine and the fuel cell. They could also be used to store energy during sailing and release this energy in a short time, for example when manoeuvring with the bow thruster. This means some equipment that has to be sized for peak loads, such as an auxiliary generator or the fuel cell, can be smaller. The disadvantages of these techniques are a more complex installation and a higher cost.

DC/DC converters are used to connect the fuel cell strings to electricity grid. Depending on the load strings can be switched on and off, the optimal strategy is subject for further research. Using a DC grid makes it possible to use batteries and super capacitors to improve stability.

7.5 System integration

So far, the separate techniques to be used were briefly discussed. The end goal is to drive the propellor shaft. As both the internal combustion engine and the electric motor have a higher rotational speed than the propellor, a gearbox is required. As long as the electric motor has a maximum speed of 1500–1800 rpm, a standard gearbox, such as the RENK T^2RECS, [48] is suitable. Other setups are possible but would cost more. In any propulsion concept, but especially when combining two power sources with a different working principle, it is important to perform a thorough torsional vibration analysis to prevent damage in the driveline.

A clutch is mounted between the internal combustion engine and the gearbox. This makes it possible to disengage the ICE from the propellor shaft and only use the electric motor for propulsion. This works when steaming at low speeds and, depending on the size of the fuel cell, also during higher speeds and manoeuvring. The electric motor does not need a clutch as it can rotate freely when not used. Another advantage is that this setup can return to port safely when there is a technical malfunction in one system that cannot be solved at sea.

The installation of both the internal combustion engine and the electric motor is dictated by the shaft line, as they both feed in on the gearbox. The other components, such as the fuel cell stacks and power converters, are more flexible in their installation location. Both the engine and the fuel cell have rules and regulations regarding their installation. Additional regulations apply when building a vessel that can use hydrogen as a fuel. Class rules, such as DNV, have additional rules for low flash point fuels. DNV Rules for Ships, part 4, chapter 3, paragraph 10 specifically describes these rules for gas only and dual fuel engines. This report does not go into detail on the rules, but the most important is that the vessel must be able to continue without interruption in diesel-only mode in case of problems with the hydrogen installation. Additionally, the switch from diesel to dual fuel mode must only be possible when a range of requisitions is met to make it safe. The piping of the hydrogen system must be double walled and the ventilation of certain spaces is bound to minimal limits. This all to ensure that a safe operation is possible. Apart from class rules, the IGC code (international code for the construction and equipment of ships carrying liquefied gasses in bulk) and IGF code (international code for ships using gases or other low-flashpoint fuels) could be applicable to a (dual fuel) hydrogen powered vessel.

D. Jansen at Conoship already created a concept design for installing the fuel cells and auxiliaries. In our case, the setup will likely be smaller, but this does not change the basic layout. Another option would be to use a containerized installation, such as offered by Nedstack. Although this is not ideal from the maintenance point of view, it could make the installation flexible, as in case of a malfunction or if the stacks have to be replaced, the complete container is removed and sent to a workshop. Especially in the case of a small fuel cell installation (between 250 kW and 500 kW), the complete installation can fit in a standard 20 foot container.

For whatever mechanical setup is chosen, the most challenging part will be the system integration. Although proven techniques will be used, the system integrator has to make sure that the installation has a stable and sturdy response in all situations without too much intervention from the vessel’s crew.

Another point of attention is the propellor. The use of a fixed pitch propellor is preferred, but care must be taken that in case of a failure of the fuel cell installation, the vessel would still be (partly) manoeuvrable with only the internal combustion engine. This could mean that the forecasted 5% efficiency gain with a fixed pitch propellor cannot be met.

Vessel layout and legislation

The vessel layout and the propulsion package do not leave much room for alternative setups. The gearbox is connected to the propellor shaft in the aft part of the vessel. As the gearbox is relatively compact, this can be done in a small section. The clutch and the internal combustion engine are put in front of the gearbox such that there is enough (maintenance) room for the engine while keeping the engine room as compact as possible. The electric motor is bolted directly to the gearbox, although a different setup with an extension shaft is possible if necessary. All other components' locations are flexible, as there is no need for a mechanical connection, only electrical. Possible layouts for this equipment have been studied within Conoship.

Class requirements largely comply with the same rules as other fuels with a low flash point. These rules are constantly developing, but one implication for the proposed design is that double walled pipes must be used. As the internal combustion engine can run on (bio) diesel only, the requirement of two completely independent fuel-containment systems and energy converters is fulfilled. Furthermore, the ship designer has to prove that the vessel is as safe as conventional powered vessels via a risk-based methodology. The rules describe redundancy (single failure of critical modules) and alarm and shutdown functions on several levels. Another point of attention is the ventilation rate, which is higher than for diesel powered vessels. The ventilation is based on the leak scenario for a room. The ventilation must dilute the hydrogen to prevent an explosive concentration.

Another legal framework is the International Code of Safety for Ships using Gasses or other Low-Flashpoint Fuels. The IGF code contains detailed prescriptive requirements for liquefied natural gas (LNG) as fuel. For fuels other than LNG, the IGF code refers to the 'alternative design' approach. This means that the IGF code does not contain specific requirements for fuels other than LNG, but these fuels can still be used if their safety level is comparable with a ship using conventional fuel.

Summary: A gearbox connects the internal combustion engine and the electric motor. A clutch is used to make it possible to disengage the internal combustion engine from the driveline. The fuel cells can be installed in a standard 20 foot container or be integrated in the vessel. Classification societies have additional rules for low flashpoint fuels, including redundancy requirements.

7.6 Control options

The ICE is a torque machine. Fuel is burned in the cylinders, creating pressure inside them. This pressure produces force on the piston. This pressure varies, and the force on the piston is nonlinear. This force is converted by the connection rod and crankshaft to a torque on the output shaft. The result is a highly fluctuating torque output. This is partly improved as an engine has several cylinders and by adding inertia in the form of a flywheel. Nevertheless, the torque produced will have some fluctuations. Orie Sakamoto researched how to model this fluctuating torque, based on a low power (100 kW) 12 cylinder diesel engine. [41].

.

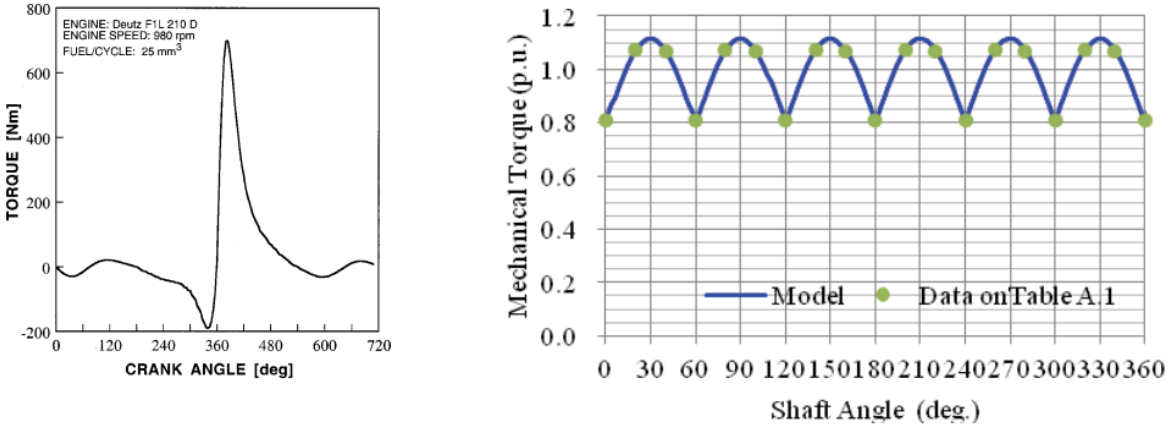

Figure 27: Torque relative to angle for one cylinder [17] (left) and (modelled) engine torque based on a model of Orie Sakamato [41].(right)

The torque of the engine in our case drives a propellor shaft. Without a governor, the engine speed would rise or fall until the torque delivered by the engine equals the torque consumed by the propellor shaft. Currently, almost all vessels are equipped with a speed governor that regulates the engine torque such that the engine speed remains constant. This leads to a continuously changing amount of burned fuel in each cylinder. Personal communication with ABC engines and a Lloyds surveyor showed that engines running on gas are vulnerable to these fluctuations in the long run. This might affect their reliability and add to maintenance costs. This is under investigation by many parties, although no clear information is available yet. Running the engine in a constant torque mode, and thus with a constant fuel supply, might help solve these issues. This would keep the engine running as constantly as possible, which is highly preferred by the engine manufacturer ABC.

However, as a vessel sails through waves, it is not possible to eliminate torque variations in the propellor shaft. This could be solved by using a controllable pitch propellor to limit load fluctuations. To a certain limit, it should be possible to maintain the torque on a certain level by continuously adjusting the propellor pitch. However, this rules out the use of a fixed pitch propellor with a higher efficiency. This also involves a fast-reacting controllable pitch propellor combined with a good adjusted controller. Additionally, whether a controllable pitch propellor can perform fast adjustments over a long time span must be determined. Normally, these propellors are built to have a constant pitch over a long time, so wear and tear might be too high with a normal CPP.

The goal is to load the diesel engine as constantly as possible. Next, control options are discussed.

Constant speed

The constant speed option is currently the most used in the maritime industry. Almost all vessels set the propellor speed with the lever on the bridge. The torque of the propellor shaft fluctuates and depends on the speed as or less fuel is injected in the ICE. Or, in case of an electric propulsion, more or less electrical energy is admitted to the electric motor. If the vessel is fitted with a controllable pitch propellor, the pitch could be controlled, but the propellor still remains at a constant speed.

In a conventional vessel with only one motor driving the propellor, the speed regulation is relatively simple. In the case of a combined system with two or more combustion engines or a combination with one or more electric motors, the system becomes more complicated. Figure 28 is a schematic representation of such a system, consisting of an internal combustion engine and an electric motor driving a propellor shaft via a gearbox. As both the engine and the motor are mechanically connected via the gearbox, they both run at the same speed. The lever on the bridge controls the speed setpoint that is fed to the governor of the ICE and the VFD of the electric motor. When the system is in a stable operating mode, the torque of the ICE and electric motor equals the torque of the propellor and the speed of the propellor remains constant. In case of a disturbance, for example, if the propellor needs more torque due to a wave, there is a mismatch in the delivered torque and the required torque. In this example this mismatch is negative, leading to a decreasing propellor speed. This decrease in propellor speed will cause a reaction of the speed controllers of the ICE and electric motor, resulting in more fuel admission and more electric current to the e-motor until there is an equilibrium again.

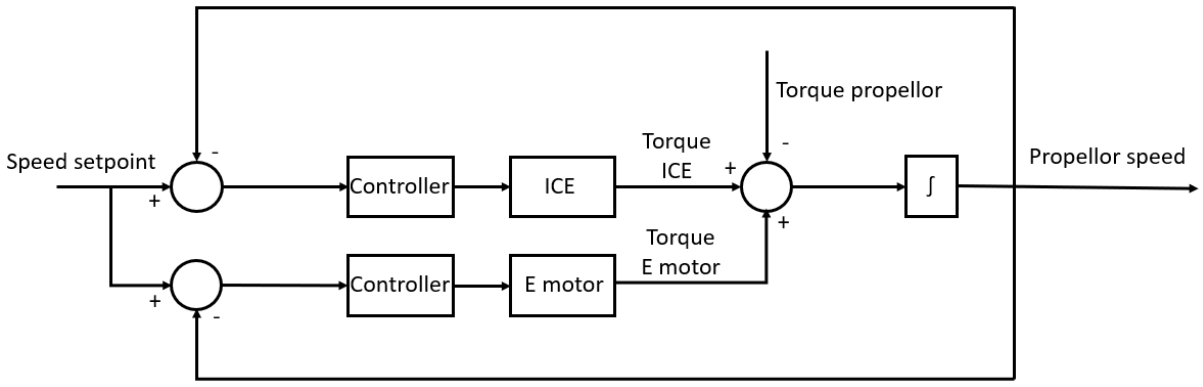

Figure 28: Block diagram of the control loop of a combined system in a speed regulation setup.

For our case with roughly a 500 kW ICE and a 250 kW electric motor, a simplified plot is shown in Figure 29. The speed of the propellor is plotted with the torque of the propellor, ICE and electric motor. There are no values on the axes and they are not to scale, as this is just a plot to clarify the response.

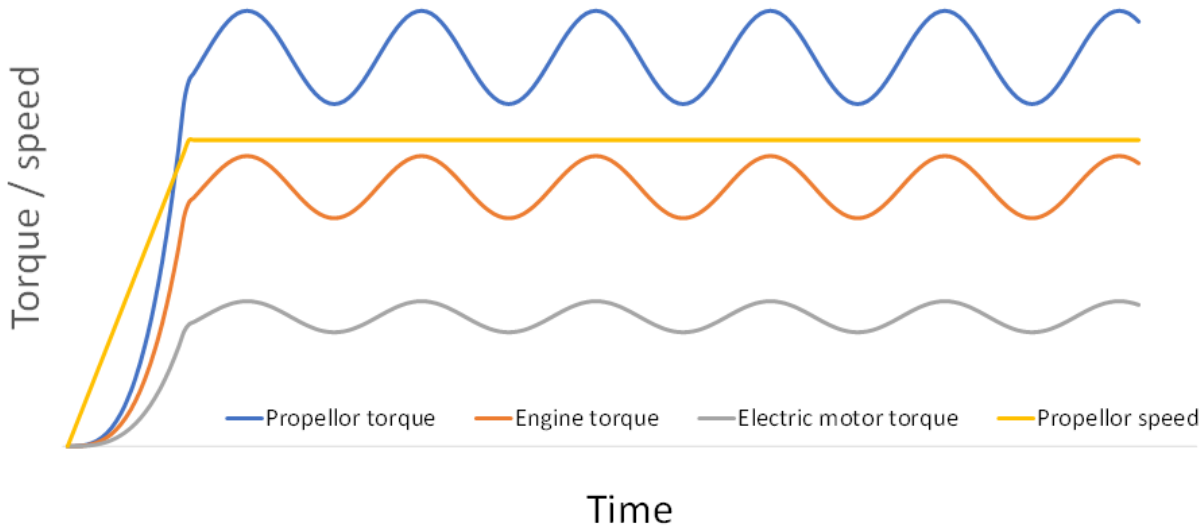

Figure 29: System response in speed control (axes have no values and are not to scale)

The plot shows a vessel starting with a zero speed. The installation is running in its normal operational region and without extreme disturbances such as a propellor coming out of the water due to heavy weather. The setpoint of the propellor is set via the yellow line, according to the propellor law. In reality the setpoint will be set in steps, causing the propellor to rotate faster than the propellor law, creating additional thrust (and losses) until equilibrium is reached. For now, however, this has no influence on the response of the system when sailing. When the vessel is at speed, the propellor speed has a fixed value. The torque on the propellor is not constant. It will contain higher frequency components induced by the propellor-hull interaction (not drawn in the plot) and lower frequency components caused by waves. As the ICE and electric motor are controlled in speed mode, the torque on both the ICE and the electric motor fluctuates. In the plot, the propellor speed is drawn in the ideal situation, so with no speed deviation. In reality, a small speed fluctuations will occur.

In this setup, the torque and power delivered by both motors are not constant. As the ICE and electric motor have different operating principles and power levels, it is important that both machines deliver power at the same rates. The electric motor, with its VFD, can react much faster, also due to the lower inertia, than an ICE. To avoid too large fluctuations, both controllers must be set carefully to prevent oscillation of the VFD. To share the load in a certain ratio, the principle of speed droop (described in Attachment A-1) can be used.

Constant torque

A different option would be to control both the ICE and the electric motor in constant torque mode. Doing so would mean that the lever on the bridge would not set the speed but the torque setpoint. As this will be strange for the crew, especially during manoeuvring, this mode might only be selected when sailing.

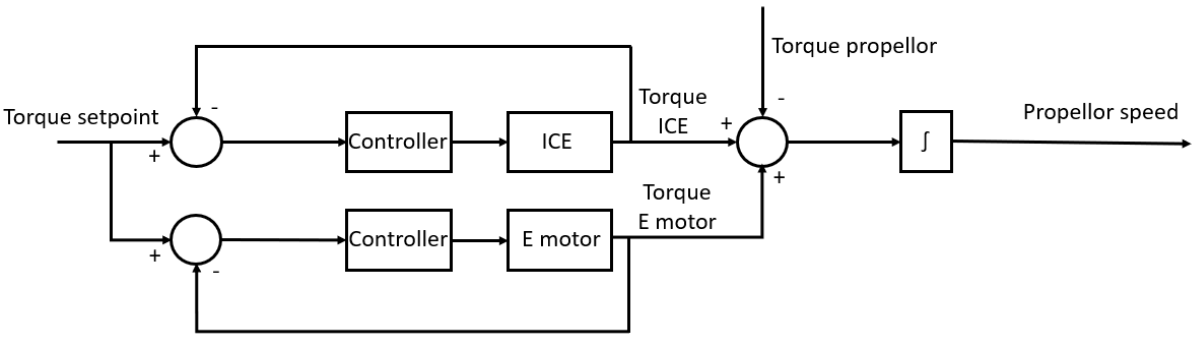

Figure 30: Block diagram of the control loop of a combined system in a speed regulation setup.

This option will lead to a fluctuating propellor speed. Currently Conoship is undecided whether a variable or constant propellor speed is more efficient. This question involves many parameters, including the effects of water on the propellor and hull and the efficiency of the ICE and electric motor.

Running in constant torque mode is not the same as constant power mode. If the speed fluctuates but the torque remains constant, the power will fluctuate linearly with the speed variation. The speed governor of the ICE and the VFD of the electric motor will therefore still continuously vary the energy and fuel flow to the motors.

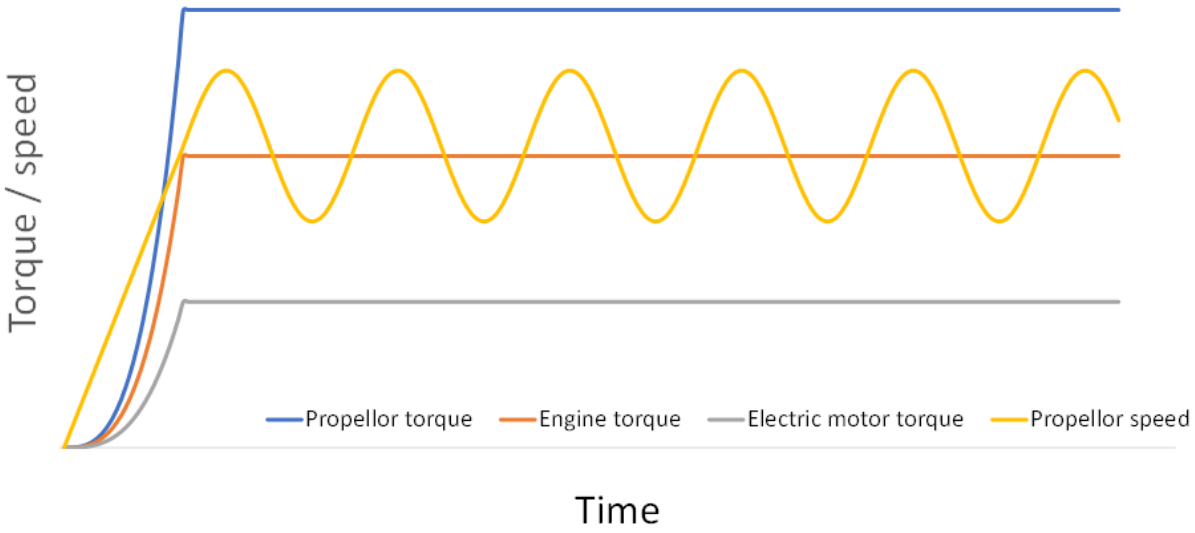

Figure 31: System response in speed control (axes have no values and are not to scale)

In reality, the torque will not be completely constant due to inertia effects and the regulating action of the governor and VFD. This control loop must include safeguards to avoid overspeed situations in case the propellor loses torque quickly. This will not happen in most situations, but when sailing in high waves there is a change that (part of) the propellor will come out of the water, resulting in a sudden loss of propellor torque. When this occurs, the system should change over to speed regulation.

Combination of speed and torque regulation

To keep the ICE running as constantly as possible, it should run in constant power mode, a constant speed with a constant torque. This implies that the diesel engine is put into constant torque mode by keeping the amount of injected fuel constant. This would lead to a fluctuating

propellor speed depending on the torque needed by the propellor. To prevent (large) speed fluctuations, the electric motor delivers the fluctuating torque, so the ICE torque and speed and the propellor speed can remain constant level.

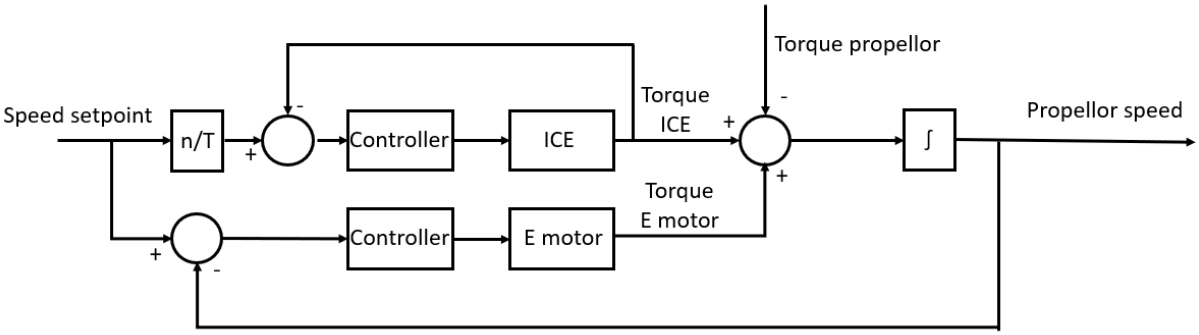

Figure 32: Block diagram of the control loop of a combined system in a speed regulation setup

The proposal above requires a sophisticated and robust overall regulator supervising both the ICE and the electric motor. Based on the position of the lever on the bridge the system will first use both the ICE and the electric motor to increase the propellor speed, likely in speed control mode. When this speed is reached, the system has to analyse the envelope of torque fluctuations on the propellor shaft. If this falls within the envelope of the electric motor, the engine is put into torque mode and the torque is lowered such that it is constant. The electric motor is used to keep the speed constant and absorb the torque fluctuations. In the event of a big torque step, such as the propellor coming out of the water, the engine immediately switches back to speed control. Figure 33 shows this principle. The vessel starts in this example from zero speed to a certain cruising speed, so the propellor torque increases according to the propellor law. Then, when at this speed the waves start. After a period of time, for this example after 3 waves, the engine enters the constant torque mode, leaving the electric motor in control of the speed.

There are systems on the market that let the engine run in a constant power mode. However, these are fully electric systems with no direct connection between the propellor shaft and the ICE. These vessels use an electric motor to drive the propellor with a constant speed, while the ICE drives a generator at a constant power. If the propellor momentarily needs less power, the surplus of energy is stored in a battery. Then this energy from the battery is used when the propellor requires more energy.

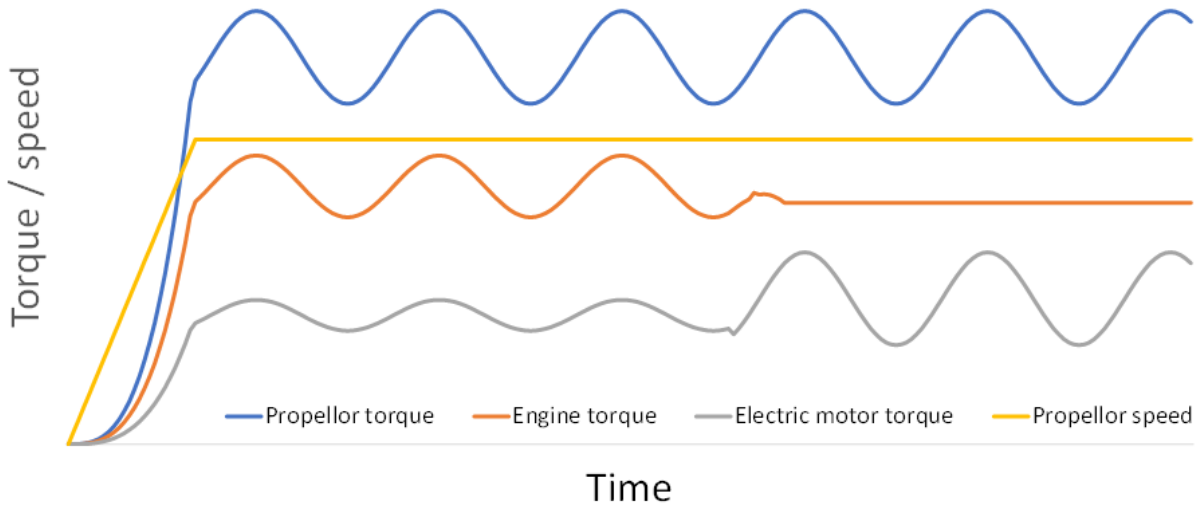

Figure 33: System response in combined torque/speed mode

Discussion about control strategies

As our main goal for this report is for the ICE to run as constantly as possible, the third option, a combination between the speed and torque control, is preferred. Unfortunately, this is also the most complicated choice. In the first two options, speed control and torque control, both the ICE and electric motor operate in the same control mode. Apart from controller settings to have a synchronous response and to have a correct load division, it uses classic control methods.

For the third option, henceforth called ‘combined control’, a more complex control strategy is needed. To make sure that the electric motor is always acting as a driving machine, and is not driven by the ICE, the control system has to ensure that it is only possible to switch to combined control if the envelope of the torque variations on the propellor shaft are within the capabilities of the electric motor. If this is not the case, it might still be possible to use the control strategy up to the limit of the electric motor to reduce the torque fluctuations as much as possible. If this point is reached, the speed of the propellor will drop and rise again until the electric motor returns to within its operating envelope.

The combined control is intended for sailing. When sailing at low speeds, the ICE is not needed and is stopped. As mentioned before, in case of a (partial) torque control, safety loops must be active to switch over the control system to speed control in case of sudden load drops.

Summary: The speed control option, with a non-constant torque load for the ICE and electric motor, is currently the most used in the maritime industry. To load the dual fuel hydrogen ICE as constant as possible a combined control option is proposed, having a speed control option when manouvring, and a constant torque mode for the ICE when sailing. The electric motor is used to compensate the torque fluctuations and keep the propellor speed constant during sailing.

7.7 Conclusion

The most promising setup is the directly driven fixed pitch propellor setup with an internal combustion engine and an electric motor driving the shaft via a common gearbox. During sailing, the combined control system is used to keep the ICE running in constant power mode. The advantages of this system are:

- The internal combustion engine can run in constant torque mode for a long time.
- As the speed is held constant by the electric motor, the ICE is running in constant power mode, the most stable operating mode possible. Both the mechanical and thermal loading of the ICE remain constant.
- The installed power is used optimally. The installed auxiliary power for the bow thruster is also used for propulsion purposes and for peak shaving of the torque variations.
- As there are two independent power sources, the vessel always has a backup to return to port safely.
- Depending on the amount of power from the fuel cells, the vessel can sail at lower speeds, and manoeuvre on only fuel cells, preventing local emissions.
- When no hydrogen is available, the vessel can continue its voyage on diesel oil only at reduced speed.
- As the electric motor is powered by a DC/AC converter it is possible to use a DC grid. This makes it relatively easy to install additional equipment, such as batteries and super capacitors, if this would be beneficial for the system response.

8 Conclusions and recommendations

Introduction

In this chapter first the research question is answered. Then the sub questions are answered and an overall conclusion is presented. The last part is are final conclusion and the recommendations.

Main research question

At the start of this research the following research question is formulated:

How can an internal combustion dual fuel engine and/or LTPEM fuel cell be integrated to form a cost effective solution to propel a short sea ship running on hydrogen?

The research question has been difficult to answer. There are several good technical setups to propel a vessel using hydrogen. The choice largely depends on unclear future developments. These include economic developments, such as the fuel prices and the size of the CO_2 penalties, and technical developments, such as fuel cell technologies and life time expectance of equipment. Additionally, personal and company preferences and strategies can, and will change during the upcoming years. These have already changed in the one and a half years of this research. The most important change is economic: at the start of the research the fuel price was not an issue and green hydrogen a must. However, during the research this shifted to a transitional point of view that green hydrogen to start with is both economically and practically unfeasible. This also influenced the choice of the configuration. If the only consideration is 'no local CO_2 emissions', a 100% fuel cell solution would be chosen, as well as being the cheapest solution for the use case.

After discussion with Conoship, a combination solution with an internal combustion engine and a fuel cell installation in a directly driven propellor shaft layout was chosen, as shown in Figure 37. This concept has the advantage of combining a proven technology with transitional package. That way, during the energy transition phase, the vessel can run on a combination of diesel and hydrogen or on diesel only. The diesel can be biodiesel to minimize the carbon footprint.

Depending on further research the size of the dual fuel hydrogen engine can vary. In this report a size of 500 kW and 750 kW were used. The fuel cell size is 500 kWe in the first case and 250 kWe in the second case.

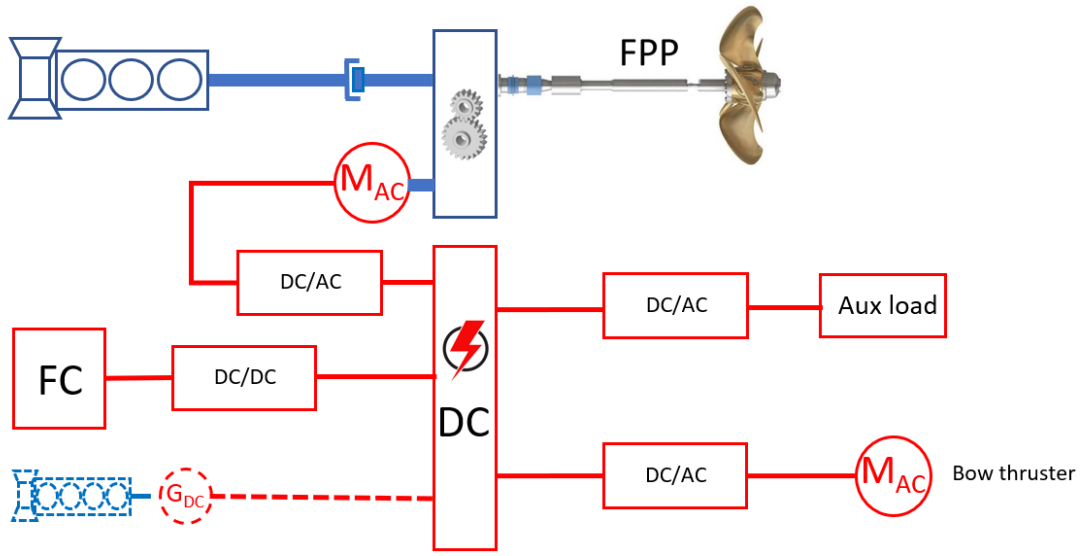

Figure 34: Selected setup with additional DC generator to run on (bio)diesel only

To be able to run on (bio)diesel only, an additional generator set has to be installed to supply the electrical consumers when the fuel cell is not in operation. The bow thruster cannot be used in that case, unless the generator set is large enough (around 300 kW). This size would also allow the generator set to supply electrical energy to the electric motor assisting the dual fuel propulsion engine. In that way, (part of) the power of the fuel cell can be compensated in case of maintenance or a breakdown.

Having this additional generator set as a backup for the fuel cell could also be necessary when using an optimized fixed pitch propellor. An optimized fixed pitch propellor provides an efficiency improvement of at least 5%. The drawback is that the required torque, in combination with a low propellor shaft speed, during manoeuvring, is too high for an internal combustion engine. An electric motor has no issues with high torques at low speed. so a combination of the two could make it possible to use an optimized fixed pitch propellor with this design.

Sub questions

What are options to propel a ship using an internal combustion engine, an LTPEM fuel cell or a combination of both, and how do these options score regarding CAPEX, OPEX, and efficiency?

Nine different designs are presented and for these designs the CAPEX, OPEX and fuel costs are calculated. These numbers are based on a use case and a use case scenario. In the CAPEX calculations the largest unknown factor is the hydrogen storage and treatment installation. For the fuel costs the development of the fuel prices in the future have the largest impact. To be

able to compare the different designs the term CO_2 penalty is introduced. All designs are compared with the reference design, being a vessel propelled with an internal combustion engine running on diesel oil. As the alternative designs have larger investment costs, but a lower CO_2 emission, it is possible to calculate the penalty per ton CO_2 emission to reach the break even point in the use case of 20 years. Figure 35Figure 38 contains the cost overview of the different designs and the CO_2 price necessary to reach the breakeven point in 20 years.

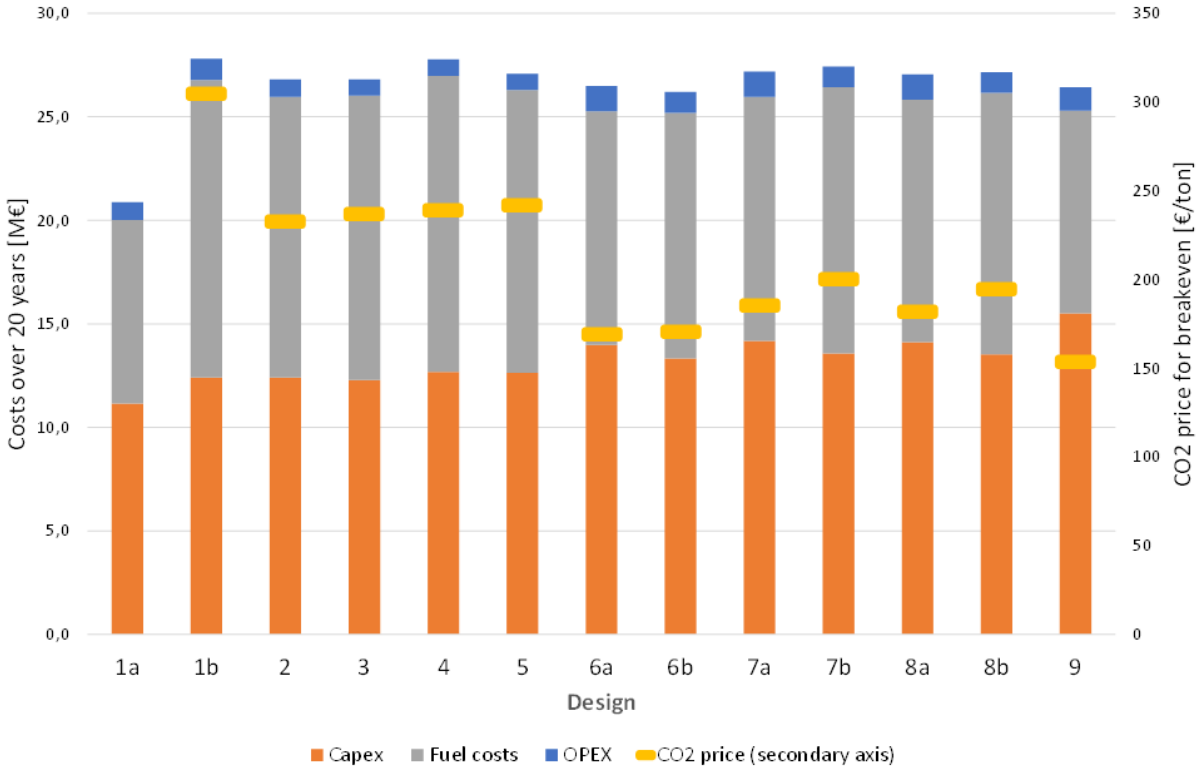

Figure 35Figure 35: Cost overview of the different scenarios and the CO_2 price necessary to reach the breakeven point (previously used as Figure 16)

How can the economic efficiency be maximized by using additional energy recovery equipment and by using a total system integration?

Heat recovery from the internal combustion engine is possible in theory, however, practically the relatively low power of the installation makes it challenging. The heat contained in the exhaust gasses and jacket cooling water can be recovered with an organic Rankine cycle. The investment for the installation is such that it just fits within the use case, but available systems are designed for a minimum internal combustion engine of 1 MW. Therefore, it remains to be seen if such a system in the proposed design is feasible.

Producing pure water with the heat for the use of NaBH4 could be an option, however, this is normally done with reversed osmosis, requiring electricity. As we have concluded before, economically producing electricity with this installation will be challenging, so the economic feasibility depends on a specific use case with NaBH4.

Heat recovery for heating purposes, such as for accommodations, is possible for both the heat from the combustion engine and the fuel cell.

Can this setup handle the vessel's power demands or are additional measures, such as batteries or capacitors, needed?

It is still unknown whether the proposed setup is fast enough to respond load changes. One reason is that the expected propellor shaft torque changes, when propelling the reference case vessel, are still unclear. Conoship and other external sources were not able to deliver this information. This could be a topic of another research project. Second, no verified data is available from the fuel cell manufacturer. According to them, load steps up to 40% have been done, but they have not shared measurement data yet. Essential information, such as time constants, were also not shared or not available. This requires further research, preferably by someone who is performing research or a thesis at the manufacturer. By using a DC grid as proposed in the chosen design it will be relatively easy to integrate batteries or capacitors if further research points out that this is necessary.

Further research should also provide more insight into the recent attention of the manufacturer on higher frequency current ripples, as batteries or capacitors might also be a solution to prevent this ripple, if present, from reaching the fuel cell. There is not much information yet available on this topic, as the manufacturer is just starting research on these current ripples and their effect on the fuel cell.

In a non-conventional electric system, what is a high-level system integration regarding control techniques?

The design used is non-conventional solution for the maritime industry. When manoeuvring the vessel, the most likely control method for both the internal combustion engine and the electric motor is speed control. When sailing in open seas, the proposed control method is constant torque control for the internal combustion engine. The electric motor will be in speed control, maintaining the propellor speed constant while filtering out the torque fluctuations of the propellor shaft. This principle is shown in Figure 36. This method requires a high-level control system to enter this mode when shifting the torque fluctuations towards the electric motor. The system must also have safeguards to switch back to speed mode when operating limits are almost reached to prevent the internal combustion engine from stalling. These techniques are not new, but the total system integration involves nonstandard combinations.

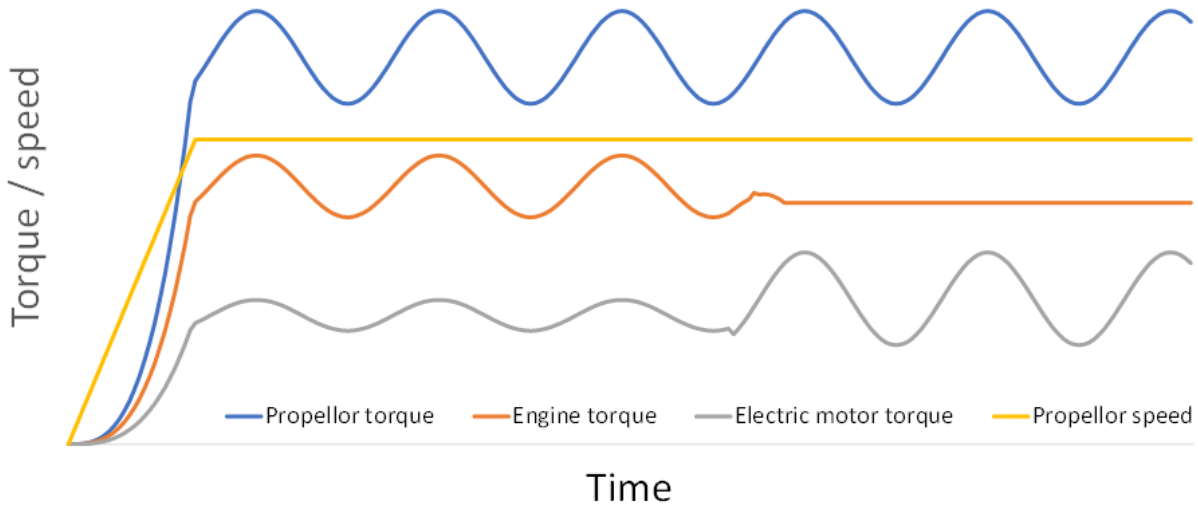

Figure 36: System response in combined torque/speed mode (previously used as Figure 33)

As the internal combustion engine speed is directly coupled to the propellor shaft, the speed cannot be varied to let the engine run at an optimal efficiency and H_2 ratio. The load can be varied at a certain speed to improve one the efficiency or the H_2 ratio. However, the efficiency of the fuel cell is the highest when operating at virtually no load. The control system must therefore also take into account the most optimal division between the engine and the fuel cell. This multiparameter control method is an important part of the complete system integration. To optimize the system, a more precise sailing pattern is needed, as the long-term economic feasibility depends not only on the efficiency of the equipment, but also on the amount of running hours, as this influences the OPEX.

What are the high-level design impacts of the options regarding vessel layout and regulations?

The general layout of the vessel is standard. The gearbox and internal combustion engine are placed in the aft of the vessel such that the engine room is as compact as possible. The electric motor can be bolted directly to the gearbox. The other parts only involve electrical connections and thus are flexible in their location.

Legislation is currently mainly focused on LNG, but the same approach is used for other fuels with a low flash point. DNV describes this approach in their ‘Rules for classification of ships’, chapters 6 and 7. The IGF code must also be followed. The ship designer must prove that a vessel using low flash point fuel is as safe as a vessel using diesel oil using a risk based approach. Practical requirements include redundancy, in our case fulfilled by the internal combustion engine being able to run on (bio) diesel only. Double walled pipes must be used and the ventilation must be sufficient that in case of a leak the hydrogen is diluted to prevent an explosive atmosphere. The type and layout of the storage system will have also have a large impact in the design, but that is not part of this thesis.

Recommendations for future research

As mentioned before, not all questions could be answered within the timeframe of this thesis. Attachment F provides Conoship the main points for future research. A multidisciplinary approach is necessary for future research, as there are still blind spots in mechanical, electrical, control and hydrodynamical topics. The total system integration must also be done with all these specializations.

To provide a proof of concept and gather more information about the application, a Simulink model of the installation should be created. This model should not only give information about the low frequency response of the system but also about higher disturbances (if present) caused by the power electronics. A complete model was not possible in this report. Nevertheless, the setup and start of such a model is described in Attachment E. This model contains all parts, such as the fuel cell, electrical installation, dual fuel internal combustion engine and the disturbances from the propellor. This model can be used to test strategies based on a single aspect, such as the dynamics of the fuel cell installation, but can also be used to develop the overall control system and its control strategies.

To validate the model, a full-scale installation should be available. MARIN is currently working on a small installation in its zero emission lab. This could be a good option in the near future (mid 2022) to validate a complete system. Parts of the model can be validated by comparing the outcomes with test data from manufacturers, if available. For the first setup, parts of a possible model are compared with a small-scale electrical setup at the Maritime Institute Willem Barentsz. Sufficient equipment is available there to build a basic setup as described in Attachment E. This small scale setup can be a base for further, low cost, research to gain more insight in parts of the installation such as the overall control system.

Overall conclusion

This research presents a design for combining a dual fuel hydrogen internal combustion engine with a fuel cell to power a short sea vessel of around 3800 GT. This design is currently more expensive to build, and to operate, than a conventional vessel running on MDO. As it is generally expected in the maritime industry that in the near future a penalty will be introduced for CO_2 emission, this difference will decrease. For the proposed design, a CO_2 penalty of 170 €/ton is necessary to reach the breakeven point in the use case of 20 years. The proposed design has the advantage that it is still possible to run on MDO or biodiesel only if hydrogen is not available. This also makes it possible to comply with the redundancy regulations from class as hydrogen is a low flashpoint fuel.

Due to the relatively small power output of the combined installation, heat recovery is limited to heating purposes of domestic systems and the accommodation.

To have the dual fuel hydrogen internal combustion engine running as constant as possible, with respect to thermal loading, and with a constant hydrogen-diesel ratio, a combined speed and constant torque control is presented. The electric motor, powered by the fuel cell, absorbs the torque fluctuations of the propellor shaft and keeps the propellor shaft speed constant. This mode of operation is only possible when sailing with a constant propellor speed. The limits of the torque fluctuations absorbed by the electric motor are subject to the size of the fuel cell and the electric motor. Further research is necessary to determine the expected torque fluctuations, the fuel cell response and the overall control system.

9

References

[1] ABB. *ABB ACS6000 MV drive course documentation*. ABB.
[2] ABB, Ed. *Energy Efficiency Handbook, chapter 5.13: HIgh efficiency motors. Towards zero emission*.
[3] ABB. *Type test report 500 kW asynchronous AC motor*.
[4] ABB. 2017. *Shipping 4.0, Navigating the 4th industrial revolution*.
[5] ABC, personal communication.
[6] Adam B Dempsey et al. 2016. A perspective on the range of gasoline compression ignition combustion strategies for high engine efficiency and low NOx and soot emissions: Effects of in-cylinder fuel stratification. *International Journal of Engine Research* 1, 21.
[7] Aina T. et al. 2012. Influence of compression ratio on the performance characteristics of a spark ignition engine. *Advances in Applied Science Research* 3, 1915–1922.
[8] Alewijnse, personal communication.
[9] Alewijnse. 2006. *MV Avalon electrische installatie*.
[10] AMW marine, personal communication.
[11] Anglo Belgian Corporation. *Product guide*. ABC.
[12] Anibal T. de Almeida et. al. 2014. Beyond Induction Motors. Technology Trends to Move Up Efficiency. *IEEE Transactions on Industry Applications* 50, 3, 2103–2114.
[13] Aradex. 2020. *Aradex datasheet DC-DC converter VP5000*.
[14] Asgeir J. Sørensen. 2012. *Marine Control Systems. Propulsion and Motion Control of Ships and Ocean Structures* Report UK-12-76. Department of Marine Technology, Norwegian University of Science and Technology.
[15] Bernd-Robert Hohn et. all. 2017. Low Loss gears. *Gear Technology* June.
[16] Conrad U. Brunner. 2011. *Energy-Efficiency Policy Opportunities for Electric Motor-Driven Systems*. Impact Energy, Zurich.
[17] Dennis N. Assanis. 2001. A Nonlinear transient, single-cylinder diesel engine simulation for prediction of instantaneous engine speed and torue. *Journal of Engineering for Gas Turbines and Power* October, 123, 951–959.
[18] DNV. *DNV Rules and standards, Rules for classification: Ships.*
[19] Gabriel Sievi et al. 2019. Towards an efficient liquid organic hydrogen carrier fuel cell concept. *Energy Environ. Sci.* 12, 2305–2314.
[20] Gaffney Cline. 2020. *Focus on Blue Hydrodgen*.
[21] gpgrootbrandstoffen.nl. *Bio diesel price*.
[22] Hans Klein Woud and Douwe Stapersma. 2002. *Design of Propulsion and Electric Power Generation Systems*.
[23] IEC. *IEC 600034-30-1 Rotating electrical machines. Efficiency classes of line operated AC motors*.
[24] J. Kolehmainen. 2011. *Dovetail rotor poles in synchronous permant magnet and reluctance machines.* Doctoral dissertation, Aalto University.
[25] James Larmini and Andrew Dicks. 2003. *Fuel Cell Systems Explained*. John Wiley & Sons.
[26] Jan Fredrik Hansen, John Olav. *Onboard DC Grid. The newest esign for marine power and propulsions*. ABB.
[27] Jason W. Bush et all. 2012. *Transformer Efficiency Assessment - Okinawa, Japan*. Idaho National Laboratory.
[28] Johnny Rengifo et. all, Ed. 2018. *Efficiency Evaluation of Induction Motors Supplied by VFDs*.
[29] Kees Kuiken. 2007. *Scheepsdieselmotoren. Deel 2*.
[30] Kees Kuiken. 2016. *Gas- and Dual-Fuel Engines I. For ship propulsion, power plants and cogeneration*. Book I Principles. Target Global Energy Training.
[31] Kerri Hart et. all. *Improved cost of energy comparison of permanent magnet generators for large offshore wind turbines*.
[32] Martin Kanalik. 2019. *Calculation of Power Transformer Losses due to Harmonic Current Flow*. 0th International Scinetific Symposium ELEKTROENERGETIKA.
[33] Mohammad Kabalo et all. *State-of-the-Art of DC-DC Converters for Fuel Cell Vehicles*. University of Technology of Belfort-Montbeliard, France.
[34] Nedstack, personal communication.
[35] Nedstack. 2020. *PemGen CHP FCPS 500. Solution Technical Proposal*. Nedstack.
[36] Nidec, personal communication.
[37] Nidec, personal communication.
[38] van Nievelt. 2019. *Maritime application of sodium borohydride as an energy carrier*. Msc thesis marine technology, TUDelft.
[39] Nitheesh Saravanan. 2008. An experimental investigation on performance, emissions, and combustion in a manifold injection for different exhaust gas recirculation flowrates in hydrogen–diesel dual-fuel operations. *Journal of Automobile Engineering* 222 Part D, 2131–2145.

[40] Olli Lamminen. 2018. *Development of a permanent magnet assisted synchronous reluctance motor*. Master's thesis, University of Vasaa.
[41] Orie Sakamoto. 2015. A diesel generator model with fluctating engine torque including magnetic saturation for transient analysis using XTAP. *Journal of Electical Engineering Technologies* 10(3), 1298–1303.
[42] Øyvind N. Smogeli. 2010. *2010Propulsion Control. presentation*. Department of Marine Technology, Norwegian University of Science and Technology.
[43] P.J.H. Wingelaar et all. 2007. PEM fuel cell model representing steady-state, small-signal and large-signal characteristics. *Journal of Power Sources* 171, 754–762.
[44] Philips Semiconductors. *Datasheet BY329 series*.
[45] Pon Power, personal communication.
[46] R.D. Geertsma et al. 2017. Design and control of hybrid power and propulsion systems for smart ships: A review of developments. *Applied Energy* 194, 30–54.
[47] Rahman, M. M., Mohammed, K., and Bakar, R. A. 2008. *Effects of Air Fuel Ratio on the Performance of Hydrogen Fuel Port Injection Engine*.
[48] Renk. 2016. *T2RECS brochure*.
[49] shipandbunker.com. *Fuel prices*.
[50] Siemens. *Transformers, product catalogue Siemens*.
[51] ST Microelectronics. 3011. *Calculation of conduction losses in a power rectifier*. ST Microelectronics.
[52] Stamford. *MX321 Automatic Voltage Regulator (AVR). Specification, installation and Adjustments*.
[53] Stamford. *PI736D Winding 312 Technical Data Sheet*.
[54] Stamford. *Stamford N200G4 generator datasheet*. Stamford.
[55] Stamford. *Stamford N250G4 Technical data sheet*. Stamford.
[56] Stamford. *Stamford S5L1D-C4 generator datasheet*.
[57] Statistics Norway. *Emission factors used in the estimations from combustions*.
[58] theglobaleconomy.com. *Urea prices*.
[59] Theodore Wildi. *Electrical Machines, Drives, and Power Systems*.
[60] TNO. 2020. *Impact assessment biobrandstoffen voor de binnenvaart* TNO 2020 R11455. TNO.
[61] TNO, E. L. V. Goetheer, personal communication.
[62] Toshiba. *Datasheet Toshiba Inuslated Gate Bipolar Transistor GT15Q102*.
[63] U.S. Department of Energy. 2012. *Energy Tips: Motor systems*.
[64] Young-Kwang Son et al. 2020. Maritime DC Power System With Generation Topology Consisting of Combination of Permanent Magnet Generator and Diode Rectifier. *IEEE Transactions on transportation electrification* 6, 2, 869–880.
[65] Zehra Ural. 2010. *Mathematical Models of PEM Fuel Cells*. Firat University, Faculty of Engineering, Denizli, Turkey.
[66] Zulhisyam Salleh, Ed. 2013. *Study on parameter determination for 1.5 kW AC induction motor*.

Appendices

A
Electrical systems

A-1 AC systems

Currently, ships are equipped with three phase AC distribution systems. A typical layout of such a system for a small cargo vessel consists of 2 generators driven by a diesel engine. The voltage is fed into a main switchboard and distributed across the vessel from there. Sometimes a shaft generator is fitted on the gearbox from the main engine.

This setup requires the diesel engines to run on a fixed speed to keep the electrical frequency stable at 50 or 60 Hz. When a second generator must be brought online, it has to be synchronized for voltage, frequency and phase angle. This requires time. Sharing the load between the two generators is achieved with the so called 'speed droop'. This causes to engine speed (and so the frequency) to decrease slightly when running on a higher load. The frequency deviation is then corrected by the power management system.

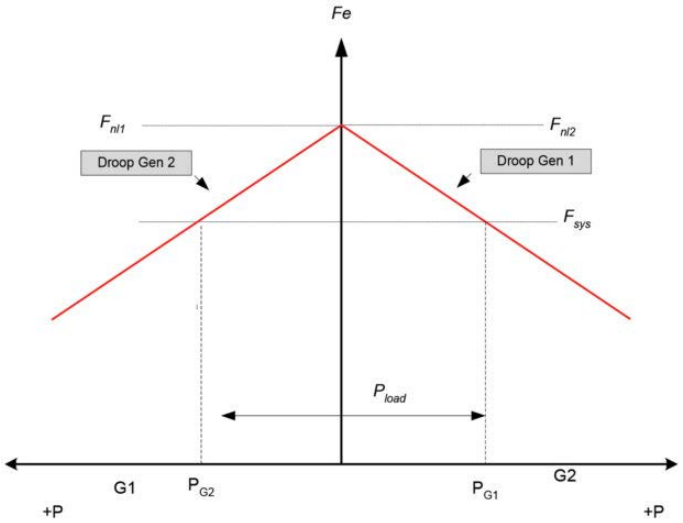

Figure 37: Speed droop to facilitate load sharing between two generators (source: www.ee.co.za)

AC generator

AC generators on ships are always synchronous, meaning that the output frequency is coupled to the rotation speed of the shaft. Asynchronous or induction generators cannot be used, as they need an external grid to operate, so they cannot recover from a dead ship situation. Due to their relatively low rotation speed, ship generators have salient poles. [59]

The voltage delivered by an AC generator relates to the change of the magnetic flux over time in the windings of the stator according to Faraday's law:

$$E = N \cdot \frac{d\phi}{dt} \qquad 2$$

The number of windings *N* in the stator is a fixed value. Therefore, the voltage is linearly related to the rotational speed and the magnetic flux. The rotational speed in a conventional

three phase generator is a fixed value to obtain a frequency of 50 or 60 Hz. This implies that the voltage solely depends on the flux. As conventional plans also have a fixed working voltage, this flux must be regulated.

Modern AC generators are brushless excitation generators. These generators are excitated with a variable DC voltage external power supply, as shown in Figure 38. This DC voltage generates a magnetic field, inducing an alternating voltage in the rotating auxiliary alternator mounted on the generator shaft. This voltage is converted to DC in the rotating rectifier and fed into the rotor windings. There it generates the magnetic flux that induces the alternating voltage in the stator.

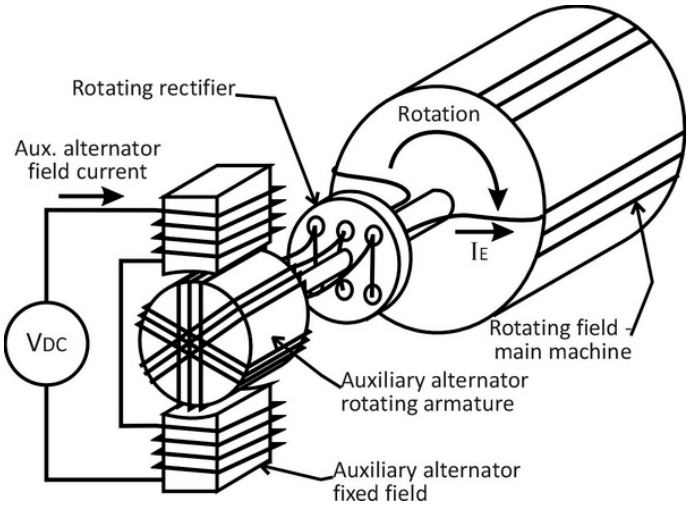

Figure 38: Schematic overview of a brushless synchronous generator. (Source: Ian McKenzie, Quora.com)

The auxiliary alternator field current is controlled with an automatic voltage regulator (AVR). This electronic device measures the output voltage of the generator and controls the field current accordingly. The AVR relies on electronics, making it a fast controller. Due to the inductance of the coils of the auxiliary and main generator, a time constant is introduced, the so called transient reactance [59]. This reactance is only noticeable during extreme load variations, such as short circuit conditions or load shedding due to the generator circuit breaker tripping.

Taking a 920 kVA Stamford PI736D winding 312 generator as an example [53], the sub transient time constant of the stator is 15 ms and the transient time constant is 162 ms. The armature time constant is 18,3 ms. The AVR used is a standard MX321 type [52]. This AVR has a response time of 10 ms and a 0 to 90% field current response of 80 ms. For this report, we focused on the response to load changes, not on failure conditions. Also, the generator operates in its nominal range so there will be no saturation of the magnetic core. Therefore, the generator voltage/current response was considered ideal.

The efficiency of a generator is influenced by:

- Ohmic conductor losses, caused by the resistance of the stator windings. These are quadratic with the current.
- Iron losses caused by hysteresis due to eddy currents in the stator and rotor laminations [59].
- Friction losses.

In no-load operation, the ohmic losses are close to zero and the losses are dominated by the iron losses and friction losses. Increasing the load, and so the current, increases the losses in the stator windings. This leads to a non-constant and non-linear efficiency. Additionally, the power factor and the output voltage influence the output current and so the efficiency. This efficiency depends the size of the generator. Figure 39 shows the efficiency of 920 kVA generator, Figure 41 that of a 287 kVA generator and Figure 42 that of a 230 kVA generator

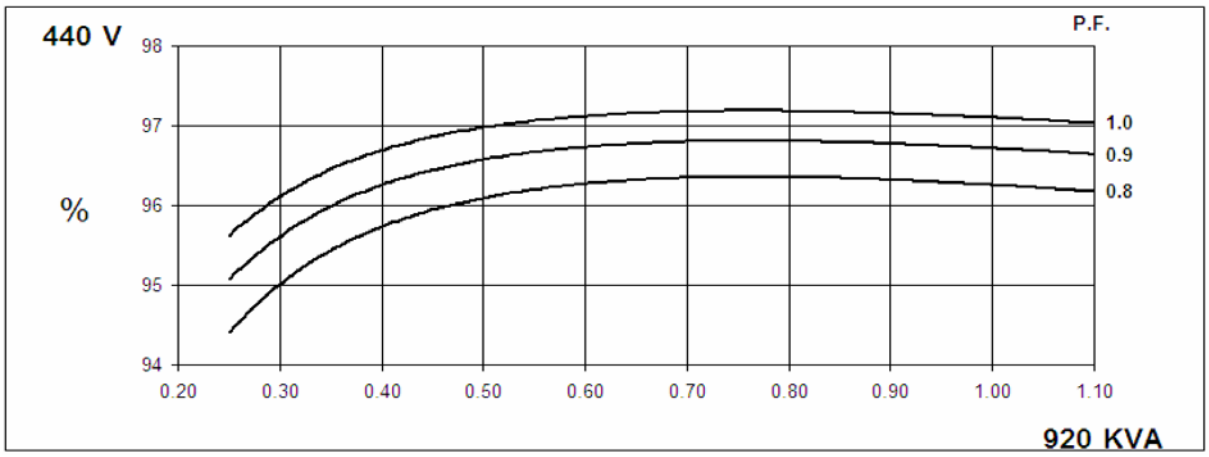

Figure 39: Efficiency of a Stamford PI736D generator [53]

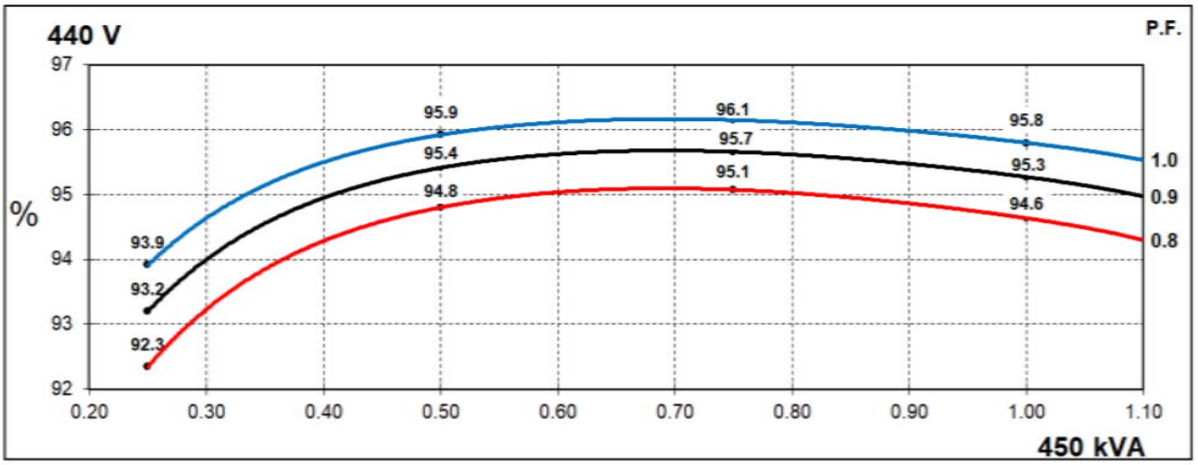

Figure 40: Efficiency of a Stamford S5L1D-C4 generator [56]

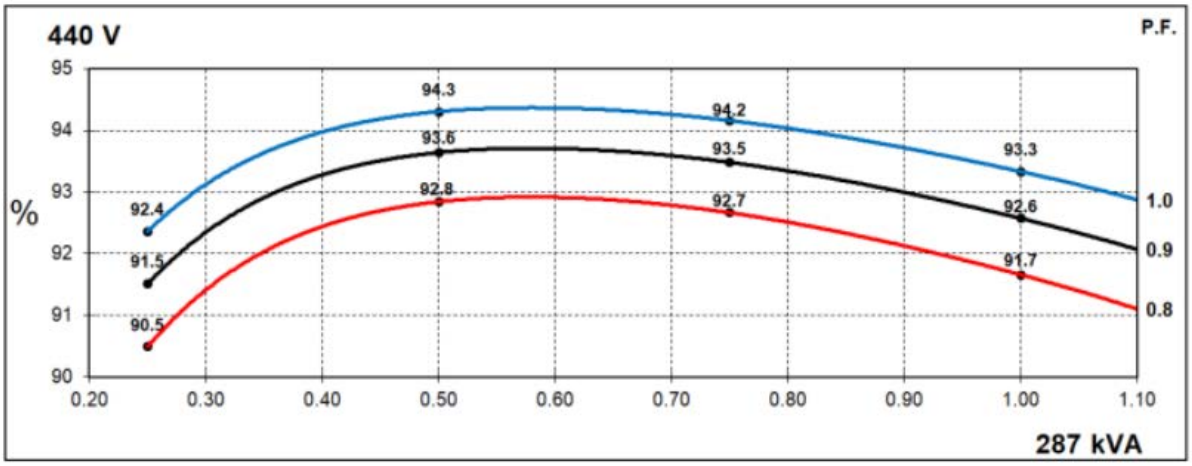

Figure 41: Efficiency of a Stamford N250G4 generator [55]

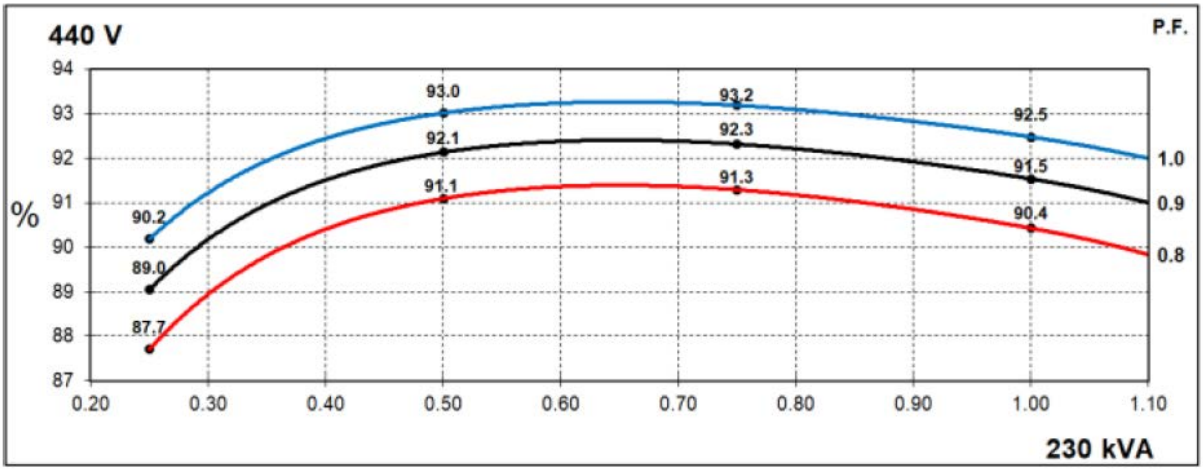

Figure 42: Efficiency of a Stamford N200G4 generator [54]

AC switchboards

Switchboards are used for distribution and protective functions. Therefore, the only losses present are ohmic losses. As the conductors are oversized for their nominal currents (as the switchboard has to withstand short circuit currents), these losses are minimal and are neglected in this report.

Transformers

The advantage of an AC voltage is that it can be easily converted to a different voltage level using a transformer. Transformers rely on a magnetic coupling between two coils. Vessels use dry transformers. The losses are both ohmic and reactance losses in the windings and iron losses in the transformer core. [59]. The same relationship as with the generator holds for the transformer. At low loads, the iron losses are relatively large. At higher loads, the ohmic losses become larger due to the quadratic relationship with the current.

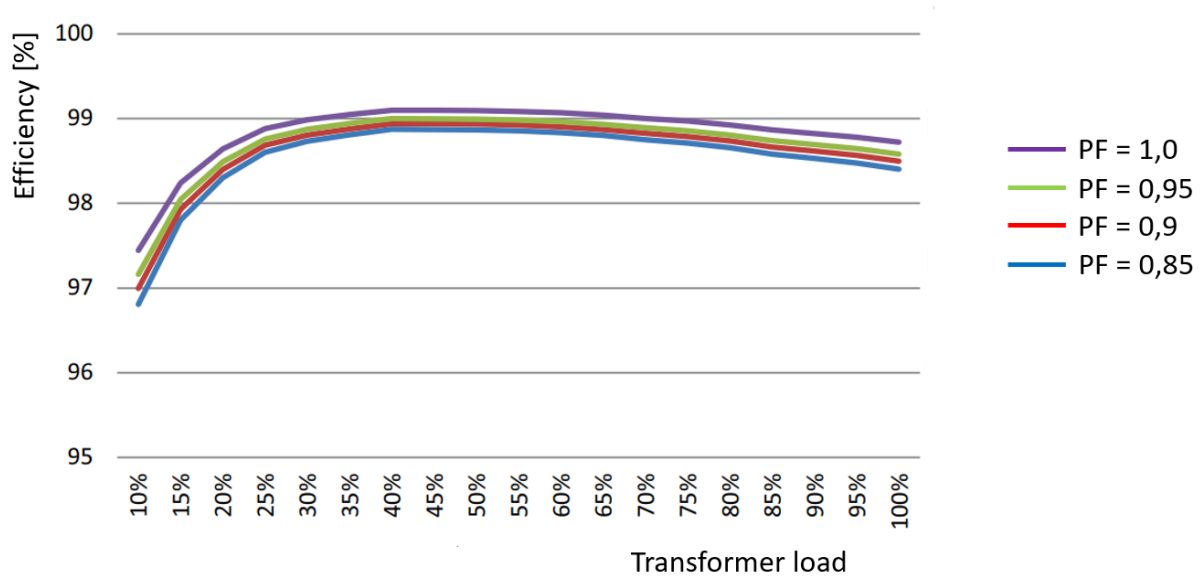

Figure 43: Efficiency plot of a high efficient 500 kVA transformer [27]

Most distribution transformer manufacturers comply with the minimum and maximum energy efficiency requirements of the US Department of Energy. For example, for a 75 kVA transformer this value is 98,6%, for a 500 kVA transformer the value is 99,14% [50]. As

shown in Figure 43, this efficiency only applies to a certain load range. No efficiency chart was available for a 400 kVA transformer, so the 500 kVA plot of Figure 43 was used.

Apart from changing the voltage levels, transformers may be used in frequency drive setups to lower the total harmonic distortion by using a 12 or even 24 pulse system with a phase change between the different supplies [59]. Transformers in this application have a lower efficiency, as the harmonic distortion of the current generates more losses in the transformer. It is difficult to calculate the exact contribution, Martin Kanalik [32] performed an experiment with a 1.25 MVA dry type distribution transformer. he found that compared to a sinusoidal source, a source containing harmonics up to the 50th order produce an additional 33% power loss. As this loss is quadratic with the current, and the current is linear with the load, we can calculate that:

$$Additional\ loss\ [\%] = \left(\frac{\%load}{100}\right)^2 \cdot 0{,}33 \qquad 3$$

The values of Figure 43 match equation 3, giving the following values:

	Transformer load			
	25%	50%	75%	100%
Transformer (500 kVA) efficiency [%]	98,7	99	98,8	98,6
Additional harmonic losses [%]	0,02	0,08	0,19	0,33
Total transformer efficiency [%]	98,68	98,92	98,61	98,27

Table 26: 500 kVA transformer losses with harmonic distortion

AC motors

AC motors can be synchronous or asynchronous. In the first case, the rotating speed is directly related to the frequency of the supply, while in the second case it is not. In practice, all motors used on vessels are asynchronous due to their simplicity of construction and reliability. Unlike synchronous motors, asynchronous motors do not require any external auxiliary field supply. In principle, the synchronous motors have a slightly better efficiency due to the absence of the slip induced rotor current and are more suitable for lower speeds. However, they are also more expensive to build.

Recently, synchronous AC motors have been developed that require no external field supply. These motorers are called reluctance synchronous motor and permanent magnet assisted synchronous reluctance motor. Their efficiency is higher than a squirrel cage motor, as there are no copper losses in the rotor. Also, the efficiency curve of synchronous technology is flatter, meaning it is less dependent on motor load. This is an important advantage, since the motor of a ship also operates in partial and variable loads. This is also valid for variable frequency applications [12].

Development of power electronic devices, such as variable frequency drives (VFDs), has enabled more energy efficient use of synchronous motors. These advanced converters enable synchronous motors to produce the starting torque without a squirrel cage. However, using a VFD increases the additional losses in the motor, which are affected from the converter's supply harmonics [40].

Squirrel cage motor

Most motors used are asynchronous, squirrel cage type. The motor has windings in the stator while the rotor has a cage. Depending on the speed difference between the rotating field in the stator and the speed of the rotor, this setup acts as a transformer. This induces a current in the cage on the rotor that is short circuited with rings on both sides of the rotor. This provides a magnetic interaction between the stator and rotor. Due to this construction, these motors have ohmic losses in both the stator and rotor, increasing quadratically with the current. The iron losses are relatively constant.

IEC/EN 60034-30-1-2014 categorizes single speed squirrel cage motors up to 8 poles according to their efficiency at the nominal operating point. These categories are:

- IE1 (standard efficiency)
- IE2 (high efficiency)
- IE3 (premium efficiency)
- IE 4 (super premium efficiency)
- IE 5 (for a future edition of this norm)

Class IE 4 is difficult to achieve but they are commercially available [3]. Looking at a 6 pole, 50 Hz motor between 500 kW and 1 MW, the nominal efficiency for IE1 is 94%, IE2 is 95%, IE3 is 95,8% and IE4 is 96,6% [23]. The actual efficiency depends on the motor load, as with the transformers. In the lower load ranges the iron losses are dominant, in the higher load ranges the losses in the windings and the cage of the rotor take over.

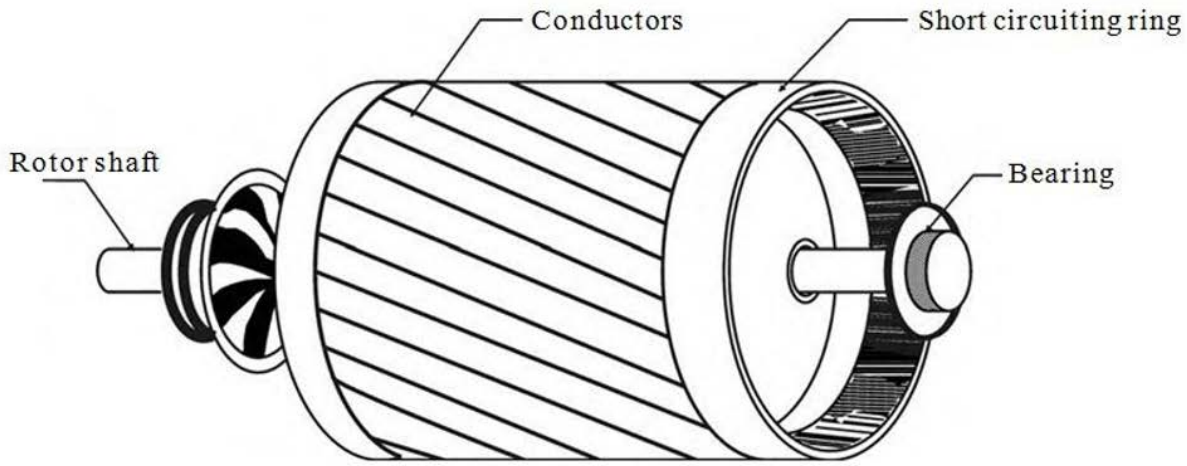

Figure 44: Schematic drawing of a squirrel cage AC motor's rotor (source: www.theengineeringprojects.com)

Even though the price of high efficiency motors may be high, the costs during motor life-cycle span can consist 97% from electric energy consumption [40].

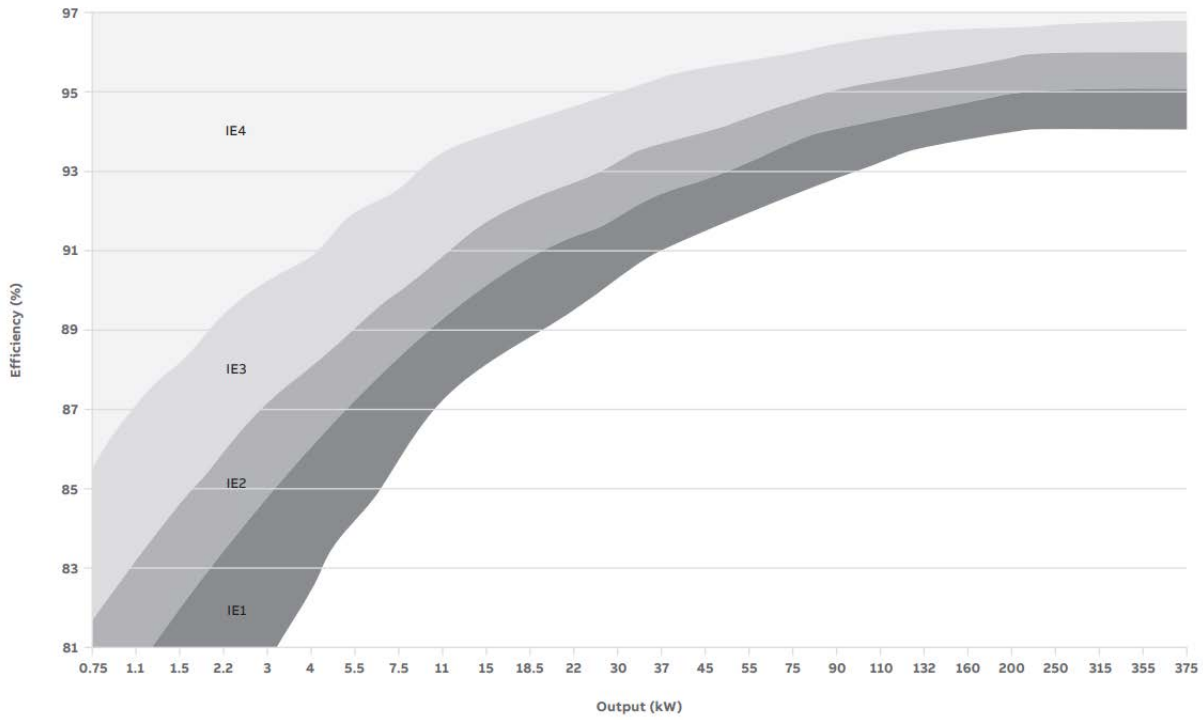

Figure 45: IE classes for a 4 Pole motor (Source: ABB [2])

Excitated synchronous motors

Synchronous motors have the same winding in the stator. Excitated synchronous motors have coils on the rotor through which a DC current is fed. This turns the coils into magnets, locking the rotor to the rotating magnetic field of the stator. As in the name, this motor requires an active excitation system. This can be achieved with carbon brushes feeding the current from the stator to the rotor or with a brushless excitation system as used in a generator.

Permanent magnet motor (PMM)

A PMM uses rare earth magnets on the rotor instead of coils. Benefits of PMMs are generally a high efficiency and high torque production. Disadvantages are high manufacturing cost because of the high price of the magnets. PMM use is popular in low-speed and high-torque applications. [40]

Reluctance synchronous motors (SynRM)

Rotors for SynRM motors designed for variable speed drive (VSD) applications do not need a squirrel cage and are simple to manufacture. The principle is based on reluctance torque. The magnetic field created in the stator follows the path of the least resistance. By shaping the rotor, the magnetic field is directed through the rotor producing a magnetic torque. This can be achieved in several ways, as shown in Figure 46. Radially laminated rotor with flux barriers has good performance, is simple to manufacture and the eddy current losses are small [24]. SynRM technology has high efficiency and high torque density compared to an induction motor and is cheaper to manufacture in mass production. The main disadvantage of a SynRM motor compared to a squirrel cage AC motor is a poor power factor, which requires an oversized frequency converter [40].

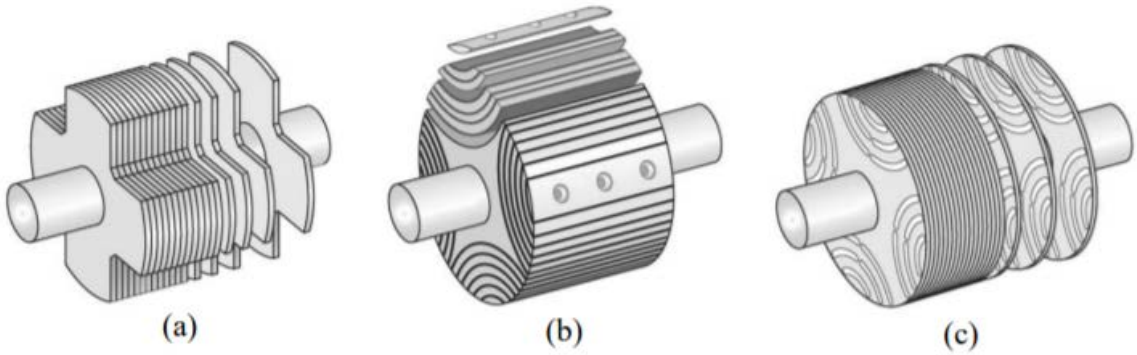

Figure 46: SynRM rotor geometries: a) radially laminated simple salient pole rotor, b) axially laminated rotor, c) radially laminated rotor with flux barriers [24]

Permanent magnet assisted synchronous reluctance motor (PMaSynRM)

PMaSynRM torque production is partly based on magnetic reluctance, as in the SynRM motor, and partly on permanent magnets, as in PMMs. Adding permanent magnets in the SynRM rotor allows the power factor to be increased [40]. Compared to the PMM, the PMaSynRM has lower manufacturing costs, but also lower efficiency. Compared to the conventional asynchronous squirrel cage induction motor, its efficiency and power density are better. PMASynRM motors are commercially available in the power range we need (around 350 kW).

Frequency drives

Whenever the frequency of an AC network must be changed, a frequency drive has to be used. When only a fixed change is needed, for example going from a 50 Hz to a 60 Hz grid, a rotary converter is used, consisting of an electric motor coupled to a generator. A variable AC frequency is obtained by first rectifying the AC voltage to a DC voltage, after which this DC voltage is inverted back to an AC voltage with the desired frequency and voltage. The DC link is smoothed with capacitors and sometimes a choke. The inverter (DC to AC) can have thyristors or transistors as active components.

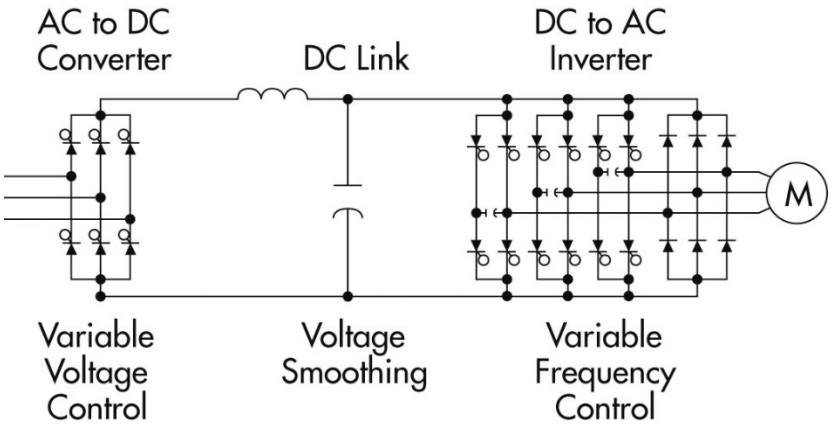

Figure 47: Pulse width modulated variable frequency drive overview (source www.nrcan.gc.ca)

Until recently, most frequency drives were pulse width modulated, controlling the power with pulses with a fixed height and a variable time. Nowadays, most drives are so called vector drives, giving an more precise control of the attached AC motor. This is achieved by separately controlling the current producing the flux and the current producing the torque. A third option is a drive controlling the flux vector, which has different names depending on the manufacturer. ABB calls this 'direct torque control' [1]. Depending on the accuracy of control needed, the electric motor can have an encoder fitted to feed back the exact rotor position to the drive. This is especially useful for vector drives to choose the correct control vector.

The efficiency of a drive mainly depends on the efficiency of the rectifier and inverter. For a general PWM drive of a 200 hp motor, the US Department of Energy states the efficiencies at 25, 50, 75 and 100% load are respectively 95%, 96%, 97% and 97% [63]. This is in line with Figure 48, giving an overview of the efficiency of drives at part load condition.

Losses in a VFD consist of ohmic losses, which are quadratically related to the output current. In contrast to a standard induction motor fed directly from the grid, the current is not proportional with the power, as a modern VFD controls the magnetic flux of the motor. This can create a fast-changing current that can create more losses, as the maximum values are higher. The losses in the power electronics are not linear with the load, as they depend on the switching frequency of the semiconductors. Depending on the operating point, the drive has many switching options, making it difficult to determine exact losses.

The efficiencies of different drives at certain static loading points were obtained from the Nidec documentation [36]. The claimed 98% efficiency of the 400 kW drive that would be needed for our setup is only true at full load conditions. From the documentation the values of Table 27 are obtained.

	Power (propellor)			
	25%	50%	75%	100%
Drive 400 kW efficiency [%]	96,58	97,82	98,25	98,55

Table 27: Nidec 400 kW drive efficiencies

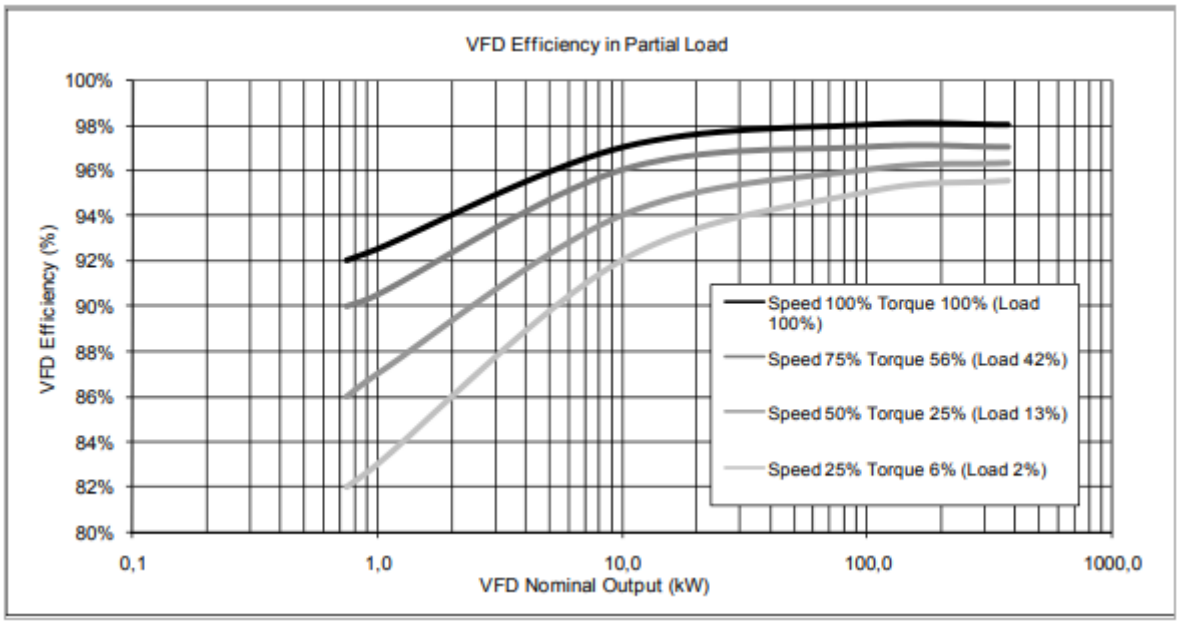

Figure 48: Variable-frequency drive efficiency at full and partial load (Source: International Energy Agency [16])

Combination of motor and drive

As we are interested in a motor to propel a vessel, we need to consider classification rules for such setups. One important rule is that if a vessel is propelled by a single shaft from an electric motor, the complete installation must be redundant. This means that the shaft must be driven by either two separate motors, each with its own frequency converter, or a single motor with separate windings, each connected to an own frequency converter. (DNV Rules for classification of ships, Part 4, Chapter 8, section 12) [18]. Other classification societies have similar rules. For this report, we use two separate electric motors mounted on the same propellor shaft, as motors with two windings are not standard and therefore more expensive. Also, the more efficient motors are not yet available in power over 500 kW.

To control the speed of the propellor shaft, the electric motors must be connected to a frequency drive. Apart from the losses in the frequency drive, this setup will cause additional losses within the electric motor. These losses originate from the regulation principle of the drive, which causes harmonic distortion of the current waves, causing additional copper losses in the motor. For a standard induction motor, these losses can be close to 3% [28]. Therefore, the losses of the electric propulsion, seen from the switchboard, consist of:

- Losses in the drive
- Losses in the motor caused by iron and copper losses
- Additional copper losses caused by the harmonic disturbance of the frequency drive

In Table 28 the efficiencies are listed for several techniques in combination with a frequency drive.

ABB offers the so called ‘IE4 SynRM motor drive packages’ with powers up to 200 kW. The total nominal efficiency for a 200 kW motor running at 1000 rpm in combination with an ACS880 drive is 94,1% [7]. A standard IE4 500 kW induction motor in combination with an ACS880 drive has a total efficiency of 91,7% [3, 28, 40]. These figures are the maximum efficiencies, they will decrease if running at lower loads. One of the most promising setups,

with respect to the total efficiency, is the Nidec 400 kW drive in combination with a Nidec permanent magnet AC motor.

	Power (propellor)			
	25%	50%	75%	100%
Nidec drive 400 kW efficiency [%]	96,58	97,82	98,25	98,55
Nidec 408 kW/3600rpm PM AC motor efficiency [%]	94,1	96,1	96,6	96,9
Total efficiency [%]	90,88	94,01	94,91	95,49

Table 28: Drive, motor and total efficiencies

For all these combinations, the shaft speed of the electric motors is too high for the propellor. Therefore, a gear reduction is necessary to drive the propellor shaft.

A-2 DC equipment

DC Generator

DC generators are not used on standard merchant vessels. Historically, DC generators were designed with field windings in the stator. The main current is generated in the rotor and fed towards the outgoing cables with carbon brushes. The combination of carbon brushes and high rotor currents requires maintenance and makes this construction relatively vulnerable.

DC generators used on non-standard vessels are mainly AC generators with a separate rectifier [4, 26]. This rectifier can be integrated in the generator or placed as a separate unit. Little information is available, but the simplest rectifier for these applications is a three phase, six pulse diode rectifier, which is suitable for this application as it is not necessary to feed back electrical energy. The rectifiers, which use diodes, are referred to as direct frond end (DFE). The losses in a diode consists of a term linearly related to the current and a term quadratically to with the current [51]:

$$P_{loss} = V_{T0} \cdot I_{F(av)} + R_D \cdot I_{F(rms)}^2 \quad 4$$

V_{T0} is the forward voltage over the diode, $I_{F(av)}$ is the average current through the diode, $I_{F(rms)}$ is the average current through the diode and R_D is the ohmic resistance of the diode. Both losses depend on the temperature. As the rectifier will be cooled, the temperature is considered constant.

To determine the losses in the rectifier, some assumptions were necessary. In general, losses are lower when the current is lower. To lower the current, we can raise the voltage. However, this is limited to the maximum voltage of the connected equipment. A common combination when using a full wave three phase rectifier is a 690V AC three phase power source, resulting in a 930V DC bus. The power factor in a DC installation will be near to 1. Therefore, the line current of the generator is calculated with:

$$I_{line} = \frac{P}{U_{line} \cdot \sqrt{3}} \quad 5$$

When using a maximum power of 1 MW and a line voltage of 690V AC, we obtained a maximum line current of 837 A. As generators are wired in star configuration the line current is equal to the phase current, the maximum current through one diode of the rectifier is also 837A. Therefore, we can select a rectifier diode with a value above this 837 A. The datasheet of such a phase leg diode module contains the graph below, showing the power loss as a function of the current.

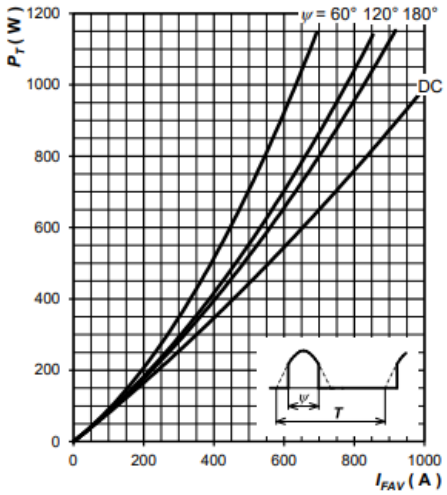

Figure 49: Power loss vs leg current for 1 phase arm [51]

In a full wave three phase rectifier, each diode conducts for 120 degrees. Although they are not completely linear, we linearized the loss. From Figure 49, the power loss per phase arm, we obtained the following relationship for a full wave three phase rectifier:

$$P_{loss\ rectifier} = 3 \cdot 1{,}375 \cdot I_{line} \qquad 6$$

For our 1 MW example, this leads to a loss of approximately 3500W at full load. The efficiency of the rectifier is 99,65%. In reality, the manufacturer will choose a different diode, as design parameters, such as overcurrent situations, must be accounted for. The losses will be roughly the same as the materials and technology are the same. For now, we assumed the efficiency of the rectifier to be 99,5%.

Another option would be using an active front end (AFE), where the diodes are replaced by switching elements, such as transistors. This option is more expensive and has higher losses, but has a lower harmonic distortion and a lower total weight. [23].

Permanent Magnet DC Generator

A new, promising development is using a permanent magnet DC generator on board vessels. This option has not been used, as the magnetic field of the rotor is not adjustable, making the output voltage linearly related with the rotational speed. By choosing the impedance of the generator carefully, the voltage can be kept within the class society limits (although slightly variable) and at the same time operate the combustion engine near its optimal operating line with a variable speed strategy. As this technology is still new and in laboratory test stage, it is not further included in this report. However, its technology should be followed as the efficiency gains could be substantial, especially for low load (DP) operations.

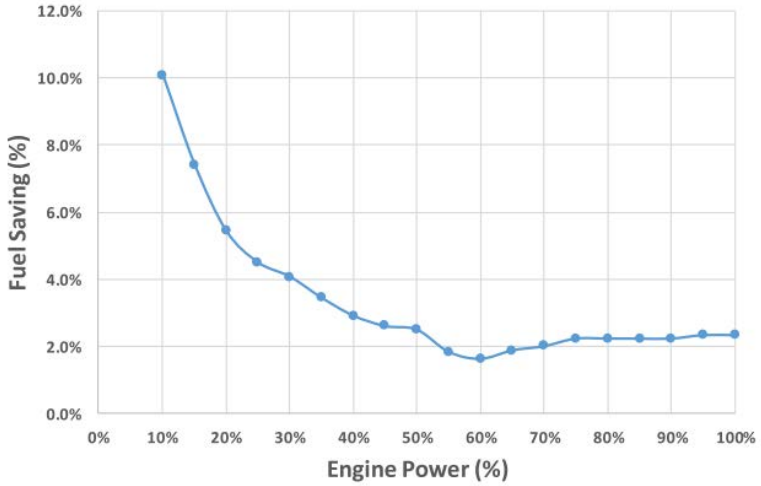

Figure 50: Fuel savings when using a PMG DC generator together with a variable combustion engine speed (Test setup with a 4 kW PMG DC generator) [64]

For this thesis, we considered the efficiency of the DC generator to be the same as the AC generator, but we added a loss of 0,5% for the rectifier, as explained in the previous section.

DC/DC Converters

DC/DC converters are electronic circuits used to change DC voltage. In AC circuits, a voltage is easily changed using a transformer, but as this relies on the alternating nature of this voltage, such a transformer cannot be used for DC voltages. The simplest converters are buck converters (lowering the voltage) or boost converters (increasing the voltage). These converters are non-isolated, meaning there is no galvanic separation between the input and output. Also, current flow is only possible in one direction.

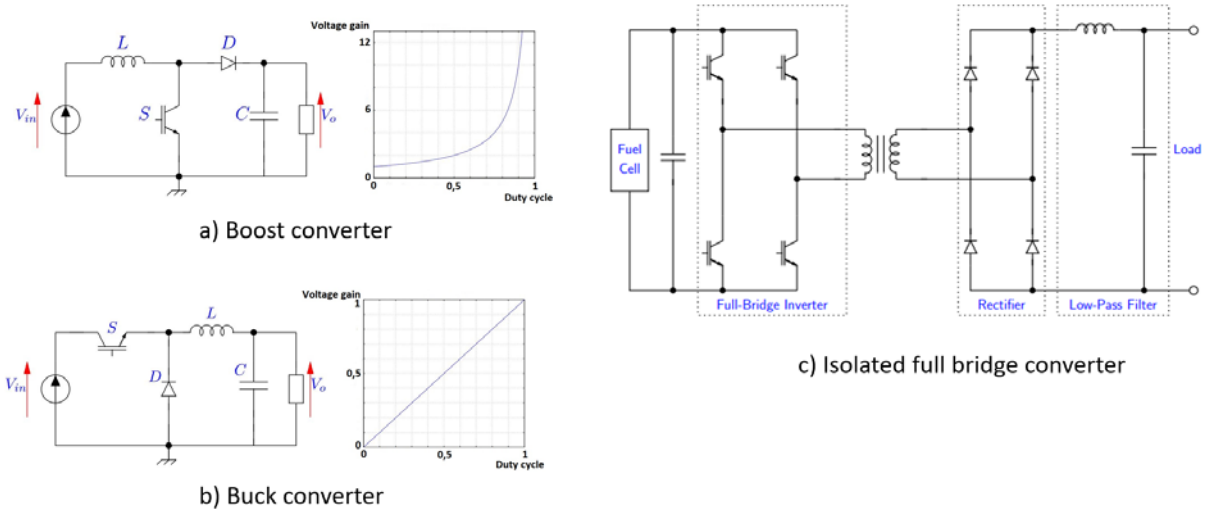

Figure 51: a) Boost converter, b) Buck converter and c) Isolated full bridge converter [33]

To achieve isolation, a transformer is incorporated in the converter. To limit the size and the losses, this transformer is not operated at 50 or 60 Hz but at several kHz. All converters shown in Figure 51 are one way only. This is sufficient for the fuel cell, but if a DC/DC converter is necessary for matching batteries or capacitors, the converter must be able to operate in two directions.

Many manufacturers are unwilling to give efficiency information apart from the maximum achievable figure. Aradex manufacturers DNV/GL type approved DC/DC converters with a maximum continuous power of 200 kW. The datasheet [13] of this product shows efficiency values for different operating voltages. As expected, this efficiency increases when the voltage increases.

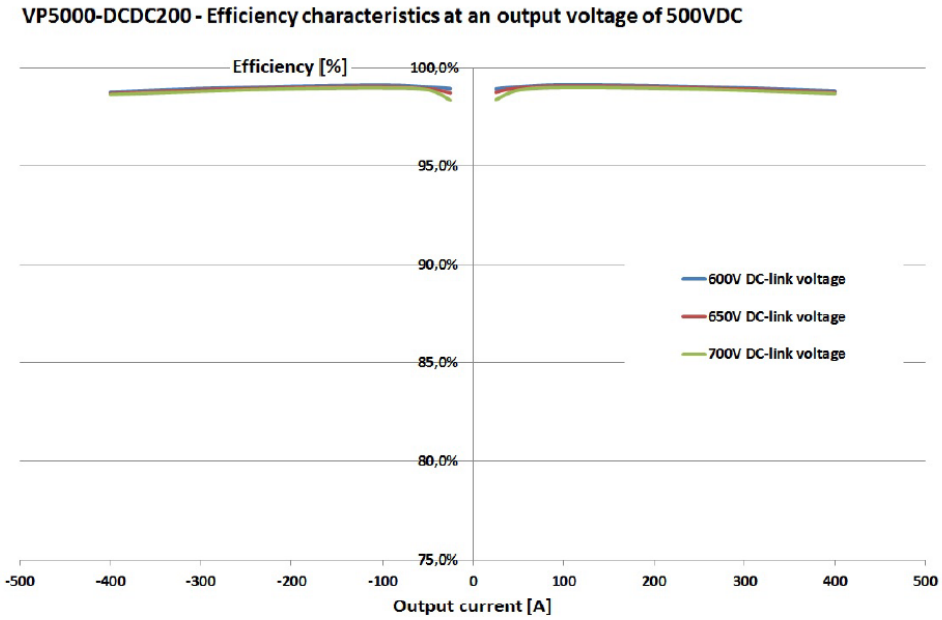

Figure 52: DC-DC converter efficiency (Aradex VP5000) [13]

Competitors likely have comparable figures. The efficiencies for a 600V, 650V or 700V DC link voltage are nearly the same.

	Power			
	25%	50%	75%	100%
DC-DC converter efficiency [%]	99,1	99,1	98,9	98,8

Table 29: Efficiency of a 200 kW DC-DC converter (Aradex VP5000)

B
Mechanical equipment

B-1 Gear box

The designs use gear boxes to convert the rotational speed of the prime movers (diesel engine or electric motor) into the lower speed of the propellor shaft. Depending on the situation, the gearbox can have one or more power take ins (PTI0) and one power take out (PTO). As the reduction a factor of 10, this is at the limit of what a single stage gearbox can do.

Losses in the gearbox can be divided into load dependent and non-load losses. When running, the gears are splashing and churning the lubrication oil in the gear box. This causes the oil to heat up. This is the main loss at no load and is speed dependent. When running at higher loads, the bearing and gear losses are more important [15]. Not much information is available about exact losses of gearboxes versus load. Klein Woud and Stapersma give a figure of 1–2% for a single step reduction gearbox, and 3 to 5% for more complex gearboxes [22]. The paper '*A cost comparison of permanent magnet generators for large offshore wind turbines*' contains a figure for 1, 2 and 3 stage gearbox efficiencies. Although this is a different application, it shows that the efficiency is nearly constant for 1 and 2 stage gearboxes. This paper has a value of 99% for a 1 stage gearbox and about 98,6 for a 2 stage gearbox [31].

For this thesis, a maximum value of 98,5% efficiency is used for a single stage gearbox with 1 power take in (PTI) and 1 power take out (PTO). For a 1 stage gearbox with 2 PTIs and 1 PTO, the maximum efficiency is 98%. In the proposed designs, with a gearbox of around 1 MW this is a loss of 15 kW for the version with 1 PTI and 20 kW for 2 PTI. This value is assumed to be nearly constant for the whole range. With this assumption, the loss percentage in our 4 operating points can be calculated.

	Power			
	25%	50%	75%	100%
Gearbox 1PTI efficiency [%]	94	97	98	98,5
Gearbox 2PTI efficiency [%]	92	96	97,3	98

Table 30: Gearbox efficiencies at different loading points

B-2 Propellor

In a conventional setup with a propellor driven by an ICE with a gearbox, a controllable pitch propellor is used. This is necessary as the ICE cannot deliver enough torque at low speeds, making manoeuvring impossible. Compared to a CPP, the efficiency of a fixed pitch propellor is higher and can even be further raised in the case an elec. Researchers on this topic claim that the minimum efficiency gain is 5% for an optimized E-motor driven FPP compared to an ICE driven CPP [Source: personal communication]. This number can increase if more tests are performed and real-life data becomes available.

The hull efficiency and other effects, such as propellor-hull interactions, are not included in this report. To compare , the boundary is set at the propellor shaft. When using a CPP, it is assumed that a power of 750 [kW] at maximum rpm is needed. For this vessel, the propellor shaft has a maximum speed of around 220 [rpm].

An FPP can be used, so in combination with an E-motor, the maximum power on the shaft is lowered by 5%, giving 712 [kW]

B-3 Diesel generator sets

Diesel generator sets used on board vessels consist of a diesel engine with a generator on a common skid. The generator can even be bolted directly to the engine casing. As these sets have relatively small power output, the combined efficiency of the engine and generator is low.

For this project, a few generator sets were selected. All but the smallest one are above the 130 kW limit from IMO tier III and thus have to comply with the rules of tier III. These rules can only be met with an SCR. The estimated urea consumption is 6% of the diesel consumption [source: personal communication with Caterpillar]. Caterpillar provided the information to calculate the values in Table 31.

	Caterpillar generators sets									
	99 ekW (C4.4)		150 ekW (C7.1)		250 ekW (C9.1)		565 ekW (C18)		945 ekW (C36)	
Load [%]	DO [kg/h]	eff. [%]	DO [kg/h]	eff. [%]	DO [kg/h]	eff. [%]	DO [kg/h]	eff. [%]	DO [kg/h]	eff. [%]
10	4,09	20,4	5,12	24,7	9,89	21,3	17,81	26,7	38,33	20,8
20	5,84	28,6	8,43	30,0	15,44	27,3	30,22	31,5	49,59	32,1
25	6,83	30,6	10,19	31,0	18,08	29,2	36,42	32,7	60,16	33,1
30	7,93	31,6	11,95	31,7	20,61	30,7	42,62	33,5	69,43	34,4
40	10,29	32,5	15,71	32,2	25,52	33,0	55,06	34,6	86,25	37,0
50	12,72	32,8	19,89	31,8	30,60	34,4	67,50	35,3	104,17	38,2
60	15,01	33,4	23,87	31,8	36,60	34,6	77,62	36,8	123,31	38,8
70	17,25	33,9	27,66	32,0	42,69	34,6	87,74	38,0	141,78	39,3
75	18,40	34,0	29,35	32,3	45,65	34,6	93,26	38,3	151,44	39,5
80	19,56	34,1	30,73	32,9	48,30	34,9	99,73	38,2	161,70	39,4
90	21,89	34,3	33,43	34,0	53,21	35,7	114,21	37,5	181,86	39,4
100	24,35	34,3	36,37	34,8	58,07	36,3	130,58	36,5	203,17	39,2

Table 31: Calculated DO consumption and efficiencies based on an LHV of 42,7 MJ/kg. All but the smallest set equipped with an SCR.

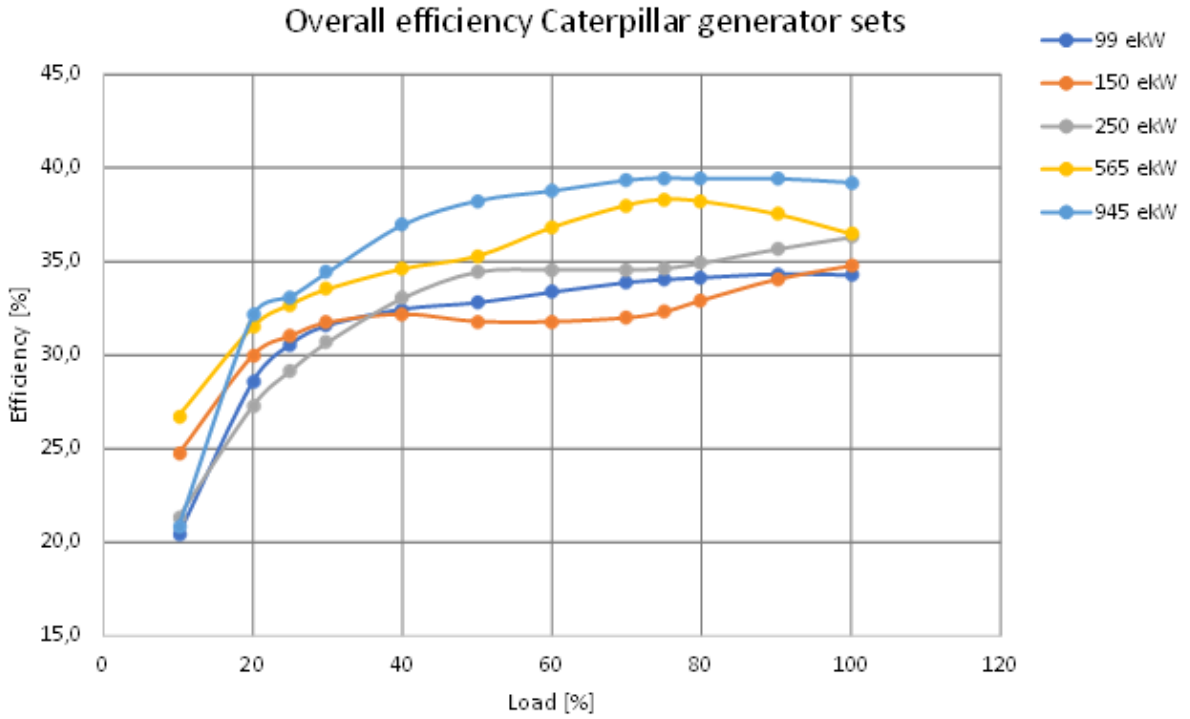

Figure 53: Overall efficiency of caterpillar generator sets, based on electrical power, fuel consumption and an LHV of 42,7 MJ/kg

B-4 Diesel and dual fuel hydrogen engine.

Efficiency and hydrogen/diesel oil ratio

First, the values were obtained for the DF engine following the propellor curve. As mentioned before, this curve follows a third order relationship between power and shaft speed. For now, we only have contour plots available for a 1 MW engine. This engine is slightly oversized. For the calculations, the efficiency values was lowered according to the relations found in Table 31, if necessary.

Power [%]	25	50	75	100
Power [kW]	250	500	750	1000
Shaft rpm [%]	63	79,4	90,9	100

Table 32: Propellor curve for a 1 MW engine

The efficiency of the engine is plotted in Figure 54. The datapoints are found in the contour plot, the lines are fourth order trendlines.

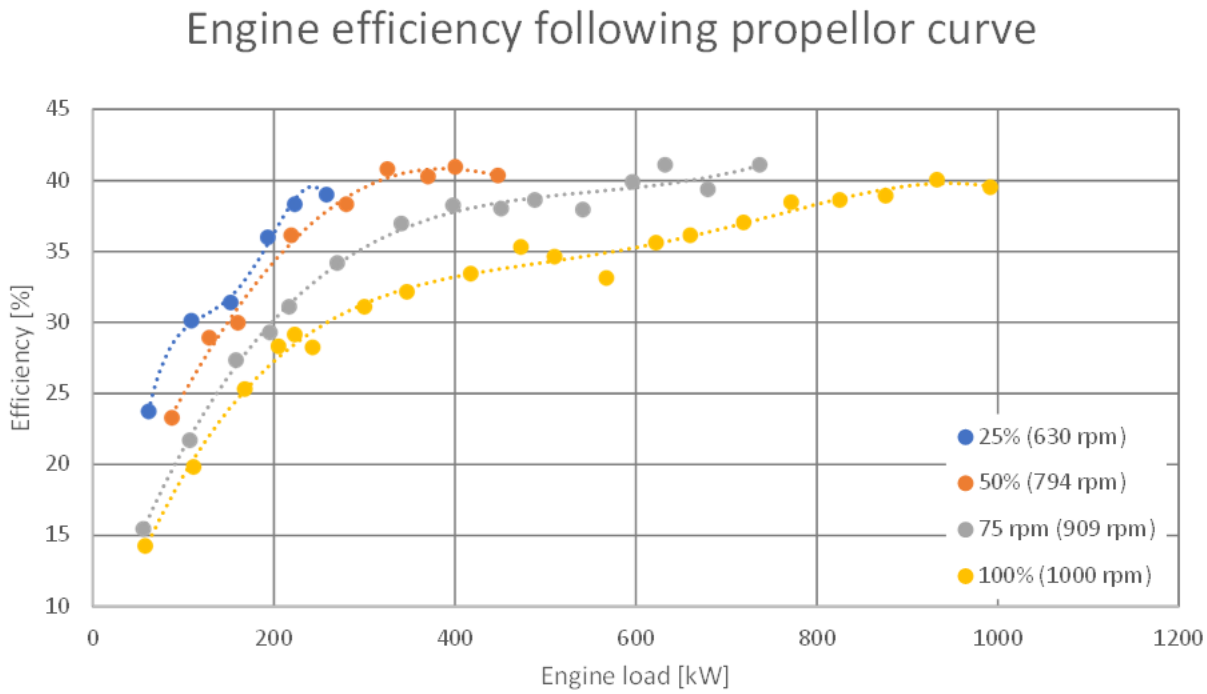

Figure 54: 1 MW DF hydrogen motor efficiency plot when operated along the propellor curve

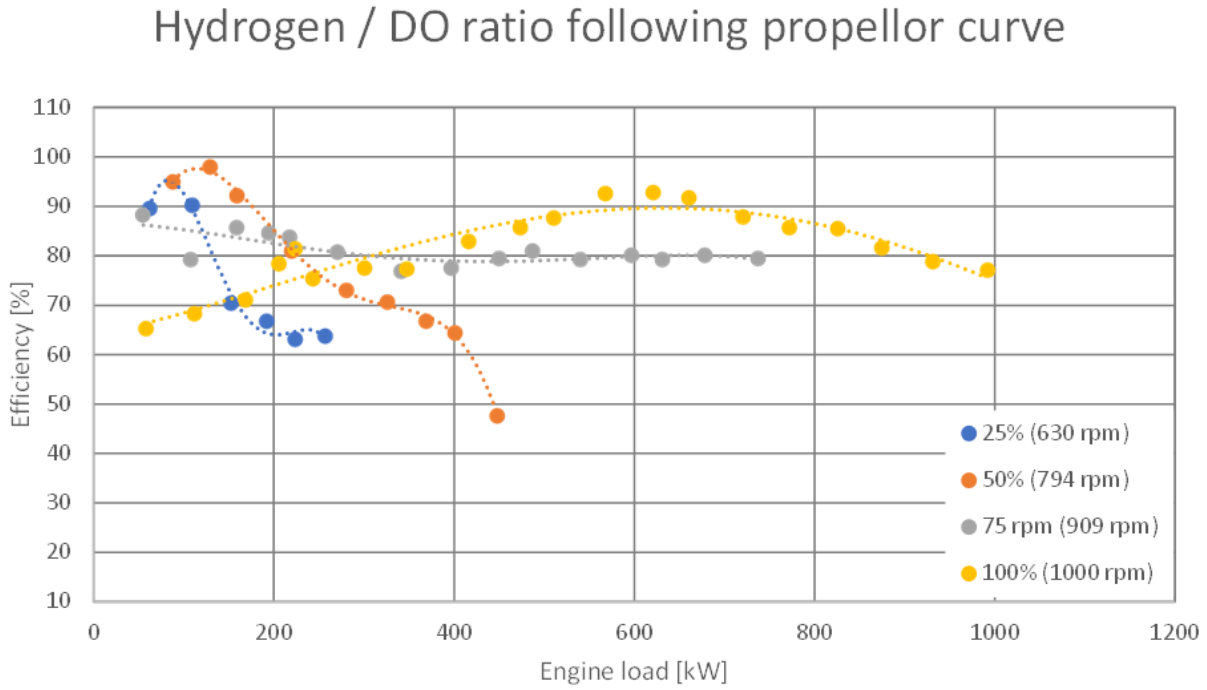

Figure 55: 1 MW DF hydrogen motor hydrogen/DO ratio plot when operated along the propellor curve

There are two possibilities for the engine to operate as a generator set. The most common setup is to use an AC system. This requires the engine speed to be constant, as the frequency of the grid has to be stable at 50 or 60 Hz.

The second option is using a DC generator set, in which case the engine speed can vary. This allows more efficient fuel consumption and/or H_2 ratio. However, the operating point of the engine in the DC setup must be within certain boundaries:

- The operating point must be within the operating envelope.
- There must be some distance between the operating point and the top line of the operating envelope to ensure fluctuations in load can be compensated for.

- Sometimes there is a conflict between operating with the highest efficiency and with the highest H_2 ratio. In that case the point is chosen somewhere in the middle, so operating with a reasonable efficiency and H_2 ratio.
- The operating points should form a continuous line to avoid large jumps in engine speed.

Figure 56 shows the plot of the efficiency, H_2 ratio and engine speed for a DC generator setup fulfilling these requirements.

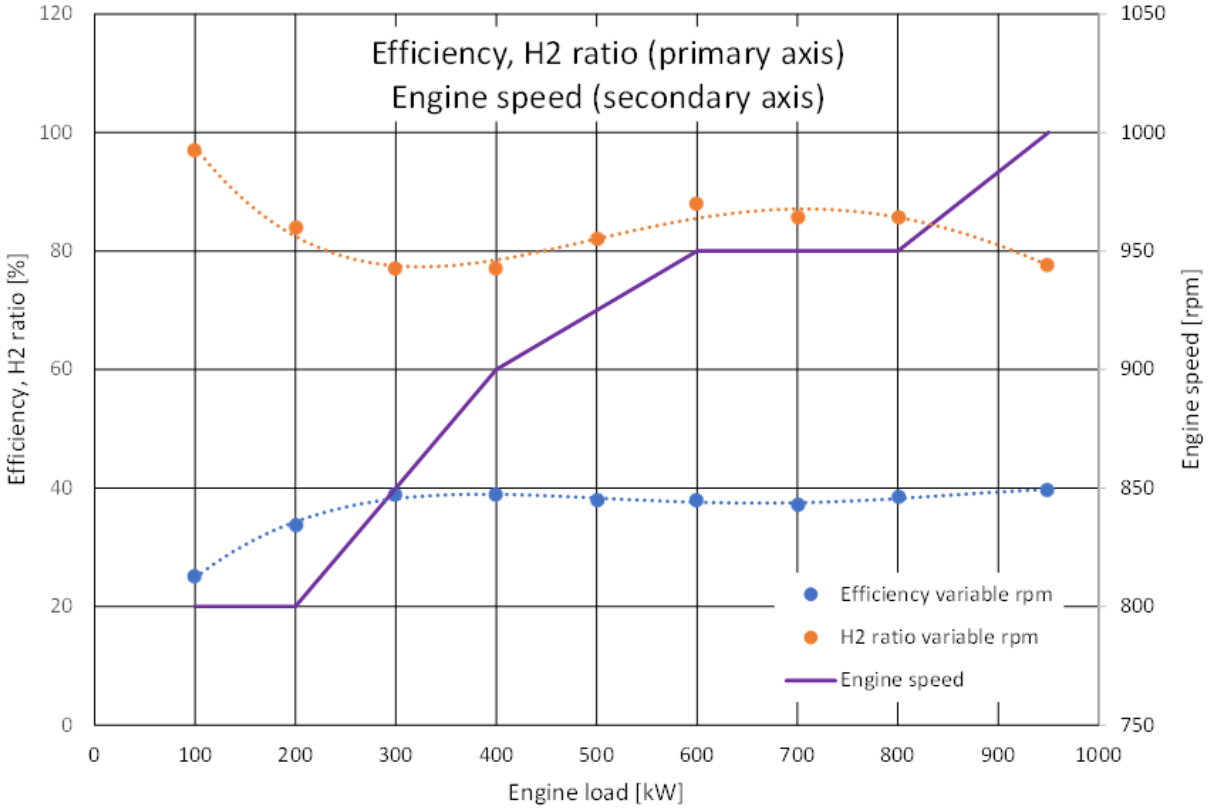

Figure 56: Plot of efficiency, H2 ratio and engine speed vs engine load for a variable speed DC generator setup

Figure 57 compares the efficiencies and H_2 ratios of the AC and DC generator setup. The efficiency in the lower regions, up to around 60% load, is higher when running with a variable speed. The H_2 ratio is also higher up to around 25% load, after which it is slightly lower compared to the AC generator setup up to 75% load. At higher loads, the differences between the two options are minimal.

All these efficiency and H_2 curves were fitted with fourth order polynomials and used in the calculations.

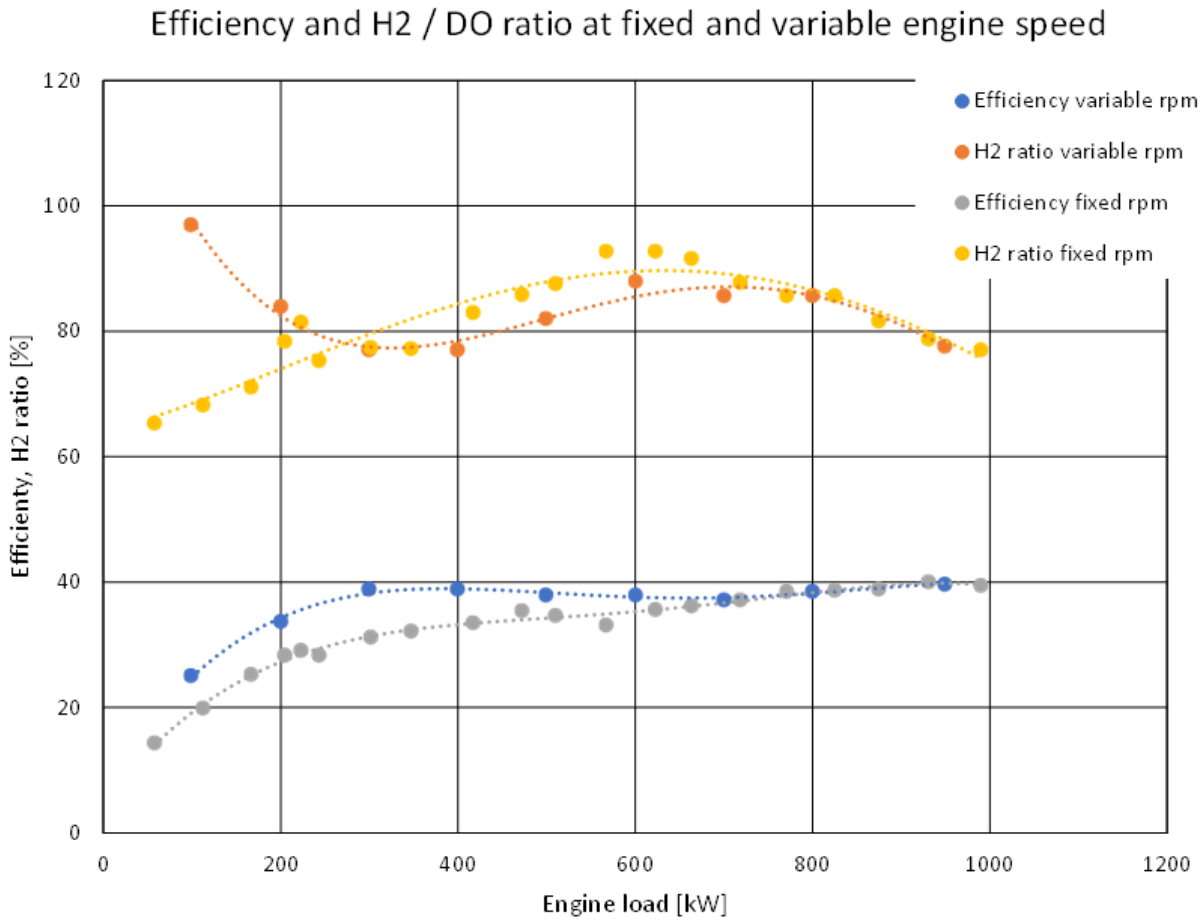

Figure 57: Plot of efficiency and H2 ratio for variable speed DG generator and fixed speed AC generator

B-5 Urea consumption

The dual fuel engine running on hydrogen and diesel does not comply with IMO tier III. Therefore, this engine also needs an SCR and urea to limit the NO_x emissions. Exact figures for urea consumption are not available, but Caterpillar uses a rule of thumb of 6% of the diesel oil consumption (mass based) when running in constant rpm generator mode [source: personal communication with Caterpillar]. Using this figure, the urea consumption was calculated for the ABC 1 MW dual fuel motor running in diesel mode.

P [%]	NOx [g/kWh]	NOx[kg/hr]	DO [g/kWh]	DO [kg/h]	Urea [kg/hr]	Urea/NOx
25	8,92	2230	245	61,25	3,675	1,65E-03
50	8,22	4110	211	105,5	6,33	1,54E-03
75	7,54	5655	207	155,25	9,315	1,65E-03
100	7,04	7040	204	204	12,24	1,74E-03

Table 33: Urea use vs NOx production for a 1 MW ABC duel fuel motor running on diesel oil in constant rpm generator mode

Table 33 shows the relation between urea use and NOx production. We used the mean value of 1,64 E-03 kg urea used for each kg NO_x produced. With this value, the urea consumption for the propellor curve and the dual fuel mode was calculated, both for diesel and dual fuel mode. As only 4 points are available for each mode, this is an approximation, but should be

sufficient for this report. The trend lines plotted are second order polynomials. The equations of these lines were used to calculate the urea consumption.

		Generator (constant rpm) mode			Propellor curve		
	P [%]	NOx [g/kWh]	NOx[kg/hr]	Urea [kg/hr]	NOx [g/kWh]	NOx[kg/hr]	Urea [kg/hr]
DO only	25	8,92	2230	3,68	14,3	3575	5,88
	50	8,22	4110	6,33	11,44	5720	9,40
	75	7,54	5655	9,315	8,6	6450	10,60
	100	7,04	7040	12,24	7,04	7040	12,24
Dual fuel	25	4,99	1247,5	2,05	15,66	3915	6,43
	50	2,81	1405	2,31	10,61	5305	8,72
	75	2,9	2175	3,57	5,74	4305	7,08
	100	5,22	5220	8,58	5,22	5220	8,58

Table 34: Urea consumption for generator mode and propellor curve

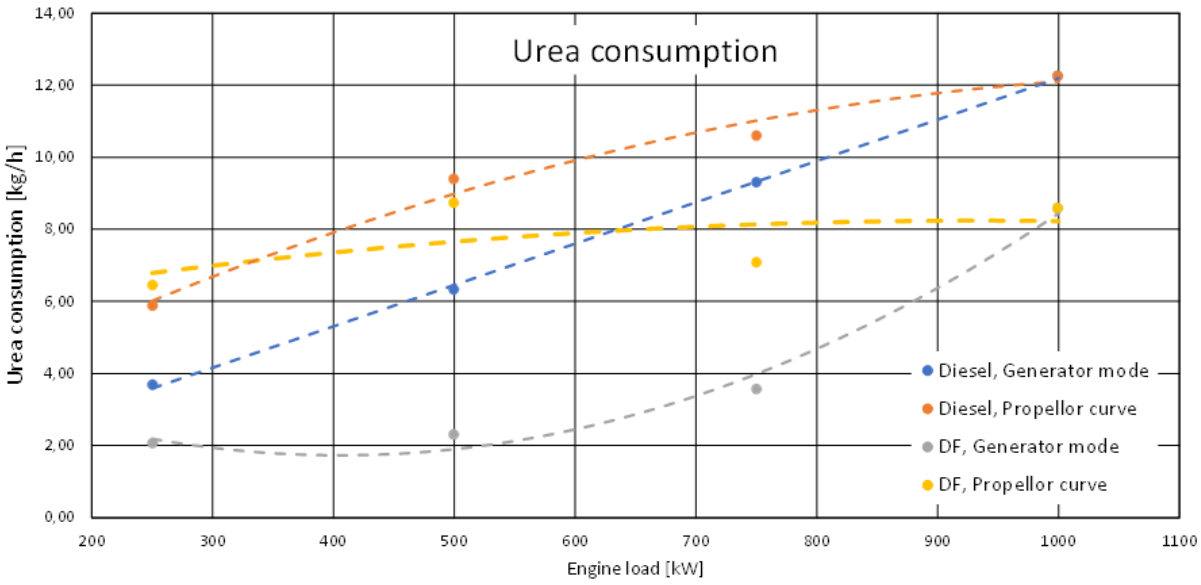

Figure 58: Urea consumption for generator mode and propellor curve

If the engine is used in a DC generator configuration, the above figures cannot be used. No information is available for other operating points. Figure 56 shows that in the lower regions, the thermal loading in variable speed generator mode is less than the propellor curve, as the engine has to deliver less power with a higher rotational speed. It is, however, higher than the engine running in generator mode. In the higher load regions, the propellor and generator curves converge to the same point. The mean value of these two curves is used to approximate the urea consumption for the dual fuel motor in the DC generator configuration.

Setup	Polynomial urea consumption (P in kW)
Diesel, propellor curve	$y = -0{,}00007543351790663 92 * P^2 + 0{,}0175464974620334 * P + 2{,}09859170948162$
Diesel, AC generator mode	$y = 0{,}011472 * P + 0{,}72$
DF, propellor curve	$y = -0{,}00003122640151316 44 * P^2 + 0{,}00581961514516398 * P + 5{,}52830568894262$
DF, AC generator mode	$y = 0{,}00001898236513037 15 * P^2 - 0{,}0153872202193163 * P + 4{,}84728252436274$

DF, DC generator mode	$y = 0{,}00000792986248952753 * P^2 - 0{,}00478380253707616 * P + 5{,}18779410665268$

Table 35: Polynomial fittings of the graphs of Figure 58

For the Caterpillar diesel generator sets, the 6% rule, as obtained from Pon Power [45], was used, as these power ratings are far below the fitted polynomials from Figure 58: Urea consumption for generator mode and propellor curve.

C
LTPEM Fuel Cell

In this thesis, an installation with a low temperature proton exchange membrane fuel cell (henceforth LTPEM FC or FC) was examined. This type of fuel cell was chosen during the literature survey based on the available information.

The LTPEM FC uses an ion conduction polymer with on each side a catalysed porous electrode. The polymer electrolyte works at a low temperature, meaning an LTPEM FC can start quickly. The membranes are also thin, resulting in a compact size. The absence of corrosive fluids means the LTPEM FC can operate in any orientation. These characteristics make this FC suitable for vehicles and other portable operations.

To obtain more insight on the working principle of a LTPEM fuel cell below a short description is found, based on the book 'Fuel Cell System Explained' by James Larmini and Andrew Dicks [25].

Working principle

The FC converts chemical energy directly into electrical energy. The basic principle of all fuel cells is the same: Hydrogen reacts with oxygen, forming water:

$$2H_2 + O_2 \rightarrow 2H_2O$$

This looks similar to a combustion process, but electrical energy results, rather than heat. This reaction takes place in two steps in two locations:

1. At the anode of the acid electrolyte fuel cell, the hydrogen gas ionises, releasing electrons and creating H^+ ions (or protons): $2H_2 \rightarrow 4H^+ + 4e^-$
2. At the cathode, oxygen reacts with electrons taken from the electrode and the H^+ ions taken from the electrolyte, to form water: $O_2 + 4e^- + 4H^+ \rightarrow 2H_2O$

Figure 59 shows the transport of H^+ ions through a membrane of solid polymer and a transport of electrons via the electrodes through an electrical circuit. At the anode, energy is released, but not at an unlimited rate. Before the reaction starts, a certain amount of energy must be supplied, the so called 'activation energy'.

If the probability of a molecule having enough energy is low, the reaction will proceed slowly. Three ways of dealing with slow reaction rates in a fuel cell are:

1. Using a catalyst
2. Raising the temperature
3. Increasing the electrode area

The first two can be applied to any chemical reaction. The third is specific to fuel cells. As the produced electrons must be removed, the only point where the reactions can take place are on the surface of the electrode. The rate at which the reaction happens is proportional to the area of the electrode. This area is not just the simple length x width area of the electrode, it also

depends on the structure of the surface. By making electrodes with a micro structure, the surface area can be increased hundreds or thousands of times.

As the LTPEM operates at a low temperature, the problem of slow reaction rate is addresed by using platinum as a catalyst. In the past, the rate of catalysis was in the order of 28 mg cm^{-2} but this has been reduced to around to around 0,2 mg cm^{-2}. Nevertheless, this led to the myth that the catalyst is a huge part of the production costs for an LTPEM FC. Only minimal amounts are used, so cost of the platinum is a small part of the total price.

As a fuel cell only produces a low voltage, several cells are put in series with an integrated channel structure for the supply of hydrogen and oxygen, a so called ‘stack’.

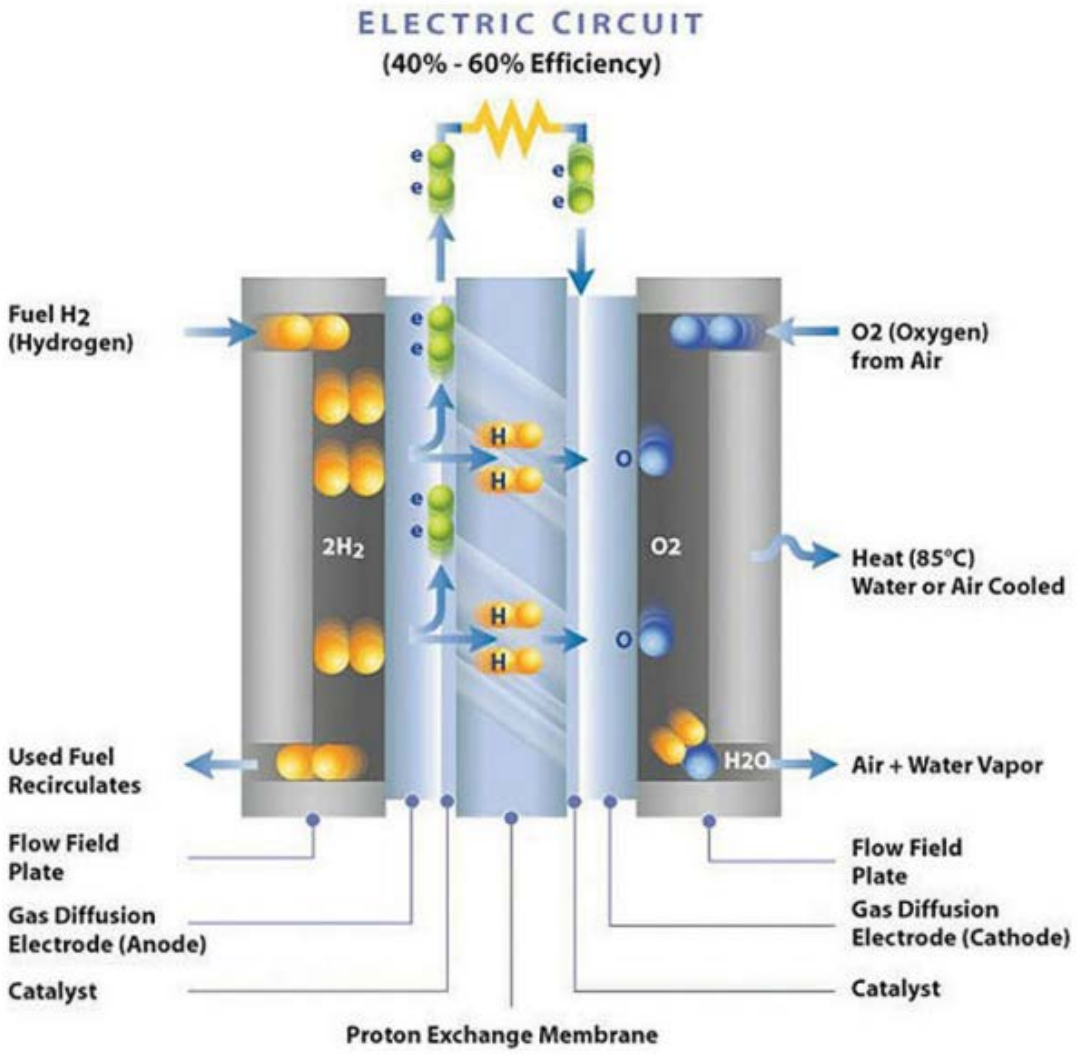

Figure 59: LT PEM fuel cell (Source: Journal of Ecological Engineering Vol. 20(9), 2019)

Energy in fuel cells

Energy released by burning a fuel in the classical way is well defined. However, the energy of a chemical input and output is harder to describe. In the case of fuel cells, the ‘Gibbs free energy’ is important. This can be defined as the ‘energy available to perform external work, neglecting any work performed by changes in pressure and/or volume’. In an FC, the external

work is moving electrons around in an external circuit. Any work performed by a changing pressure and/or volume in the FC is not used.

The Gibbs energy is defined in terms of enthalpy and entropy:

$$G = H - T \cdot S \qquad 7$$

This chemical energy has two similarities with ordinary mechanical potential energy:

- The point of zero energy can be defined almost everywhere.
- The change of energy is important for our calculations.

When working with chemical reactions, the zero-energy point is normally defined as pure elements in the normal state at standard temperature and pressure (25°C, 0.1 MPa). When using this convention, the 'Gibbs free energy of formation' G_f is used instead of the 'Gibbs free energy'. When also using the 'enthalpy of formation' instead of just 'enthalpy' the G_f of the input of an FC operating at standard temperature and pressure is zero.

To calculate the change in G_f, the G_f of the products and reactants must be calculated:

$$\Delta G_f = G_{f\ products} - G_{f\ reactants} \qquad 8$$

Working with chemical reactions, it is common practice to consider the quantities of molecules per mole. Formula 8 is then written as:

$$\Delta \bar{g}_f = \bar{g}_{f\ products} - \bar{g}_{f\ reactants} \qquad 9$$

Applying this to a basic LTPEM fuel cell is straightforward. The basic reaction is:

$$2H_2 + O_2 \rightarrow 2H_2O \qquad 10$$

This is equal to:

$$H_2 + \frac{1}{2}O_2 \rightarrow H_2O \qquad 11$$

Combining this with formula 9, we obtain:

$$\Delta \bar{g}_f = \bar{g}_{f\ H_2O} - \bar{g}_{f\ H_2} - \frac{1}{2}\bar{g}_{O_2} \qquad 12$$

The Gibbs free energy of formation G_f is varies with temperature and the state of the substances (liquid or gas). As the FC operates at a constant temperature this is not a big drawback and the G_f is easily obtained from tables.

In an ideal world, the chemical reaction would be reversible and all Gibbs free energy would be converted to electrical energy. For each water molecule formed, two electrons pass through the external circuit. So for each mole of hydrogen used, 2N electrons pass the external circuit where N is Avogadro's number. One electron has a charge of -*e*. Therefore, the charge flowing in our case is:

$$-2 \cdot N \cdot e = -2 \cdot F \ [coulombs] \qquad 13$$

F is the Faraday constant, the charge on one mole of electrons. Electrical work performed is defined by multiplying the charge by the voltage. *E* is the symbol of the voltage of our fuel cell, so:

$$Electrical\ work\ done = -2 \cdot F \cdot E \ [J] \qquad 14$$

Considering a reversible system, the electrical work performed is equal to the Gibbs free energy released, giving:

$$E = \frac{-\Delta \bar{g}_f}{2 \cdot F} \qquad 15$$

Equation 15 is the theoretical reversible open circuit voltage of the LTPEM fuel cell running on hydrogen, assuming pure hydrogen and oxygen at standard pressure (0.1 MPa) and a no-load operation. As the $\Delta \bar{g}_f$ decreases if the temperature is increased, so does the open circuit voltage.

C-1 Efficiency

Within thermodynamics, the maximum efficiency is limited to the Carnot efficiency:

$$Carnot\ limit = \frac{T_1 - T_2}{T_1} \qquad 16$$

Fuel cells are not subject to this Carnot limit. Therefore, the electrical energy produced was compared with the heat that would be produced when burning the same amount of fuel. This heat is the change in 'enthalpy of formation', $\Delta \bar{h}_f$. This said, looking at formula 11, it is obvious that water can be formed as a liquid or as a gas. When forming steam, $\Delta \bar{h}_f$ equals -241,83 [kJ mol^{-1}], when water is formed $\Delta \bar{h}_f$ equals -285,84 [kJ mol^{-1}]. The difference between these two is the molar enthalpy of vaporisation of water. The higher value is referred to as the 'higher heating value' (HHV), the lower value as 'lower heating value (LHV).

With this information, the maximum efficiency can be calculated:

$$Maximum\ efficiency = \frac{\Delta\bar{g}_f}{\Delta\bar{h}_f} \cdot 100\% \quad (17)$$

It is important to state whether this efficiency is based on the LHV or HHV, as the LHV gives a higher maximum efficiency.

Form of water produced	Temperature [°C]	$\Delta\bar{g}_f$ [kJ mol^{-1}]	Maximum EMF [V]	Efficiency limit [%]
Liquid	25	-237,2	1,23	83
Liquid	80	-228,2	1,18	80
Gas	100	-225,2	1,17	79
Gas	200	-220,4	1,14	77
Gas	400	-210,3	1,09	74
Gas	600	-199,6	1,04	70
Gas	800	-188,6	0,98	66
Gas	1000	-177,4	0,92	62

Table 36: $\Delta\bar{g}_f$, maximum EMF and efficiency limit (HHV basis) for hydrogen fuel cells [25]

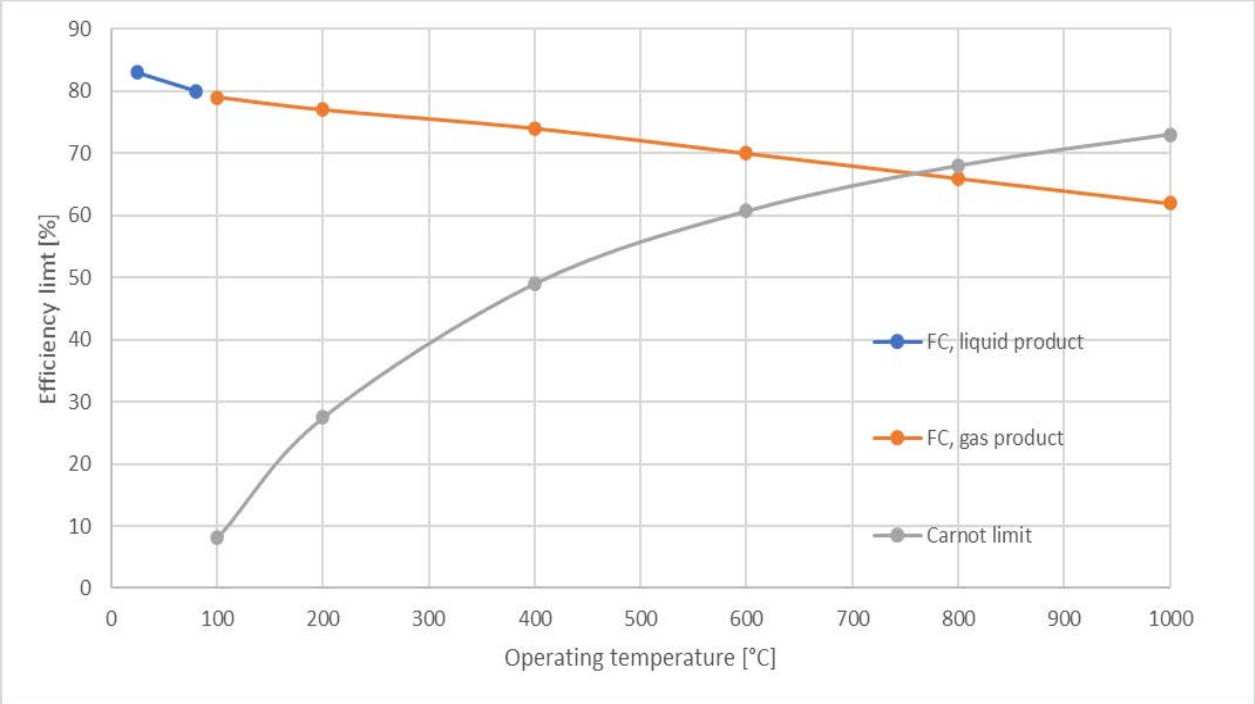

Figure 60: Maximum hydrogen FC efficiency (reference HHV) at standard pressure and Carnot limit with a 70 °C exhaust temperature

In Figure 60, the theoretical efficiency of a hydrogen FC is plotted. This suggests that lower temperatures result in a better efficiency. However, the internal voltage losses are lower with

higher temperatures (this is discussed more later). Also, the exergy of the waste heat of a fuel cell is higher if it is available at a higher temperature.

Table 36 shows a relation between the maximum EMF and maximum efficiency of an FC. If all energy for the hydrogen fuel cell would be transformed into electrical energy, the EMF would be:

$$E = \frac{-\Delta\bar{h}_f}{2 \cdot F} \qquad 18$$

Using an HHV gives an EMF of 1,48 [V], while a LHV gives an EMF of 1,25 [V]. This assumes that the efficiency of the FC is 100%. In reality, the cell efficiency of the FC based on the HHV is:

$$\eta_c = \frac{V_c}{1{,}48} \cdot 100\% \qquad 19$$

In this formula, V_c is the actual cell voltage of the FC. Formula 19 assumes that all fuel is converted into electrical energy. In practice, a part of the fuel cannot be used, as explained later in this paragraph. To correct for this, a 'fuel utilisation coefficient' is defined as:

$$\mu_f = \frac{mass\ of\ fuel\ reacted\ in\ the\ cell}{mass\ of\ fuel\ input\ to\ the\ cell} \qquad 20$$

Combining formula 19 and 20 gives the overall fuel cell efficiency based on the HHV:

$$\eta_{FC} = \mu_f \cdot \frac{V_c}{1{,}48} \cdot 100\% \qquad 21$$

Cell voltage

The theoretical voltage of an FC is given by formula 15. In practice, however, the cell voltage varies with current density. The main observations are:

- Even the open circuit, voltage is less than the theoretical voltage.
- There is a rapid initial fall in voltage.
- After this initial fall, the voltage falls less rapidly and more linearly.
- Sometimes there is a higher current density at which the voltage falls rapidly.

Figure 61 shows the voltage for a typical low temperature, air pressure, fuel cell. If an FC is operated at a higher temperature, the reversible voltage falls. However, the difference between the no loss value and the actual operating voltage decreases, as shown in Figure 62. What causes these voltage drops is described in the next paragraphs.

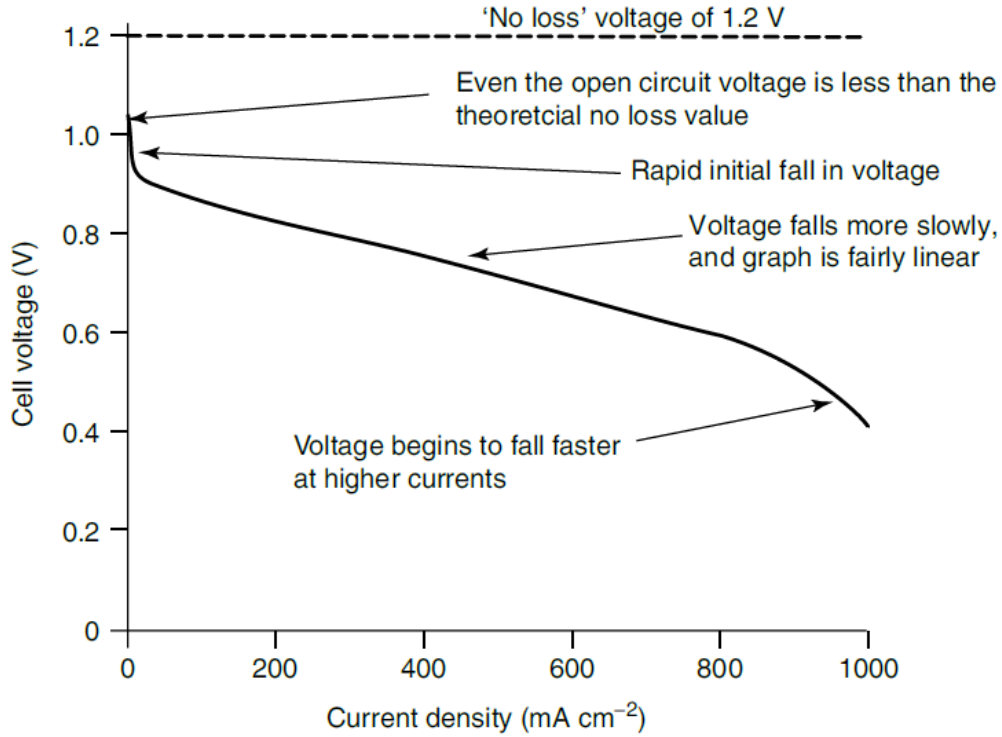

Figure 61: Voltage for a typical low temperature, air pressure, fuel cell [25]

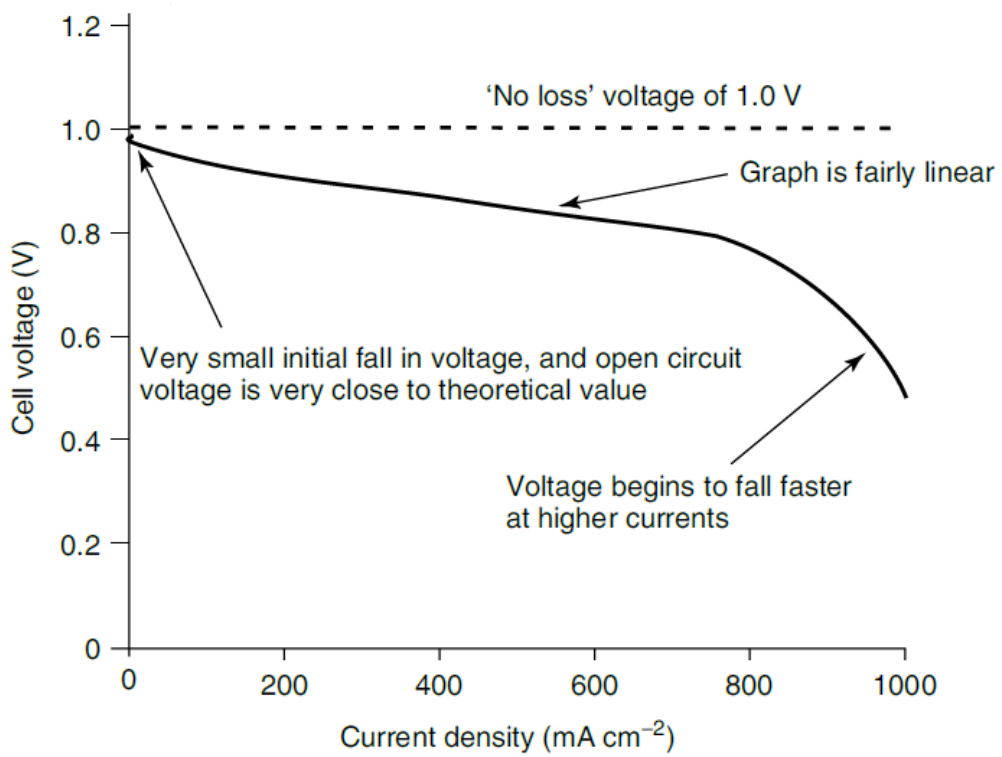

Figure 62: Voltage of a typical air pressure fuel cell operating at about 800 °C [25]

Activation losses

As the fuel cell relies on a chemical reaction, we must deal with slow reactions taking place on the surface of the electrodes. A part of the voltage generated by the FC is lost in driving the chemical reaction that transfers the electrons to or from the electrode. This voltage drop is

very non-linear. In low temperature fuel cells, the voltage drop due to activation loss mainly occurs at the cathode. The equation describing this voltage drop is:

$$\Delta V_{act} = A \cdot ln\left(\frac{i}{b}\right) \quad 22$$

A and b are constants that depend on the electrode and cell conditions and *I* is the current density. A typical value for A is 0,06 [V] [25], while b is equal to i_0. This i_0 is the current flowing through the membrane in a no-load condition. The no-load current in the membrane is caused by the equilibrium reaction:

$$O_2 + 4e^- + 4H^+ \leftrightarrow 2H_2O \quad 23$$

This causes a continual backward and forward flow of electrons through the membrane. For a PEM fuel cell using air at normal pressure and 30 °C, i_0 is around 0,04 [mA cm^{-2}].

The voltage for a fuel cell is the theoretical voltage *E* minus the activation voltage:

$$V = E - A \cdot ln\left(\frac{i}{i_0}\right) \quad 24$$

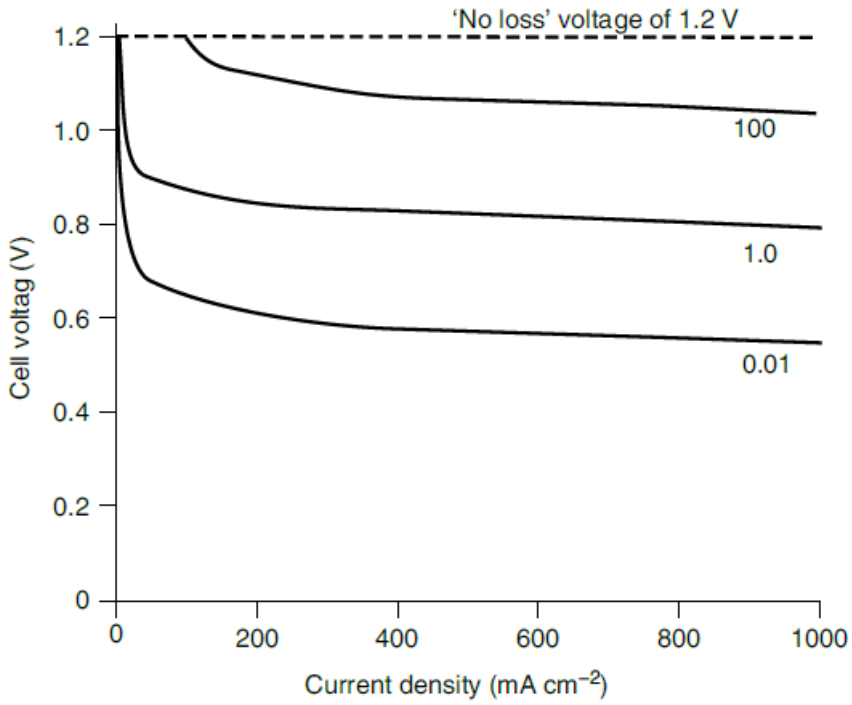

Figure 63: Voltage drop assuming losses due to activation voltage on one electrode for i_0 values of 0.01, 1.0 and 00 [mA cm^{-2}] [25]

Options to decrease the activation losses are:

- Raising the cell temperature.
- Using more effective catalysts.

- Increasing the roughness of the electrodes.
- Increasing the reactant concentration, for example using pure oxygen.
- Increasing the pressure.

Fuel Crossover and Internal Currents

The function of the membrane is to only conduct the ions. In reality, however, small quantities of fuel and electrons will pass the membrane. If fuel passes the membrane, this is called 'fuel crossover'. The effect is that fuel or electrons pass the membrane without generating electricity, thus causing a loss. In hydrogen fuel cells, the major loss is the transfer of electrons at the cathode interface.

If we include these losses in internal current density i_n and include this in formula 24, we obtain a formula including the activation losses and fuel crossover/internal currents:

$$V = E - A \cdot ln\left(\frac{i + i_n}{i_0}\right) \qquad 25$$

Plotting this formula for a typical low temperature fuel cell with E = 1,2 [V], A = 0,06 [V], i_0 = 0,04 [mA cm^{-2}] and i_n = 3 [mA cm^{-2}] gives the following graph:

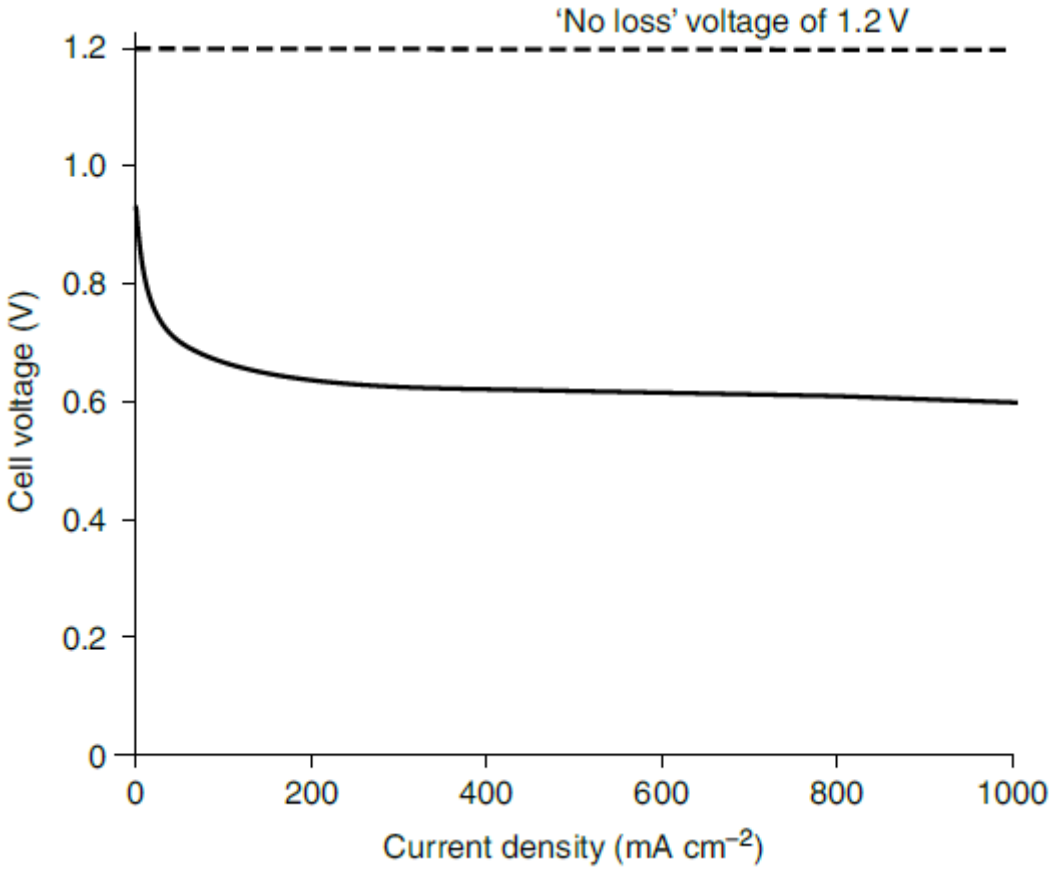

Figure 64: Fuel cell voltage modelled using activation and fuel crossover/internal current losses only [25]

This figure shows that the zero-load voltage is below the theoretical cell voltage, contradicting the general behaviour of, for example, batteries.

Ohmic losses

Ohmic losses are the simplest to understand and are similar to any other electrical circuit described by Ohms law:

$$V = I \cdot R \qquad 26$$

In most fuel cells, the resistance is dictated by the membrane or electrolyte. As the other losses are described in relation to the current density, formula 26 was rewritten to use the current density and the resistance corresponding to 1 cm^2, the so called area-specific resistance (ASR), expressed in $k\Omega\ cm^2$:

$$\Delta V_{ohm} = i \cdot r \qquad 27$$

Minimizing this loss is mainly achieved by a proper choice of materials and construction. The most important ways to reduce the resistance are:

- Using electrodes with a high conductivity.
- Choosing the appropriate materials for the bipolar plates and cell interconnections and have a well-designed fuel stack construction.
- Making the membrane or electrolyte as thin as possible.

Mass transport or concentration losses

The reactants in the fuel cell are hydrogen and oxygen. As hydrogen is used, the inlet pressure will be higher than the pressure at the end of the fuel cell. This influences the output voltage. The same applies for the oxygen. In LTPEM fuel cells, the oxygen is taken from the air, lowering the partial pressure of the oxygen and the total pressure of the mixture. Some theoretical models exist to calculate the voltage drop caused by this lowered partial pressure, but they are not usable in practical low temperature fuel cells. Another approach is entirely empirical and gives a very good fit to the results. It uses the equation:

$$\Delta V_{trans} = m \cdot \exp(n \cdot i) \qquad 28$$

Typically, m is about $3 \cdot 10^{-5}$ V and n about $8 \cdot 10^{-3}\ cm^2\ mA^{-1}$. The solution to minimize this loss is to have a fast-reacting hydrogen supply and a good air circulation to avoid nitrogen build-up. In LTPEM fuel cells, the removal of water is also important.

Total of the losses

Combining the losses, the fuel cell voltage is:

$$V = E - i \cdot r - A \cdot ln\left(\frac{i + i_n}{i_0}\right) + m \cdot \exp(n \cdot i) \qquad 29$$

The value of i_n is in reality very small and is mainly used for explaining the initial fall in voltage. It has little impact on operating losses and is difficult to measure. Also, i_0 is nearly always greater than i_n, so we can rewrite the activation voltage drop to:

$$\Delta V_{act} = A \cdot ln\left(\frac{i}{i_0}\right) = A \cdot \ln(i) - A \cdot \ln\,(i_0) \qquad 30$$

The second part, related to the i_0, is a constant term. It is used to calculate the practical open circuit voltage E_{oc}:

$$E_{oc} = E + A \cdot \ln\,(i_o) \qquad 31$$

This open circuit voltage will always be less than the theoretical voltage, as the small i_0 generates negative logarithms. Combining equation 29 with equation 31, we obtain the equation to calculate the cell voltage V_c:

$$V_c = \ E_{oc} - i \cdot r - A \cdot \ln(i) + m \cdot \exp\,(n \cdot i) \qquad 32$$

This simple equation gives an excellent fit with the results of real fuel cells [25].

In the literature a different formula from Wingelaar was found: [43]

$$V_c = \ E_{oc} - i \cdot r - A \cdot \ln\left(\frac{i}{i_0}\right) + B \cdot ln\left(1 - \frac{i}{i_l}\right) \qquad 33$$

This is the same formula, however the last term describing the concentration losses is different compared to formula 29. The difference is that formula 29 is based on empirical data for low temperature fuel cells, while formula 33 is based on the limiting current i_l and concentration coefficient *B*.

Water management

Without going too much into detail, water management is important in an LTPEM fuel cell. There must be enough water in the polymer electrolyte to facilitate the proton conductivity. However, there must not be so much water that the electrodes are bonded to the electrolyte flood. This will block the pores of the electrodes or the gas diffusion layer. Ideally, the water formed in the fuel dell would keep the electrolyte at the correct level of hydration. The air used to bring in the oxygen blows over the cathode and dry out any excess water. The membrane electrolyte is so thin that water would diffuse from the cathode side to the anode, keeping the whole electrolyte well hydrated.

In reality, there are some complications. During the operation, H^+ ions move from the anode to the cathode, pulling water molecules with them. Especially at high current densities, this can cause the anode side of the membrane to dry out, even if the cathode is well hydrated.

Also, at temperatures over 60 °C, the air will dry out the electrodes faster than the water is produced by the reaction. One way to overcome this is to humidify the air, hydrogen or both before they enter the fuel cell. Lowering the air supply to just the flow for the stochiometric rate is not possible, as the concentration loss, and so the drop of partial pressure of the oxygen through the cell, will be high enough to influence the generated voltage. In practice, the stoichiometry will be at least 2.

In larger FC stacks, the challenge is that the water balance must be correct throughout the whole cell. For example, the air at the end of the cell might have a higher water content, so less water will evaporate at that part of the cell. Whether an FC needs humidification of the supplied air or hydrogen depends on the design. The system can be run even if it is not well designed.

Heat losses

The cell voltage V_c is always lower than the theoretical cell voltage. The difference between these figures is not converted into electricity but into heat. The theoretical cell voltage is 1,48 [V] if the water produced is in liquid form and 1,25 [V] if the water produced is in vapour form. The cases in which water ends as vapour in an FC are rare, so most of the times the value of 1,25 [V] is used. The heat generated is:

$$Heating\ rate = n \cdot I \cdot (1{,}25 - V_c)\ [W] \qquad 34$$

Or in terms of electrical power:

$$Heating\ rate = P_e \cdot \left(\frac{1{,}25}{V_c} - 1\right)\ [W] \qquad 35$$

In small fuel cells (<100 W) convected air alone can be used to cool the cell and provide sufficient air to evaporate the water. For bigger cells, a fan is needed to supply enough cooling air through the cell.

Although enough cooling air can be supplied to the cell to remove the generated heat, this excessive flow will lead to dry air in the cell, dehydrating the membrane. To overcome this in larger cells (>100W), the cooling air is separated from the air supplying the oxygen. The cooling air is fed through cooling air channels in the bipolar plates. Air cooling in this way is mostly performed for fuel-cells with a capacity up to 2 kW. Fuel cells of 5 kW and up are water cooled, while in-between fuel cells can have either or both cooling systems.

Efficiency of a real fuel cell

The theoretical efficiency depends on the fuel cell voltage. As the cell (and membrane) ages, the cell voltage, and so the efficiency, decreases. Nedstack provided documentation [35] containing the efficiency and hydrogen consumption for a new stack and after 24000 hours of operation. The latter fuel cell is still working well, but as no further data is available, we considered this the technical lifetime for now. As the degradation is linear according Nedstack, we can use the mean value for the efficiency and hydrogen consumption.

For this report, a fictional 250 kWe FC was used. In reality, the documentation available is for a 500 kW FC, but this unit is built from 6 strings of each 104 kWe. Depending on the load, one or more strings can be switched on or off. The advantage of running on fewer strings is that fewer stack replacements are necessary as the running hours are lower. The disadvantage is that the loading on each string is higher, leading to lower efficiency. Which strategy is more economical is not determined in this thesis.

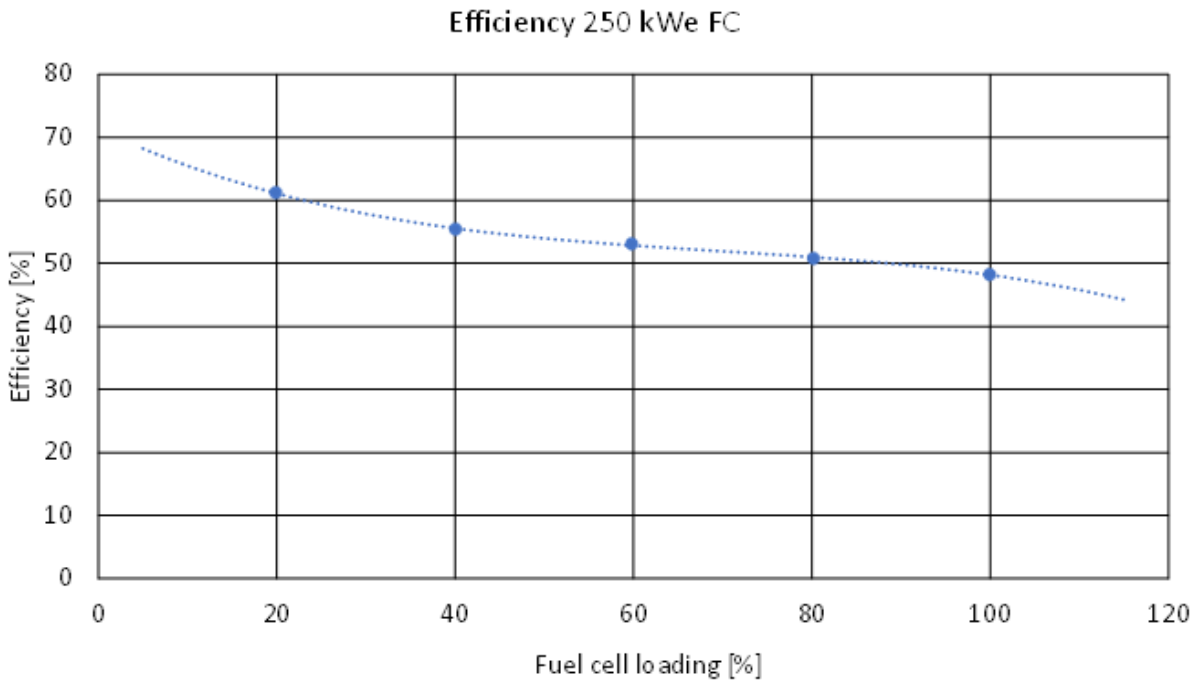

Figure 65: Mean efficiency of a 250 kW FC

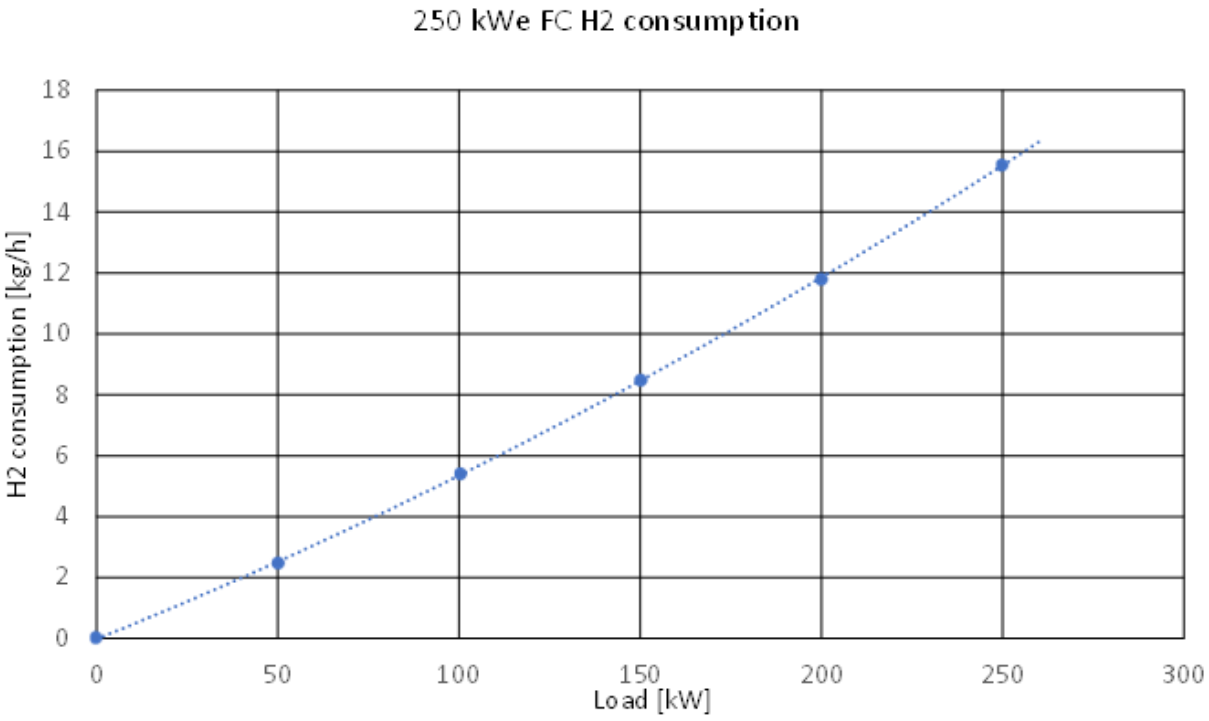

Figure 66: Mean hydrogen consumption of a 250 kW FC

D
Combustion engine

General

Internal combustion diesel engines have a long history in shipping. They are a reliable, simple way of converting chemical energy into mechanical energy. This paper does not focus on the complete theory of internal combustion engines and readers are expected to posses basic knowledge about this energy converter. Section 7.2 describes some specific dual fuel technology. Below, additional information is provided about the emission control and the operating range of internal combustion engines.

Emission control

New vessels over 24 meters long with a gross tonnage over 500 GT and an engine power of over 130 kW have to comply with IMO Tier III when sailing in a NECA (NOx emission control area). This is the case for our vessel.

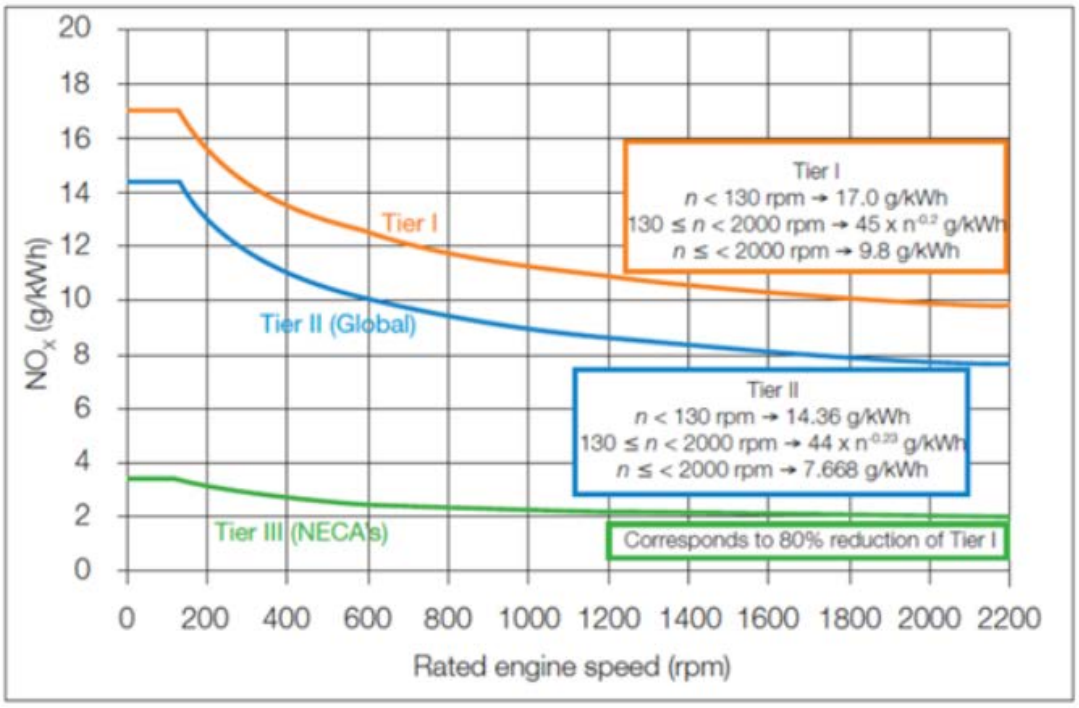

Figure 67: IMO Tier I, II and III limits (source: bergermaritiem)

NOx is formed when the nitrogen from the combustion air reacts with oxygen. The amount formed depends on the temperature and how long the mixture is at this temperature. This is the base of the so called ‘diesel-paradox’: higher temperatures increase the Carnot efficiency, but this leads to a higher NOx production.

As how long the mixture spends at higher temperature depends on the rated speed, this is not something the engine manufacturer can change. Therefore, lower speed engines are allowed to produce more NOx, as can be seen in Figure 67.

Another issue is soot formation. The region where soot is formed depends on the type of fuel used and the air to fuel ratio in the mixture. Figure 68a shows NOx and soot formation regions for a diesel engine. The NOx region lies in the higher temperature, higher efficiency region of the engine. Figure 68b shows that the locations of soot and NOx formation are not the same in a flame of burning fuel [6].

For this thesis, we ignored soot formation and accepted that an internal combustion engine produces NOx. Currently no engine can meet tier III regulations without an exhaust gas treatment. This treatment is usually a selective catalytic reduction (SCR). In an SCR, ammonia is injected into the exhaust gasses in a reactor containing a labyrinth with a catalytic surface. The catalyst on this surface needs a temperature between 300 and 400°C to convert the nitrogen oxides, forming nitrogen and water. Many reactions are possible but equations 36 and 37 show the most common ones. [29]

$$4\,NO + 4\,NH_3 \rightarrow 4\,N_2 + 6\,H_2O \qquad 36$$

$$6\,NO_2 + 8\,NH_3 \rightarrow N_2 + 12\,H_2O \qquad 37$$

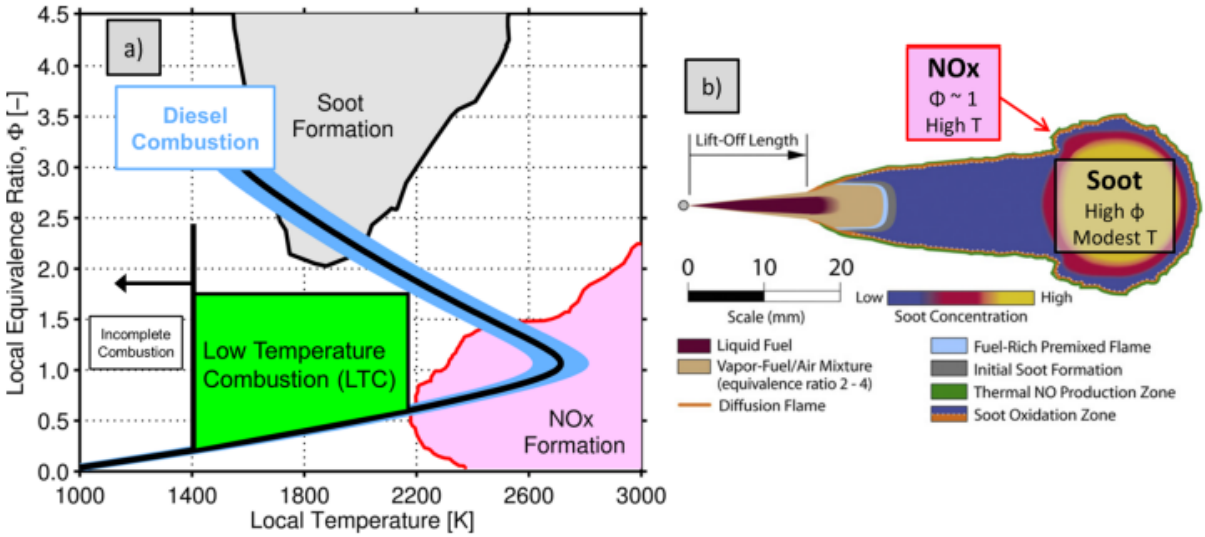

Figure 68: a) NOx and Soot formation regions for a diesel engine. Local equivalence ratio defined as the local air to fuel ratio divided by the stochiometric fuel ratio. b) Conceptional model of mixing limited diesel combustion illustrating the locations of NOx and soot formation. [6]

The ammonia is injected into a urea solution, consisting of urea dissolved in water. At 80 °C, ammonia is formed from the urea. The amount of urea needed varies in different sources, between 4 –6% of the diesel use, mass based. Engine manufacturer Caterpillar indicates 6% of the diesel consumption [45].

Engine loading, efficiency and fuel consumption

A combustion engine has no fixed efficiency or specific fuel consumption (g/kWh). These depend on the load and on the engine speed. For vessels driven with mechanical drivetrain consisting of an internal combustion engine, gearbox and fixed pitch propellor, the engine

speed is dictated by the vessels speed. The power needed follows the so called ‘propellor curve’:

$$P \approx n^3 \qquad 38$$

Figure 69 shows a contour plot containing three propellor curves. The blue dashed line is the propellor curve for which the vessel is designed. Due to fouling of the hull or waves, this curve can shift upwards towards the green dashed line. During the design, this off-design condition has to be specified to avoid that the propellor curve exceeding the operating envelope of the engine. In this example, the green off-design condition line is out of the engine envelope at the top.

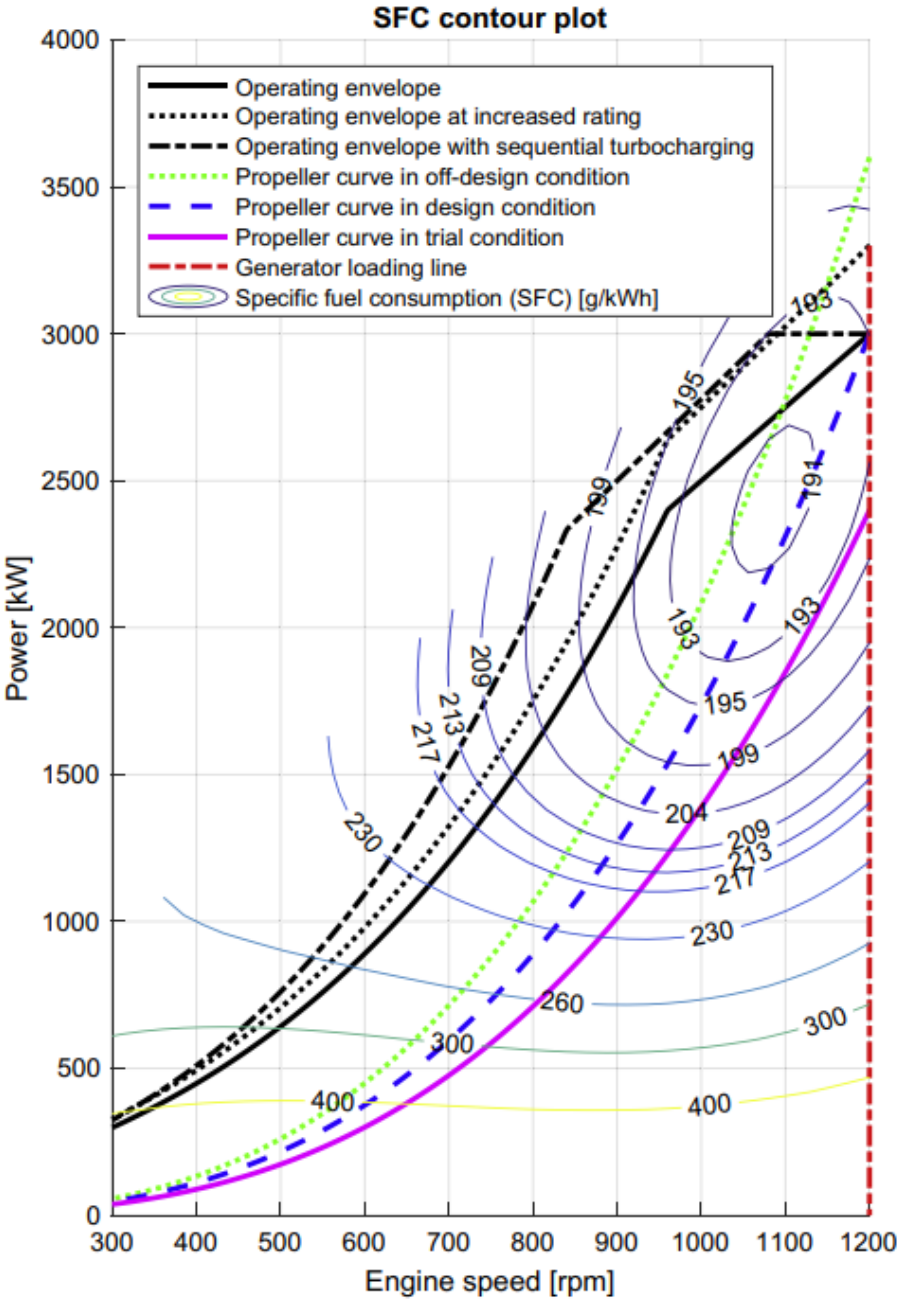

Figure 69: SFC contour plot showing three engine envelopes and three propellor curves [46]

If the ship is fitted with a CPP, the engine speed can be varied within certain limits while maintaining the same vessel speed. This allows, for example, a higher engine speed to enable using a shaft generator or to have more torque available during manoeuvring.

If the engine is driving an AC generator, the red dashed line is followed. When a DC generator is used, the engine speed can be varied as long as the operating point falls within the engine envelop. This allows us to choose the operating point, such that the specific fuel consumption is as low as possible. In this example, if we load the AC generator with 1500 kW, we have a fixed rpm of 1200 and an SFC of 213 [g/kWh]. If a DC generator is used, we could lower the engine speed to 1000 rpm, giving an SFC of 200 [g/kWh].

E
Simulation recommendations

General

To continue with the setup and recommendations, a simulation model should be used. However, a complete simulation could not be developed within the timeframe of this thesis. Additionally, data is not yet available. This attachment provides a start to such a simulation. A general outline is presented and a few topics are examined in more detail. This setup should be interpreted as a starting model that can be used as a base for further research. The model contains many highly specialized topics. For example, modelling the fuel cell itself is relatively simple, but incorporating a complete model including the hydrogen and air supply regulating systems could be a topic for its own research project. The same applies for the electrical side of the installation.

Background

With a simulation, the different components can be sized and the system response can be forecasted. Also, a model is useful to test control strategies for the combined controller. Another issue to investigate is the current ripple in the fuel cell current. As mentioned before, Nedstack is working on this is a topic, as it might influence the lifetime expectations of the fuel cells.

This current ripple depends on several factors, such as:

- Torque variations due to waves (less than 1 Hz)
- Torque variation due to propellor (a few hundred Hz)
- Current ripples caused by the power electronics (several kHz)

Small torque variations caused by the combustion process in the ICE might also feed back into the electrical system. As these are in the range of a few hundred Hertz, potentially the most harmful for the fuel cell according to Nedstack, this should be included in the simulation.

To create and validate a simulation model, the following steps must be taken:

1. Propellor torque data of an actual vessel must be acquired and analysed to know the amount of electrical energy needed to compensate the torque fluctuations. Preferably, several datasets should be available for different loading and environmental conditions. The state of the hull and propellor could also be taken into account to correct for the fouling of these components. The sampling speed of the datasheet must be high enough to include the propellor-hull disturbances.
2. The dynamic response of the fuel cell must be available, including the response during larger load steps. The influence of external equipment, such as the gas valves, blowers and compressors, during these larger load steps should be included and, if necessary, optimized.
3. The response of the DC chopper and the drive of the electric motor must be known.
4. Torque fluctuations produced by the internal combustion engines should be measured or obtained via the manufacturer.

Once the points above are known, they could be an input for a complete simulation model. Based on this simulation, the following questions could be (partly) answered:

- What is the optimal size of the fuel cell to facilitate in both peak shaving and electrical power supply within the boundaries set by the expected wave spectrum?
- What is a good control strategy for both the ICE and electric motor in each stage of the voyage?
- What is the frequency spectrum and amplitude of the expected fuel cell ripple?
- Will it be beneficial to install batteries or super capacitors to optimize the peak shaving or minimize the ripple of the fuel cell current?
- Optionally, the auxiliaries of the fuel cell could be included to seek improvements to make the response fit better in our application.

Current status

The workflow above contains several highly specialized topics that requires input from both mechanical and electrical engineers. To create a complete model, a multidisciplinary workgroup could first work on the separate topics and then integrate the parts into a complete model. The model then has to be validated. Discussions with the system integrators showed that so far, most installations are built using common sense and experience.

It is not possible to continue with a simulation in this report. No propellor shaft data is available yet within Conoship. The lectorate ‘Maritime innovative techniques (MIT)’ from the Maritime Institute Willem Barentsz is starting the TODDIS project (Transferring Operational Data into Design Information for Ships). One of their interests is to obtain this kind of information from operational vessels, but currently they are not yet working on these datasets. Many vessels are equipped with torque measurement equipment, but not all log and store this information with a high enough frequency and accuracy. Lode Huijgens is currently working at TU Delft and might be able to assist in this matter, but such information would be too late to implement in this report. Other companies, such as MARIN, could also have information available. In the last weeks of this thesis, lecture notes from Asgeir J. Sørensen about ‘marine control systems’ were found and briefly examined [14]. These notes examine different types of control, including speed, torque and power control, mainly from the control perspective. These notes could be helpful for a follow up into control strategies. The accompanying presentation also contains useful information [42].

Another area where too little information is available is the fuel cell. Nedstack is not using simulation tools yet, at least not that was known to my contact person. It could be useful to Conoship and Nedstack to have someone develop such a model. Currently, most research in Nedstack is conducted practically, but for the system integration, a simulation could be useful. There are many scientific papers on this topic and a standard fuel cell model is also available in Simulink. The section about the fuel cell in this chapter describes such a scientific model and the general Simulink model. The research currently conducted in Nedstack on possible limitations of the current ripple could also impact the design considerations.

Simulation and validation

The model should be based on the chosen setup, shown below. Two mechanically interlocked machines, an internal combustion engine and an electric motor, drive a propellor shaft. The ICE at first provides a larger output power compared to the electric motor, but this is not a requirement. A start could be roughly 3:1 with an ICE of 750 kW and an FC of 250 kW.

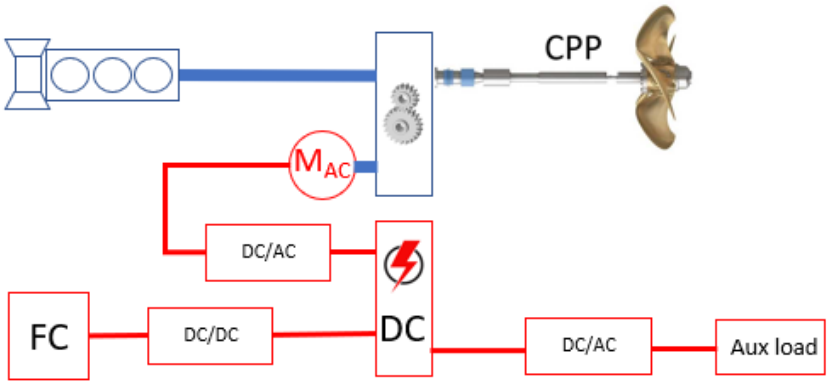

Figure 70: System layout

The simulation setup is roughly the same. It consists of an electrical part and a mechanical part. All sub parts can be modelled and validated separately.

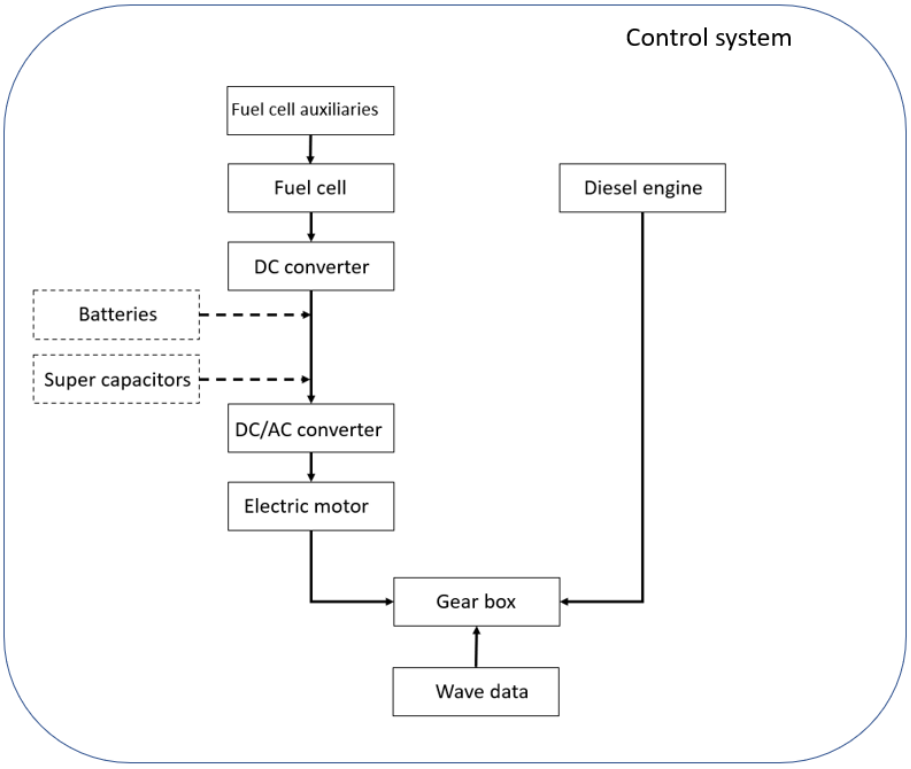

Figure 71: Overview of simulation blocks

Figure 71 shows an overview of the simulation blocks. Depending on the research questions, the blocks can be simple or more detailed. For example, when using the simulation to work out control strategies, the exact content of higher harmonics in the current ripple is likely not relevant.

Validating the model will be a challenge, as many components are involved. The strategy should therefore be to validate the sub models one by one. Some components, such as the fuel

cell, could be validated with the help of the manufacturer. For other components, validated models might already exist and should just be modified for this purpose.

Test setup

To have a small test setup available, some experiments were performed in the electrical laboratory of the MIWB. Sufficient equipment is available to help now and in the future with small-scale tests with electrical equipment up to around 1 kW. Due to the laboratory's flexible setup, parts of the simulation model can be tested alone or in a combination.

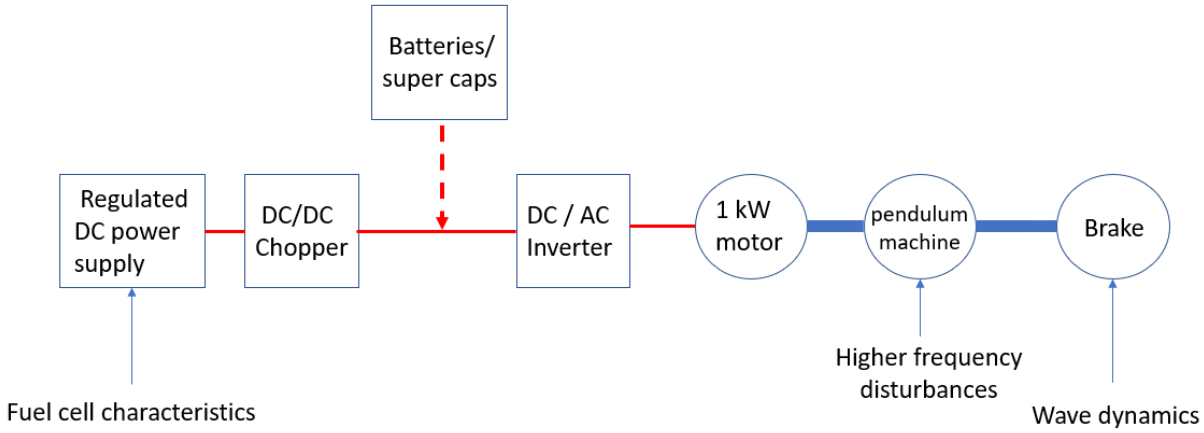

Figure 72: Overview of a small-scale validation setup (red lines are electrical connections, blue lines are mechanical connections)

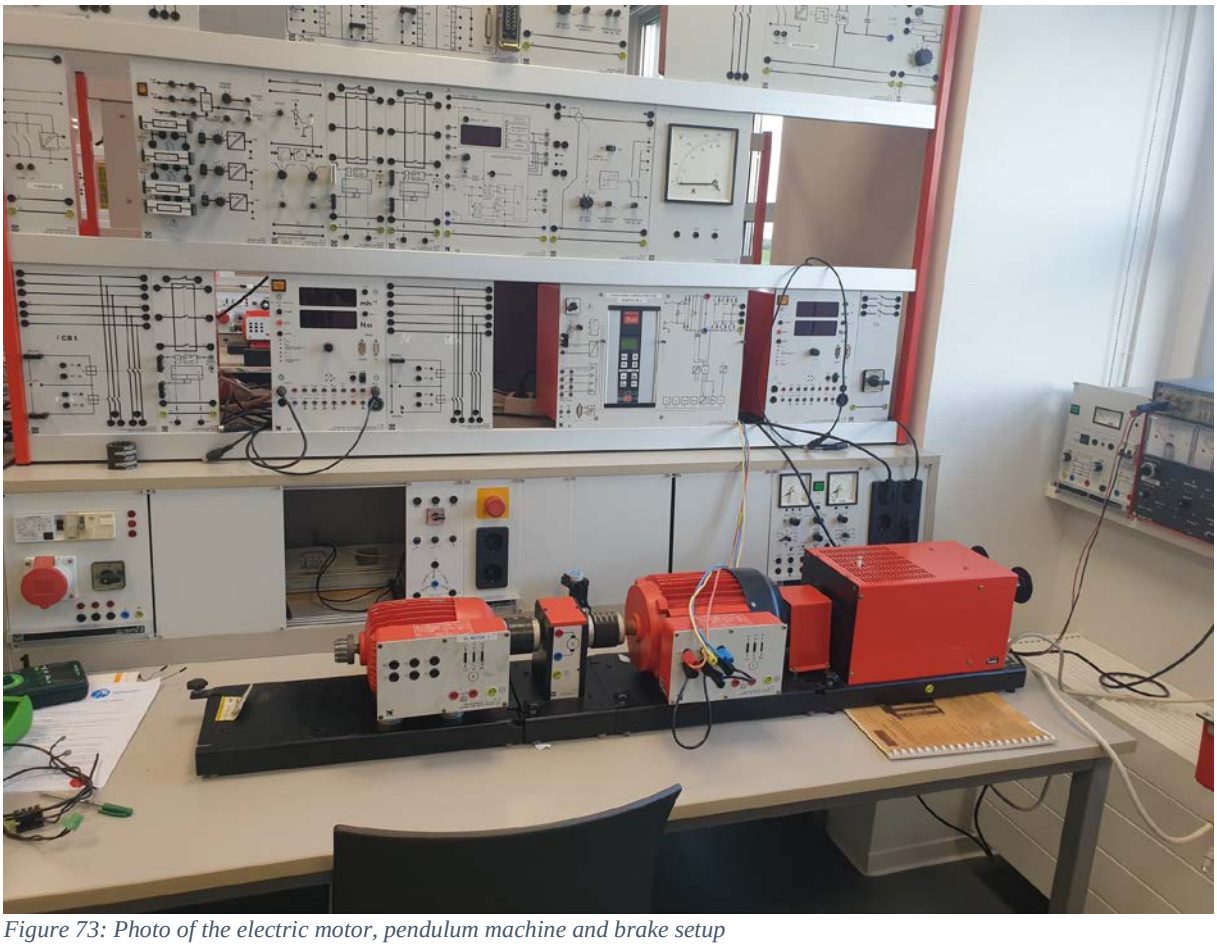

Figure 73: Photo of the electric motor, pendulum machine and brake setup

Figure 72 is an overview of the possible configuration of the validation setup. The red lines are electric connections, the blue lines mechanical connections. As the current assumption is that the internal combustion engine will run in constant torque mode, or in constant power as long as the speed remains constant, the response of this engine does not need to be modelled. However, the higher frequency torque variations generated by the combustion process should be examined, possibly by including a pendulum machine. This machine can generate quickly changing torque variations and is therefore suitable to simulate the propellor-hull interference torque variations. If only the lower frequency disturbances generated by waves need to be examined, a magnetic powder brake could be used instead. On the electrical side, a fuel cell (simulator), a DC/DC chopper and a DC/AC inverter are used to drive the electric motor.

Fuel cell

As described in Attachment C, the fuel cell voltage is not constant, but decreases with the current drawn. However, the curve describing this (Figure 61) is only valid in steady state situations. Using a fuel cell in real applications likely involves a system integration containing power converters to obtain certain voltage levels, as in our case. This generates currents steps and other dynamics in the output of the fuel cell that are not described by the steady state equations.

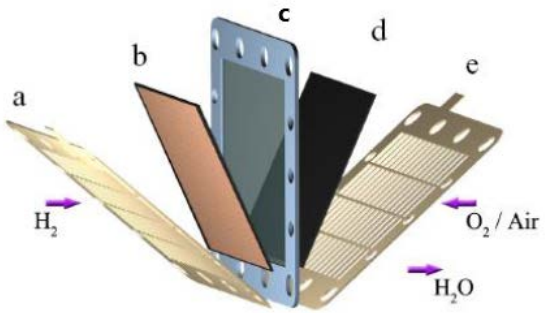

Figure 74: Schematically drawn PEM fuel cell with a) metal plate (anode), b) diffusion layer, c) membrane, d) diffusion layer and e) metal plate (cathode) [43]

Due to the construction of the fuel cell, several materials act as a capacitance. As there are two electrode-electrolyte interfaces (the anode-membrane and cathode-membrane), the fuel cell might have two charge double layer capacitances, resulting in two time constants. Furthermore, the anode and cathode reactions speeded up by platinum catalyst may result in an adsorption time constant. This is because the hydrogen adsorbs to the platinum catalyst surface, as a result of hydrogen ion discharge. As the hydrogen transfers, an immediate voltage response occurs, while the current of the system is not directly influenced because the proton transport through the membrane is slow. This results in a phase shift between current and voltage and an additional time constant. [43]

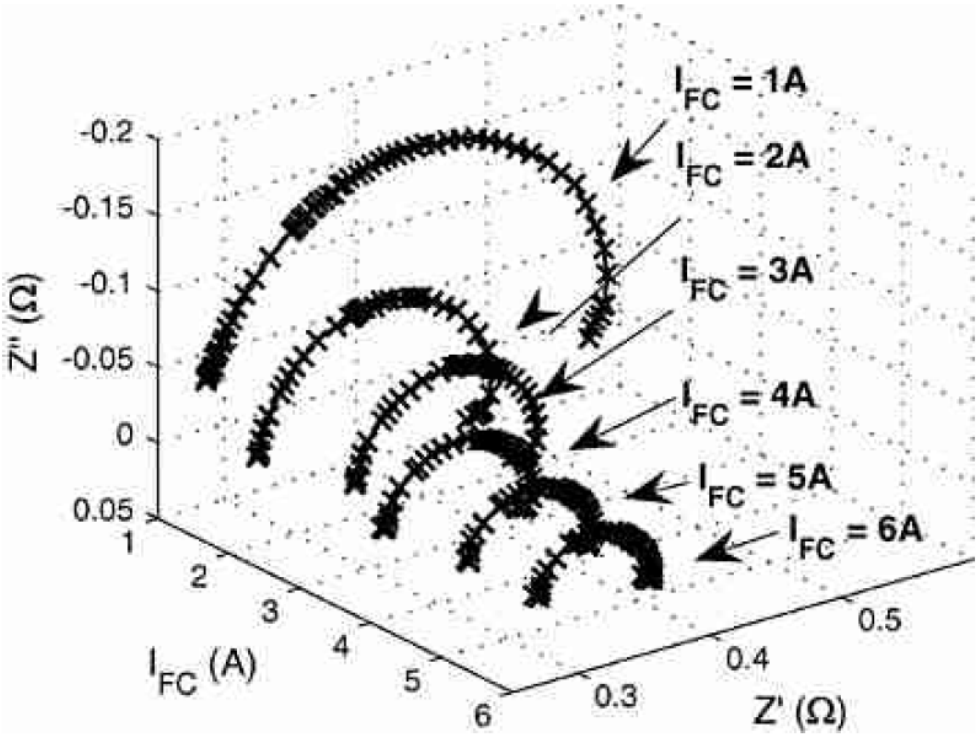

Figure 75: Impedance plots of a fuel cell in range from 1 to 6A. Z' and Z'' are the measured real and imaginary impedance components, respectively [43]

Wingelaar performed impedance spectroscopy measurements on a fuel cell at different currents and frequencies. The results are plotted in Figure 75. The right side of the semi-circles correspond to a frequency of 0,01 Hz, the left side to 45 Hz. At all currents, a large capacitive semi-circle is measured, which is caused by charge double layers effects. On the right side (low frequency), some inductive behaviour occurs, probably caused by the adsorption of hydrogen to the platinum surface. Based on these measurements, Wingelaar proposed a third-order ladder network. This network contains two double layer capacitors, C_{DL} and C_R, and one adsorption inductor L_A.

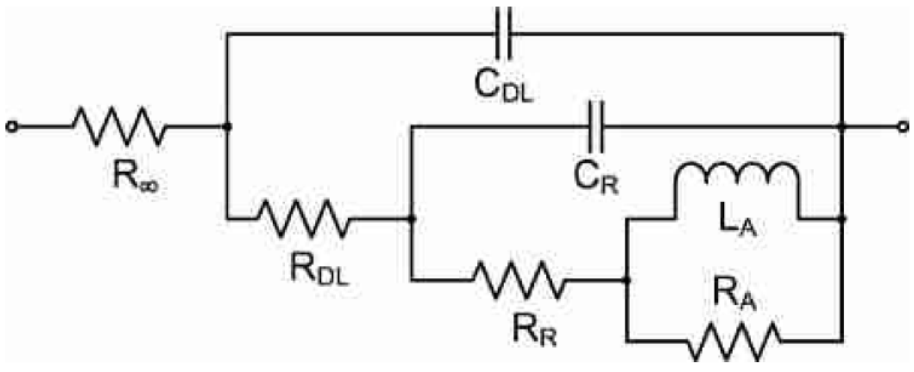

Figure 76: Third-order ladder network for fitting impedance spectroscopy data as proposed by Wingelaar [43]

The bulk resistor R_∞ has a constant character, while the adsorption resistor R_A tends to slowly decrease with increasing current set points. The two double layer resistors (R_{DL} and R_R) show non-linear behaviour dependent on the fuel cell current. The first double layer capacitor C_{DL} and the adsorption inductor L_A can be considered constants. The second double layer capacitor

C_R cannot. By performing steady-state and step measurements, the values for the non-constant components can be fitted.

Based on the theory presented above, Zehra Ural Bayrak and M.T. Gençoğlu described a large and a small signal model [65]. In the large signal model, the charge double layer is modelled with one capacitor C_{DL}, a series resistor R_S and a parallel resistor R_P.

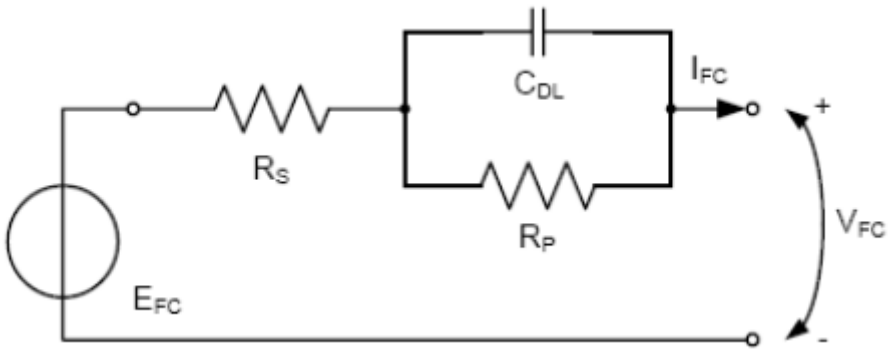

Figure 77: Equivalent dynamic circuit model of a PEM fuel cell for large signals [65]

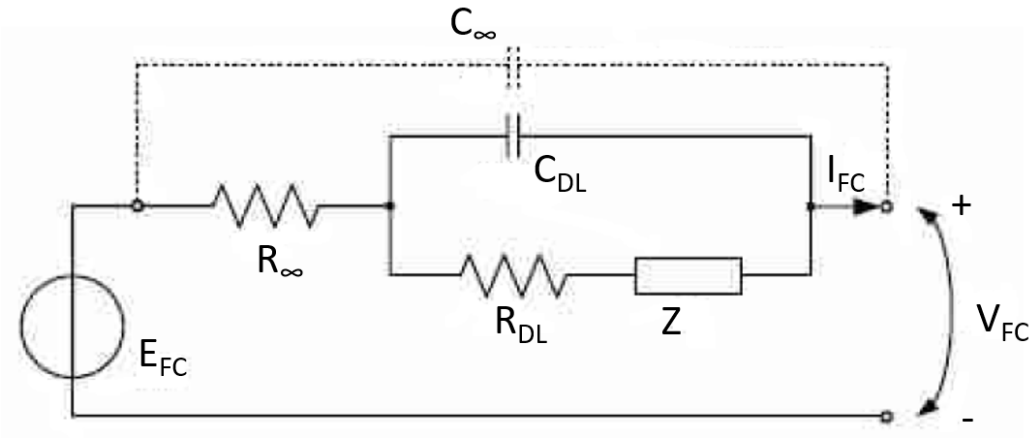

Figure 78: Equivalent dynamic circuit model of a PEM fuel cell for small signals [65]

The small signal model in Figure 78 has a double layer capacitor dominating a part of the frequency domain. The adsorption reactions can cause additional time constants, modelled with the unspecified impedance *Z*. All electrode-material systems have a geometrical capacitance C_∞ and bulk resistor R_∞ in parallel, leading to the dielectric relaxation time of the basic material. R_{DL} is a reaction resistor.

The findings in these reports suggest that for looking into higher frequency phenomena, such as the disturbances induced by the diesel engine and possibly by the propellor, a different model must be used then for the lower frequency changes induced by the waves. The reports do not have definitions of ‘high’ and ‘low’ frequencies, so this should be investigated further.

In Simulink, a standard fuel cell model is included. The Simulink model uses an approach as presented in equation 32, combined with the time delay caused by the capacitances. Figure 79 shows this simplified model.

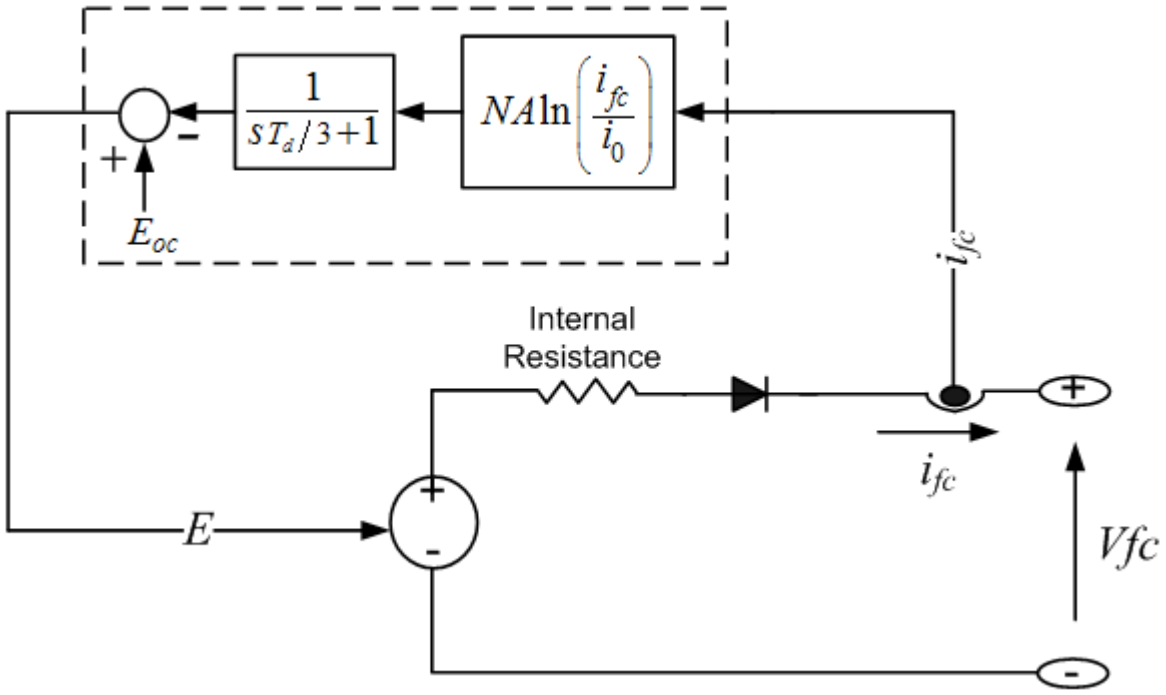

Figure 79: Simulink model of a fuel cell (source: www.mathworks.com)

This model is likely suitable to describe the fuel cell response to low frequency changes and thus for a first estimation for the fuel cell size and the control strategies. If measurements can be taken at Nedstack, the time constants can likely be identified.

For the validation setup, a controllable DC power supply is available with a range of 0–230V and a maximum current of 6A. This power supply can be controlled with an external 0–10V DC signal. For now, the (steady state) voltage curve from Nedstack was fitted with a 5th order polynomial (Figure 105). The current of the DC power supply was measured with an isolation amplifier and fed into a Siemens S300 PLC. This PLC was used because it is available in the laboratory. A different setup can be used, such as a PC with an analog input/output card and a code in python or a different software language. In this case, an SCL program block was used to calculate and scale a 0–10V output signal that controls the power supply. A first order time delay can be included, ora custom response built.

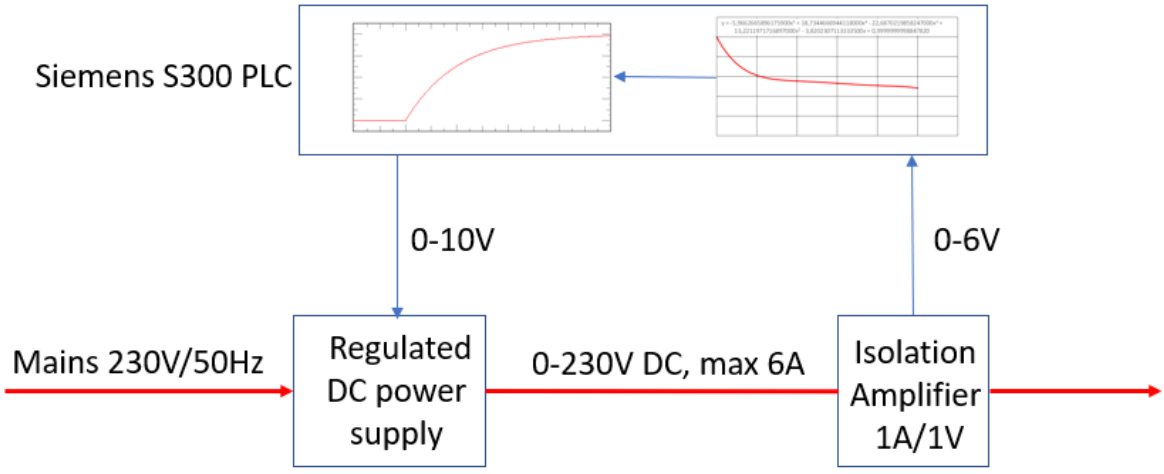

Figure 80: Hardware setup of fuel cell simulator

This response must be verified as is in line with that of a real fuel cell, as this setup is controlling the output voltage but not the output current. The current likely also has a time delay, as described earlier. The used power supply cannot limit the current to a certain value based on an external input. Additionally, the capacitors in the power supply. might need to be removed or a different power supply used, especially when observing higher frequency influences.

For now, the setup follows the fitted curve with an adjustable time delay in the voltage response.

DC boost converter

Higher voltages generally mean less current and therefore less losses. Therefore, a boost chopper was used to increase the voltage of the fuel cell. This was also added in the test setup, as the DC/AC converter needs a DC voltage of 240V DC, while the controlled power supply delivers less than 230V DC.

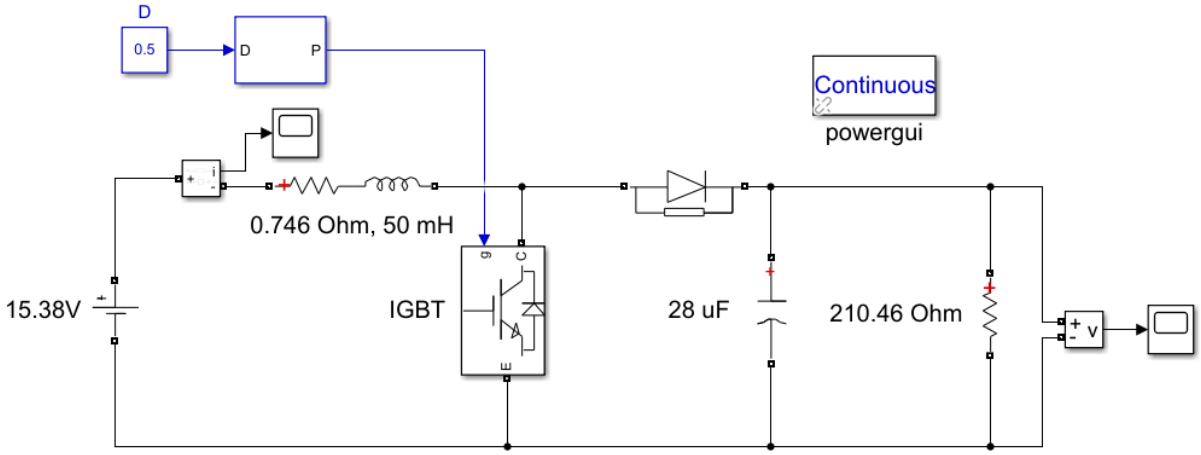

Figure 81: Simulink model of the DC boost converter

A boost converter uses an inductor to store and release energy. Figure 81 shows the Simulink model of the boost converter. On the left side, an ideal voltage source of 15,38 V is placed. This voltage was chosen as it is the same voltage measured for the first (low voltage) test setup in the laboratory. Following the positive line, a current sensor is passed and then a non-ideal inductor. Ideally, this inductor should have an inductance of 50 mH, but when the maximum allowed DC current of 5A was applied to the inductor, a voltage drop of 3,73 V was measured across it. This means a resistance of 0,746 Ω was present. The insulate base bipolar transistor (IGBT) is of the type GT15Q101 [62] with an external snubber circuit to protect the IGBT. The snubber resistor has a value of 100Ω and the snubber capacitor has a value of 0.033 µF. The internal resistance of the IGBT was not found in the datasheet, so it was set to 0,001Ω. The diode (BY329-1000 [44]) after the IGBT has the same snubber circuit and a forward voltage of 1.5V. The internal resistance of this diode was also set to 0.001Ω, as no resistance is found in the datasheet. The capacitors have a combined value of 28 µF and the load resistors are 210,46 Ω.

The IGBT is switched on and off by a pulse width modulator (PWM) module. This is a square wave generator with an adjustable t_{on}/t_{off} ratio, and thus an adjustable duty cycle. If the IGBT is switched on, the inductor is charged with energy. The load during that time is fed by the capacitor. If the IGBT is switched off, the energy from the inductor is discharged and added

to the potential of the ideal voltage source, as this voltage source and the inductor are placed in series. This raises the voltage above that of the capacitor. This causes the diode to conduct and the load and capacitor to be supplied with a higher voltage. The higher the duty cycle, the more energy is stored and released in the inductor and the higher the output voltage.

The output of the boost converter was evaluated at a switching frequency of 400 Hz and a duty cycle of 0,8. The output was logged with a DATAQ datalogger at a sample rate of 40 kHz per channel and compared with the simulation.

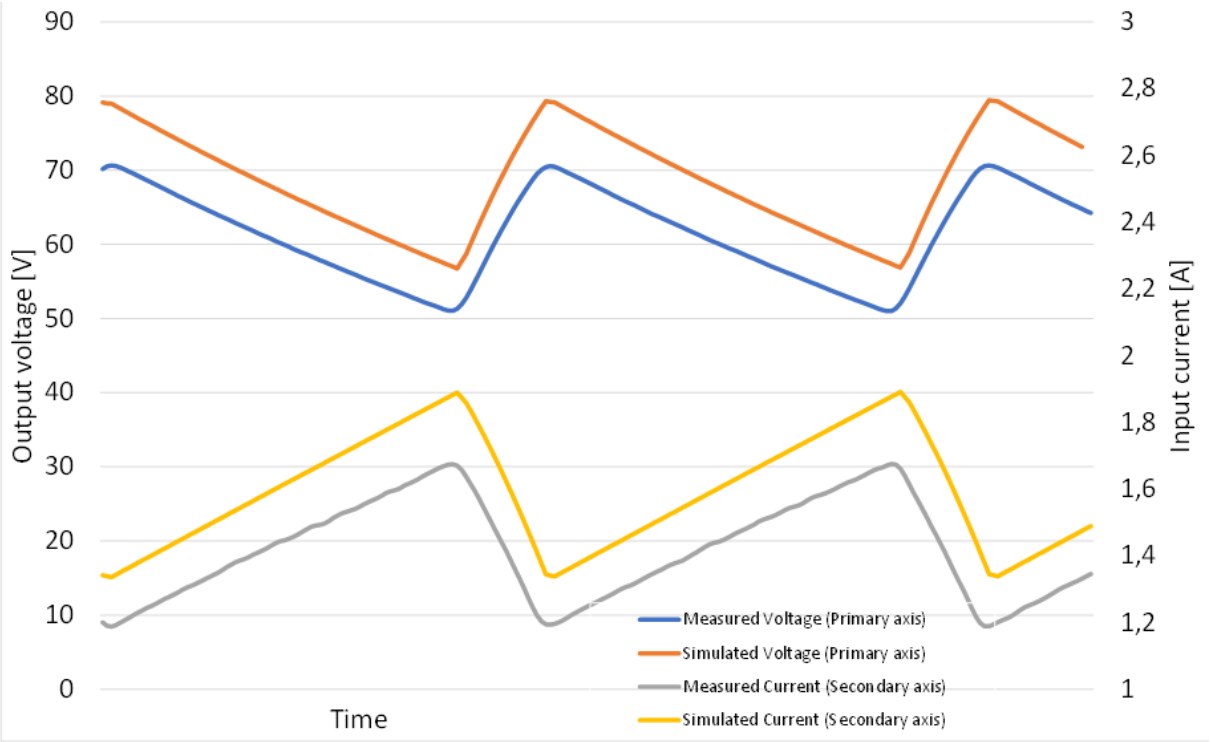

Figure 82: Comparison of the simulated DC boost converter and the experimental setup

The response of the simulation was in line with the measurements. The simulated values are higher than measured, but the trend is the same. The driving force behind the current is the voltage, so since the measured voltage is lower the current is as well.

To identify the sensitivity of the components, the values were varied in the Simulink model. Attachment H-3 shows the table and plots of the sensitivity analysis for the capacitor value, supply voltage, inductance of the coil and the duty cycle. The duty cycle has the largest influence and as that is visually set with a scope, the chance of inaccuracies is high. Setting the duty cycle to 0,77 in the simulation, or a reduction of 3,7%, lowered the simulated voltage value to the same peak and bottom value as the measured value. The maximum simulated current value in that case fell from 112% to 92,6% of the measured value. This shows that for future experiments, the duty cycle is of prime importance compared to the tolerances of the components value.

Experiments were also performed at higher frequencies. The measured quantities did not change much, but due to the datalogger limitations and noise in the test, a good comparison was not possible. As expected, the current and voltage ripple significantly decreased with a higher switching frequency. At a constant load and with a switching frequency of a few kHz, the ripple should be very low.

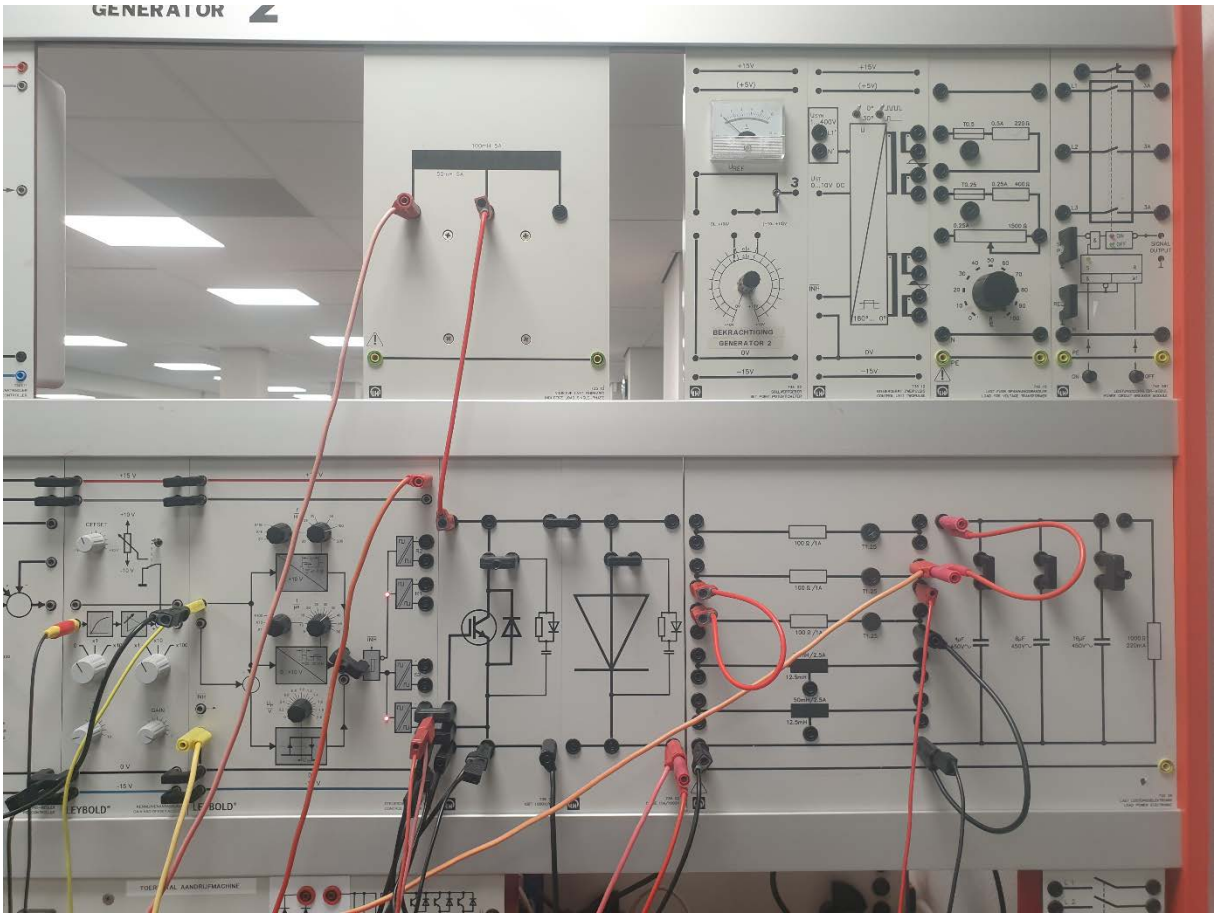

Figure 83: Photo of the boost converter setup

Internal combustion engine and constant torque mode

The engine was modelled as a constant block. In the experimental setup, an electric motor was used with a constant torque controller. The torque was measured with a built-in deflection bridge. This measured value was used to keep the torque constant.

Electric motor

The electric motor was a standard 1 kWe squirrel cage motor, as it was available in the electric laboratory. A model of a squirrel cage motor is available in Simulink. This model relies on a few rotor and stator constants. These constants can be obtained by performing a DC, zero load and a locked rotor test, as described in a publication of Zulhisyam Salleh [66]. The DC test was performed with a DC voltage of 9,18 [V] applied to one stator winding. This resulted in a stator resistance of:

$$R_s = \frac{9{,}18}{0{,}932} = 9{,}85\ \Omega \qquad 39$$

Next, the no-load test was performed, resulting in a total power of 112,7 [W], a phase voltage of 228,69 [V] and a line current of 1,34 [A]. This was used to calculate the magnetic inductance:

$$\theta = cos^{-1} \cdot \frac{P_{phase}}{I_L \cdot U_P} = cos^{-1} \cdot \frac{37{,}567}{1{,}34 \cdot 228{,}69} = 82{,}96\ [°] \quad (40)$$

$$I_m = I_0 \cdot sin\theta = 1{,}34 \cdot \sin 82{,}96 = 1{,}33\ [A] \quad (41)$$

$$L_m = \frac{U_p}{2 \cdot \pi \cdot f \cdot I_m} = \frac{228{,}69}{2 \cdot \pi \cdot 50 \cdot 1{,}33} = 0{,}547\ [H] \quad (42)$$

The locked rotor test was also performed with the motor connected in a star configuration. This test showed a total power of 299,1 [W], a line voltage of 102,7 [V] and a line current of 2,336 [A].

$$\theta = cos^{-1} \cdot \frac{P_{phase}}{I_L \cdot U_P} = cos^{-1} \cdot \frac{99{,}7}{2{,}336 \cdot 59{,}29} = 43{,}96\ [°] \quad (43)$$

$$Z_{sc} = \frac{U_p}{I_L} = \frac{59{,}29}{2{,}336} = 25{,}38\ [\Omega] \quad (44)$$

Once the stator resistance was calculated, the rotor resistance could be too:

$$R_r = Z_{sc} \cdot \cos\theta_{sc} - R_s = 25{,}38 \cdot \cos 43{,}96 - 9{,}85 = 8{,}42\ [\Omega] \quad (45)$$

$$X_{eq} = Z_{sc} \cdot sin\ \theta_{sc} = 25{,}38 \cdot \sin 43{,}96 = 17{,}62\ [\Omega] \quad (46)$$

Depending on the construction of the motor, the division between rotor and stator leakage reactance was divided based on empirical equations. In our case, an equal percentage, belonging to a class A and class D motor [66] gave the best fit in the measurements below. The inductance was calculated to be:

$$L_{ls} = L_{lr} = \frac{X_{eq}/2}{2 \cdot \pi \cdot f} = \frac{8{,}81}{2 \cdot \pi \cdot 50} = 28{,}04\ [mH] \quad (47)$$

With the parameters calculated, the Simulink model was compared with the actual motor with the help of a magnetic powder brake with a built-in deflection bridge. This brake only functioned up to 4,6 Nm, around 70% of the maximum power of the motor.

During the test, the current was measured with an ammeter and the speed was measured with a contactless rpm meter. During the first test, the speed vs torque behaviour was already excellent. All deviations were less than 0.5%. The current, however, was lower than measured by up to 12,5%. This indicates that the parameters influencing the actual power delivery, such as the rotor resistance, are well dimensioned. The magnetic components, however, can be improved. As the deviation is relatively constant over the whole range, it was likely a small deviation in the leakage reactance and therefore the mutual inductance was slightly lowered. This resulted in a better fit, with a maximum deviation of 6%. The results are shown in Table 37 and Figure 84.

Torque	Measured values			Simulation 1					Simulation 2			
T [Nm]	n [rpm]	I [A]		n [rpm]	Dev. [%]	I [A]	Dev. [%]		sim I2	Dev. [%]	n [rpm]	Dev. [%]
0	1498	1,4		1499	0,07	1,27	-9,29		1,46	4,29	1498	0,00
1	1483	1,405		1485	0,13	1,29	-8,19		1,48	5,34	1484	0,07
2	1469	1,453		1470	0,07	1,34	-7,78		1,54	5,99	1469	0,00
3	1452	1,643		1454	0,14	1,47	-10,53		1,64	-0,18	1453	0,07
4	1432	1,862		1438	0,42	1,63	-12,46		1,78	-4,40	1436	0,28
4,6	1423	1,954		1427	0,28	1,74	-10,95		1,89	-3,28	1426	0,21

Table 37: Comparison between measured values and simulation values for a 1 kW electric motor

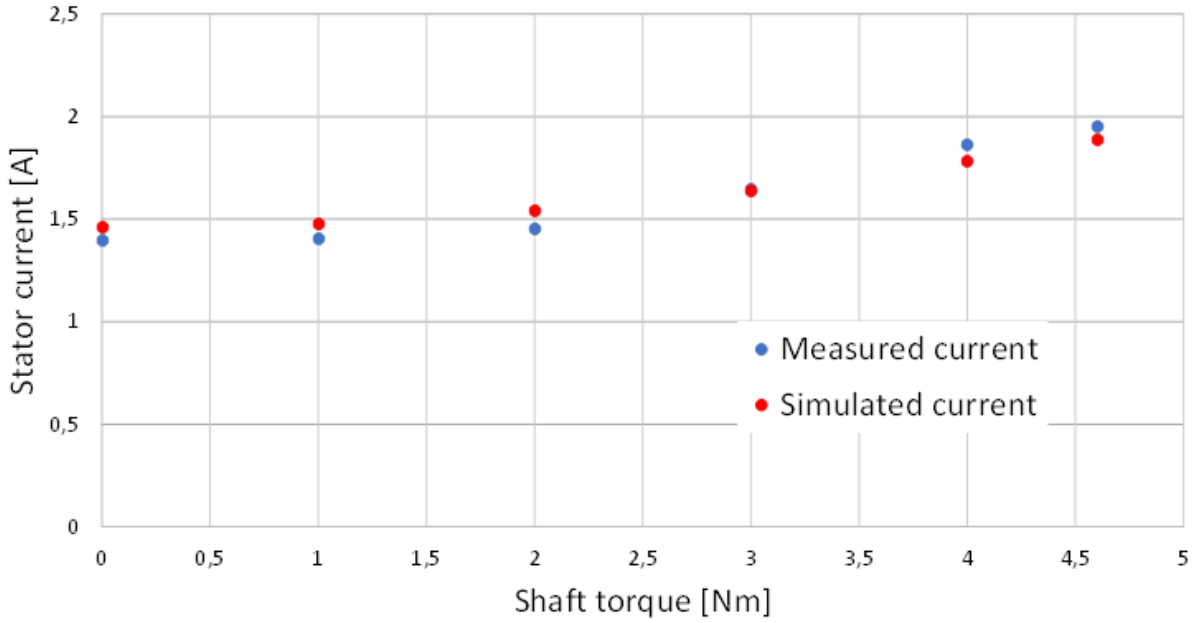

Figure 84: Plot of the measured and simulated current of a 1 kW electric motor

Propellor load

The propellor load was generated with a magnetic powder brake. This brake is controllable with an external voltage between 0 and 10 V. The response was checked with some measurements and was nearly linear between 1 and 4 Nm, although some hysteresis was present. Figure 85 shows the response of the brake.

The dynamic response of the brake to a step change was also measured and plotted. The steps used were 0 V to 5 V and 0 V to 10 V. The step to 5V corresponds with 2,1 Nm and to 10V with 5 Nm. To compare these step loads, the measurements were normalized to 1 p.u. Both a step up and a step down were performed.

The responses were measured with a datalogger and plotted in the figures below. The steps were plotted on a per unit basis. For fast changing, accurate load changes, the magnetic powder brake is not the best option due to the time constant. It might be useful for torque fluctuations caused by waves but that can only be verified when the data sets become available. Another option is to use the pendulum machine for the propellor load as well.

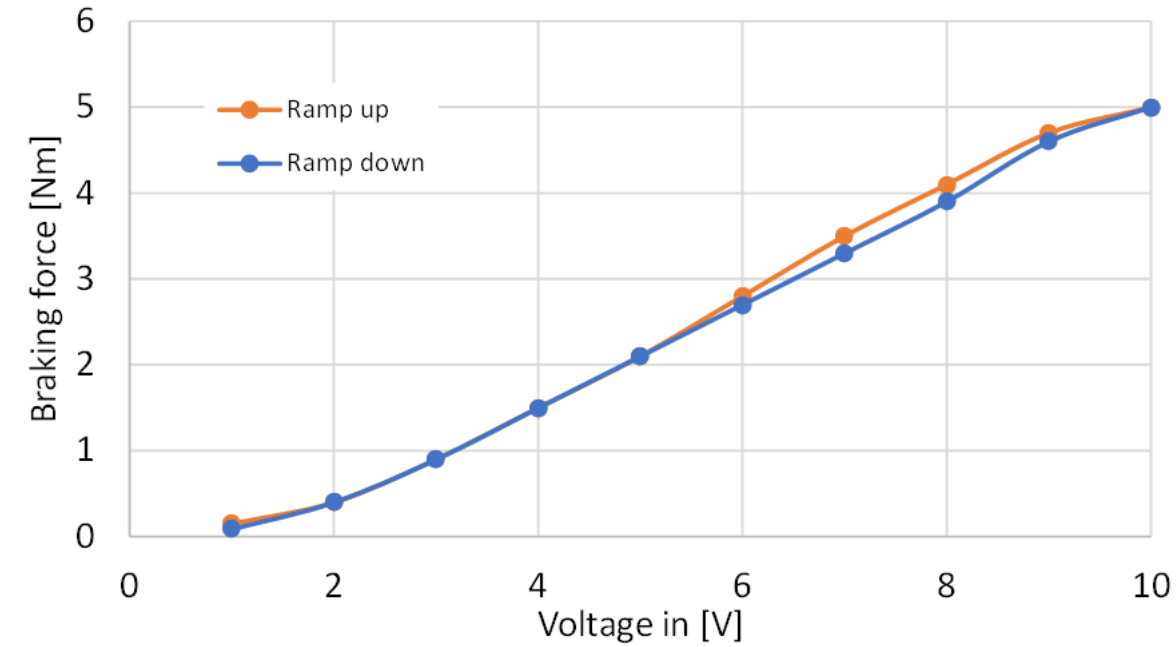

Figure 85: Magnetic powder brake response to a ramp up and a ramp down

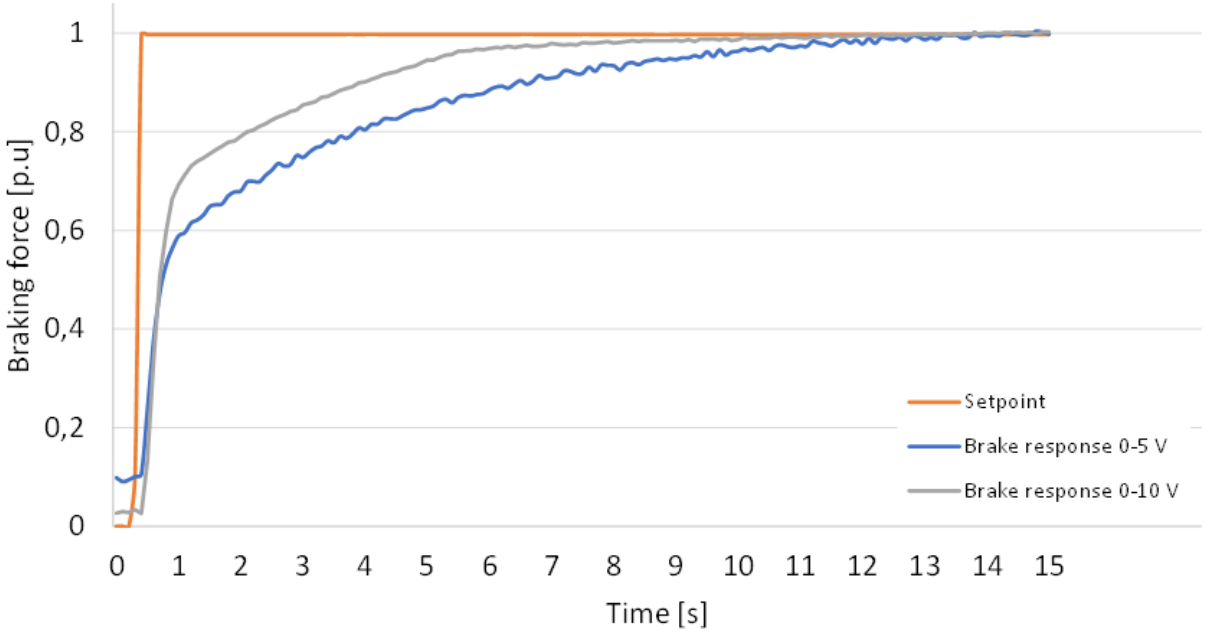

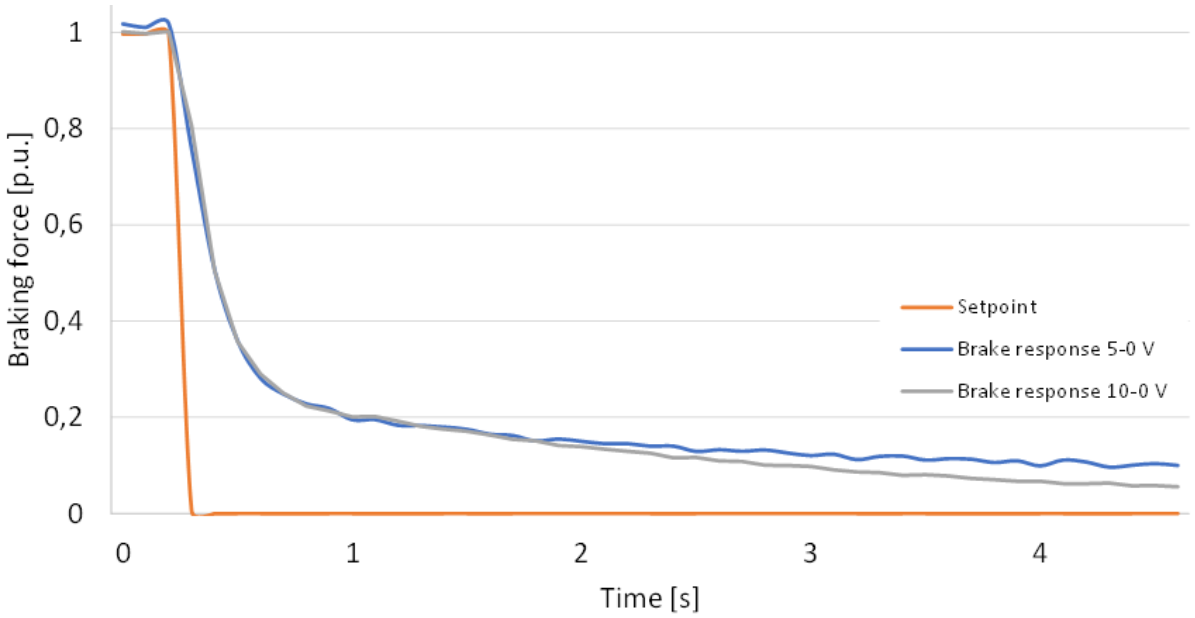

Conclusion and discussion

This attachment is intended as a first step towards a usable simulation for future research. It is not a finished project and it should not be used as the only possible approach. Two items, the electric motor and the boost converter, were simulated and compared to a real experimental setup. The results look good so far, but a validation with a larger or full-scale setup must be performed to determine any scaling effects. Ideally, the simulation and small-scale setup will be found to be accurate enough to use as a base for further development.